AN ABSTRACT OF THE THESIS OF

Kenneth Charles Walsh for the degree of Doctor of Philosophy in Physics presented on Dec 16, 2009.

Title: Hartree-Fock Electronic Structure Calculations for Free Atoms and Immersed Atoms in an Electron Gas

Abstract approved: _____

Henri J.F. Jansen

Electronic structure calculations for free and immersed atoms are performed in the context of unrestricted Hartree-Fock Theory. Spherical symmetry is broken, lifting degeneracies in electronic configurations involving the magnetic quantum number m_ℓ. Basis sets, produced from density functional theory, are then explored for completeness. Comparison to spectroscopic data is done by a configurational interaction of the appropriate L and S symmetry. Finally, a perturbation technique by Löwdin is used to couple the bound atomic states to a neutral, uniform background electronic gas (jellium).

Hartree-Fock Electronic Structure Calculations for Free Atoms and Immersed Atoms in an Electron Gas

by

Kenneth Charles Walsh

A THESIS

submitted to

Oregon State University

in partial fulfillment of
the requirements for the
degree of

Doctor of Philosophy

Presented Dec 16, 2009
Commencement June 2010

Doctor of Philosophy thesis of Kenneth Charles Walsh presented on Dec 16, 2009

APPROVED:

Major Professor, representing Physics

Chair of the Department of Physics

Dean of the Graduate School

I understand that my thesis will become part of the permanent collection of Oregon State University libraries. My signature below authorizes release of my thesis to any reader upon request.

Kenneth Charles Walsh, Author

ACKNOWLEDGEMENTS

Academic

I would like to thank the Oregon State University physics department for continuously supporting me on my journey to graduation. Specifically, I am forever indebted to my advisor Dr. Henri Jansen. His patience and insight are seemingly endless. Countless times I entered our research meetings extremely nervous and left strangely calm. His ability to douse the fires of uncertainty made him the perfect match for my continuous doubts. Every faculty member has, at some time, provided either physical or motivational help. Dr. Krane was an inspiring mentor on my road to becoming a better teacher. My office mates, specifically Skye and Jared, provided an atmosphere inducive to intellectual thought.

Personal

I am personally indebted to both my parents whose unconditional support always told me I could. When I didn't believe in myself, they did. Thank you mom and dad, for giving me the opportunities in life that led me to achieve my dreams. The Weis family, especially Cath, saw me through the hardest times of my career and I am forever thankful. To all of my friends, Ben, Logan, Ryan, Sam, Chris, Justin and many more, I thank you for adding texture to the mundane concerns of graduate school. To my love Marissa, I know it is your strength that I've built on to make my final push. Your belief in me has made my resolve stronger and I forever thank you. Finally I would like to thank the rest of the world because, after all, we live in the ultimate many-body problem and are all correlated.

TABLE OF CONTENTS

TABLE OF CONTENTS (Continued)

TABLE OF CONTENTS (Continued)

LIST OF FIGURES

LIST OF FIGURES (Continued)

LIST OF TABLES

HARTREE-FOCK ELECTRONIC STRUCTURE CALCULATIONS FOR FREE ATOMS AND IMMERSED ATOMS IN AN ELECTRON GAS

1. INTRODUCTION

My advisor Dr. Jansen, early after agreeing to work with me, asked if I wanted to *use tools to model atoms* or *create tools for modelling atoms*. The work presented here is designed to lay the ground work for a new tool created to model atoms, both free and immersed in a gas of free electrons. The end goal of such a tool is to model atomic impurities in metals accurately.

Previous work [1][2] has explored the approach of an atom in an electron gas in the context of Density Functional Theory (DFT). Spherical [3] and non-spherical [4] calculations of this type have shown promise as fundamental tools. Density functional and Hartree-Fock (HF) theory are both used to approximate solutions to the many-body Schrödinger equation. The natural question is then, *how would the immersed atomic system work if modelled with HF theory*? With this goal in mind an alternative question quickly arose, *would using a spherically symmetric converged DFT calculation, for the HF basis states, improve completeness*? This work solves the many-body HF Schrödinger equation for free atoms and atoms immersed in an electron gas, using basis sets generated from DFT.

The first step in modelling an atom, immersed in an electron gas, is to model the atom itself. To provide complete control over electronic configurations we've broken both spatial and spin symmetries. This freedom to explore all electronic configurations

increases the value of this tool but also increases complexity. Interactions between states of the appropriate symmetry lift degeneracies in the energy levels of the atom. The ground state electronic configurations can then be tested if they obey Hund's rules [5]. Various basis sets can be generated by adjusting parameters in DFT. These basis sets are tested for completeness. Along with the kind of basis states, the number, or size of the basis set is also tested for completeness. I call this "exploring the space". This flexibility lays a good foundation for future work. Computations performed here can be a foundation for more complicated calculations.

A third question, the answer to which I felt necessary to validate the work, was *how do the energies calculated by HF compare to spectroscopic experiments*? The answer to this question resulted in a side project, to couple the orbital and spin angular momentum of many configurational state functions. Not as trivial a problem as presented in introductory texts [6][7], this required expressing a completely anti-symmetric coupled L and S state in terms of the uncoupled l, m and s, m_s states. For many electrons this becomes tedious and an algorithm to account for all cases had to be formed. The end result is a configuration interaction comparison to spectroscopic data that fits nicely.

Finally, the immersion into an electron gas could be implemented. The idea is to couple the free atom to a jellium background. Metals have many free electrons but maintain a net neutral charge. To achieve this a static uniform background positive charge will offset the free electron negative charge. Observing how the atoms electronic states shift while increasing the coupling with the free electrons will explain the effects of an impurity atom in a metal. A brief exploration into spreading out the basis states attempted to simulate the effects of an immersion. This didn't increase the degrees of freedom of the system as it doesn't actually couple any bound states to any other states. As a consequence, it simply increased the total energy. To successfully lower the energy, state space had to be increased. Unfortunately HF doesn't take kindly to large state

space, as the computation time increases like M^4, where M is the number of basis states. The method must account for interactions of a set of free electron states on a set of bound electron states, without simply adding the spaces together.

A perturbation technique posed by Löwdin [8] presented a solution to the problem of coupling two slightly interacting systems. The method treats the influence of the free electrons as a small perturbation on the bound electrons and folds that interaction back into the space of just the bound electrons. This technique is applied under the iterative context of HF and the final converged atom is influenced by the electron gas. Through multiple function expansions the immersed Fock matrix is derived. A Bessel function expansion [9] [10] limits the maximum density of free electrons that can be solved. For those densities in which the system can be solved, the feature of lowering the total energy of an atom immersed in an electron gas is shown. The model even appears to distinguish between larger energy advantages to immersion, for those elements that are metallic. To forecast what the model would predict for greater electron densities, the immersion dependency on the change in total energy is extrapolated.

The work presented here not only produces results for comparison but also sets the stage for further research. A more complete set of heavier free atoms modelled, with their spectroscopic comparisons, could warrant interest. Improving the immersions to include larger densities and generating more a thorough list of converged atoms would also be of interest. In reality this work is the launching point for many, more complicated systems, from field dependencies to impurity clusters, to full band structure calculations of all these systems. We have built a fundamental tool to be used to model sophisticated many-body systems.

2. HARTREE-FOCK THEORY

The techniques shown in this work are based on those posed by D. Hartree and V. Fock [11][12][13]. The methods approximately solve the many-body Schrödinger equation. All derivations use the natural Hartree atomic units where $e = m_e = \hbar = 1/4\pi\epsilon_0 = 1$. The unit for energy, the hartree, equals two Rydbergs. Lengths are measured in units of bohr radii.

2.1 The Many-Body Problem

Solving the problem of multiple bodies, mutually interacting, is of great interest in physics. The problem can be explicitly solved for one and two particle systems. For systems of three particles and greater (many), no closed form analytical solution exists. The best hope is to make appropriate assumptions and approximations to come near a correct solution. Different techniques work well in approximating a given problem. Determining which problem solving scheme should be used depends on the nature of the question.

Electronic interactions arise from different forces than gravitationally attracted celestial bodies, but the many-body problem persists on all scales. At the atomic scale, the equation developed by Schrödinger to describe quantum phenomena must be satisfied. This work models the atomic world and at the core is a method to approximate solutions to the many-body Schrödinger equation.

2.1.1 Free Electron Gas

Before modelling particle systems it helps to describe a single particle. Newton described macroscopic bodies like baseballs and planets but for accurate descriptions of

microscopic bodies on the atomic scale, quantum descriptions are required. General static quantum systems satisfy the time independent Schrödinger equation 2.1.

$$\widehat{H}\Psi(\vec{r}) = E\Psi(\vec{r}) \tag{2.1}$$

$\widehat{H}$ is the *Hamiltonian operator* which performs operations on a wave function $\Psi(\vec{r})$, to extract information about the energy of a system. The connection to experiment is that this wave function, when multiplied by its complex conjugate $\Psi^*(\vec{r})\Psi(\vec{r})$, is equal to the probability amplitude of finding the particle. This probability amplitude must satisfy:

$$\int \Psi^*(\vec{r})\Psi(\vec{r})d\vec{r} = 1 \tag{2.2}$$

This says you have a *one hundred percent chance* of finding the particle, somewhere in space.

Since the potential energy of a free particle is zero the only term in the Hamiltonian is the kinetic energy, $\widehat{T}$.

$$\widehat{H} = \widehat{T} = -\frac{\overrightarrow{\nabla}^2}{2m} \tag{2.3}$$

Exact solutions to the problem of a free particle with kinetic energy exist [6]. The functions that satisfy this problem are plane waves, and the energies associated with these plane waves are those of a free particle.

$$\Psi_k(\vec{r}) = \frac{1}{\sqrt{V}}e^{\pm i\vec{k}\cdot\vec{r}}, \quad E_k = \frac{\hbar^2 k^2}{2m} \tag{2.4}$$

Finite volumes have a discrete set of allowed k wave vectors due to finite space requiring the solutions go to zero at the boundary. As the volume gets larger the k values become more continuous.

2.1.2 Hydrogen Atom

The least complicated system involving the interaction between bodies is that of two particles attracted to each other. This can be thought of as a single particle attracted

to a central potential created by a second particle. This is the case for the hydrogen atom. Since the gravitational force between an electron and a proton is 39 orders of magnitude smaller than the Coulomb force, gravity will be neglected. For macroscopic bodies with no net charge, gravity is the dominant force, but the shape of the gravitational potential is the same as that of the Coulomb potential. The mass of a proton is roughly 1836 times that of an electron. For this reason the motion of nuclei can be neglected and a static coordinate system can be used with the origin at the nucleus. With these assumptions the problem is that of an electron in a central Coulomb potential created by a static nucleus. The nuclear Coulomb potential operator $\widehat{V}_n$, is negative the inverse of the distance between the two charges with e^2=1.

$$\widehat{V}_n = -\frac{1}{|\overrightarrow{r}|} \tag{2.5}$$

With the kinetic energy operator for a single particle and the potential operator above, the Schrödinger equation for the simple hydrogen atom can be written as follows.

$$\widehat{H}\Psi(\vec{r}) = (\widehat{T} + \widehat{V}_n)\Psi(\vec{r}) = -\frac{\overrightarrow{\nabla}^2}{2m}\Psi(\vec{r}) - \frac{Z}{r}\Psi(\vec{r}) = E\Psi(\vec{r}) \tag{2.6}$$

The discrete set of solutions to this equation are exact and can be readily solved [13]. The normalized wave functions contain information about the probability of where to find the electron under the influence of the central Coulomb potential.

$$\Psi_{nlm}(r,\theta,\phi) = \sqrt{\left(\frac{2}{na_0}\right)^3 \frac{(n-l-1)!}{2n(n+l)!}} e^{-\frac{\rho}{2}} \rho^l L_{n-l-1}^{2l+1}(\rho) \cdot Y_{lm}(\theta,\phi) \tag{2.7}$$

In the above equation $\rho = \frac{2r}{na_0}$ and a_0 is the Bohr radius equal to $\frac{4\pi\epsilon_0\hbar^2}{m_e e^2}$. The functions that describe the probability density in the radial direction are the generalized Laguerre polynomials $L_{n-l-1}^{2l+1}(\rho)$. Angular information about an electron in a hydrogen atom comes from the spherical harmonics $Y_{lm}(\theta,\phi)$. The discrete solutions are identified by a set of integers called the quantum numbers. n is the principal quantum number, l is the angular momentum quantum number and m is the magnetic quantum number. The allowed values of the hydrogen quantum numbers are: $n = 1, 2, 3...\infty$; $\quad l = 0, 1, ..., n-1$; $\quad m = -l, ..., l$.

2.1.3 Many Electron Atoms

One and two particle systems are important because they constitute the only systems that are analytically solvable. This is important but most interesting problems involve more than two bodies. For many-body systems there is no closed form analytical solution. If the assumptions of the hydrogen atom persist and other electrons are added, new operators arise in the equations. The Coulomb repulsion between the i^{th} and j^{th} electron has the following associated electron-electron Coulomb operator.

$$\widehat{V}_{ee} = \frac{1}{|\overrightarrow{r_i} - \overrightarrow{r_j}|} \tag{2.8}$$

Writing down the Schrödinger equation for each particle yields a problem that no math has solved: a coupled set of second order differential equations. Coupling occurs through the electron-electron Coulomb potential. The consequence of this coupling is that the Coulomb energy of the i^{th} electron depends on the position of the j^{th} electron and *vice versa*. Consider the many-body Schrödinger equation with the assumption of a total wave function comprised of separable single particle states φ [13].

$$\left(\widehat{H}_i + \widehat{H}_j + \frac{1}{|\overrightarrow{r}_i - \overrightarrow{r}_j|}\right)\varphi_i(\overrightarrow{r}_i)\varphi_j(\overrightarrow{r}_j) = E\varphi_i(\overrightarrow{r}_i)\varphi_j(\overrightarrow{r}_j) \tag{2.9}$$

The equation for the energy of the i^{th} particle would be:

$$\widehat{H}_i\varphi_i(\overrightarrow{r}_i) + v_j\varphi_i(\overrightarrow{r}_i) = E\varphi_i(\overrightarrow{r}_i) - \left(\int \varphi_j(\overrightarrow{r}_j)H_j\varphi_j(\overrightarrow{r}_j)\right)\varphi_i(\overrightarrow{r}_i) \tag{2.10}$$

with

$$v_j = \int \frac{|\varphi_j(r_j)|^2}{|\overrightarrow{r}_i - \overrightarrow{r}_j|} d\overrightarrow{r}_j. \tag{2.11}$$

The equation for the j^{th} particle would be the same with each index changed. These are hopelessly coupled equations, through the Coulomb potential v_j. Closed form analytical solutions to these equations do not exist. The best hope is to make approximations and then solve the system numerically. All many-body problems are solved approximately.

The precision of the solutions then depends heavily on how your assumptions and approximations are chosen. This point is especially important with regards to computational time and desired precision.

2.2 Basic Theory: Hartree-Fock

The theory used to approximate the many-body electron problem was first developed by Douglas Hartree. The technique was posed as a way to find many-body wave functions by solving N-coupled equations for N-spin orbitals. John Slater [14] and Vladimir Fock independently realized the method didn't account for the antisymmetric nature of fermions and the exchange energy associated with them. This method, coined Hartree-Fock theory (HF), could then be used to solve quantum systems of electrons. Systems that can take advantage of approximate solutions to the electronic Schrödinger equation include nuclear, atomic, molecular and solid state. In all of these systems the basic principles behind Hartree-Fock hold true but different assumptions and approximations may be made.

2.2.1 Assumptions, Approximations and the Fock operator

To set the ground work needed to derive the Hartree-Fock equations a number of assumptions and approximations must be made [13]. These are specific to the problem of a single, stationary, non-relativistic atom.

Born-Oppenheimer approximation - The total wave function can be separated into two parts.

$$\Psi_{total} = \psi_{electronic} \otimes \psi_{nuclear} \tag{2.12}$$

This can be justified because of the mass mismatch between the electrons and nuclei. The motion of the nuclei have little dependence on that of the electrons. Since this work only models single atoms, mutual interaction of nuclei, is not needed. A result of this assumption is zero kinetic energy of the nucleus.

gravity - The large disparity between Coulomb and gravitational forces justifies ignoring all gravitational effects.

non-relativistic - The atoms modelled are light enough (Z<36) to ignore relativistic effects in the momentum operator. (reference something)

central potential - The nuclear potential is assumed to be a central potential. This fact justifies the use of spherical harmonics for the angular portion of the wave functions. Interactions with other electrons will cause the overall potential to not be central.

spin orbitals - The spin orbital $\psi_i(\overrightarrow{r_i};\sigma_i)$ represents the total state of an electron. Each spin orbital is assumed to be orthogonal and can be separated into a spacial function $\phi_i(\overrightarrow{r_i})$ and a spin state $\chi(\sigma_i)$.

$$\psi_i(\overrightarrow{r}_i;\sigma_i) = \phi_i(\overrightarrow{r_i}) \otimes \chi(\sigma_i) \tag{2.13}$$

basis set - Each spin orbital is expanded into a set of wave functions called the basis set. The variational method is used to minimize the energy and form a generalized eigenvalue problem. Solutions to this problem require a linear combination of finite, not necessarily orthogonal, basis sets. The features of the basis set will be varied to explore its precision.

spin dependence - Since relativistic effects are ignored the electron spin is added *ad hoc*. Effects that are spin-dependent such as spin-orbit or spin-spin coupling must be added as corrections after the electronic Schrödinger equations have been solved.

Fermi-Dirac statistics - The total wave function must always be antisymmetric under the exchange of particles. Energy eigenfunctions are then assumed to be determined through a single Slater determinant of single particle wave functions.

electron correlation - The correlation energy is the difference in energy between the exact solutions to the non-relativistic many-body Schrödinger equation and that of HF.

$$E_{correlation} = E_{exact} - E_{HF} \tag{2.14}$$

The interaction of electronic ensembles is only taken into account ad-hoc. This is one of the shortfalls of standard Hartree-Fock theory.

electron exchange - When using the Slater determinant to anti-symmetrize the total wave function, electron exchange effects are completely accounted for. This is one of the benefits of Hartree-Fock theory.

With these assumptions the total Hamiltonian operator ($\widehat{H}$) is comprised of a kinetic ($\widehat{T}$), a nuclear Coulomb ($\widehat{V}_n$) and an e-e Coulomb ($\widehat{V}_{ee}$) operator for every electron in the system.

$$\widehat{H} = \widehat{T} + \widehat{V}_n + \widehat{V}_{ee} = -\sum_{i=1}^{N} \frac{\overrightarrow{\nabla}_i^2}{2m} - \sum_{i=1}^{N} \frac{Z}{r_i} + \sum_{i=1}^{N} \sum_{j>i}^{N} \frac{1}{|\overrightarrow{r}_i - \overrightarrow{r}_j|} \tag{2.15}$$

N is the total number of electrons. The e-e interaction sums over every particle's interaction with every other particle.

2.2.2 Total Fermion Wave Function: Slater Determinant

For a single particle, or a electron in a central potential created by static proton, a single wave function is all that is required to describe the system. It would seem reasonable then to form the total wave function of a system of particles as a product of individual wave functions.

$$\Psi = \prod_{\alpha=1}^{N} \psi_\alpha(\overrightarrow{r}_\alpha; \sigma_\alpha) = \psi_1(\overrightarrow{r}_1; \sigma_1)\psi_2(\overrightarrow{r}_2; \sigma_2)...\psi_N(\overrightarrow{r}_N; \sigma_N) \tag{2.16}$$

Here σ_α is a spin index for the α^{th} particle. The problem with this assumption is that electrons are among a class of particles called fermions. Two fermions cannot be in the same state and the same location, at the same time. This means any wave function describing a system of such particles must be antisymmetric under exchange of particles. To satisfy this requirement Fock and Slater implemented a determinant on the location

of the particles [14].

$$\Psi = \frac{1}{\sqrt{N!}} \begin{vmatrix} \psi_1(\overrightarrow{r}_1;\sigma_1) & \psi_1(\overrightarrow{r}_2;\sigma_2) & \dots & \psi_1(\overrightarrow{r}_N;\sigma_N) \\ \psi_2(\overrightarrow{r}_1;\sigma_1) & \psi_2(\overrightarrow{r}_2;\sigma_2) & \dots & \psi_2(\overrightarrow{r}_N;\sigma_N) \\ \vdots & \vdots & \ddots & \vdots \\ \psi_N(\overrightarrow{r}_1;\sigma_1) & \psi_N(\overrightarrow{r}_2;\sigma_2) & \dots & \psi_N(\overrightarrow{r}_N;\sigma_N) \end{vmatrix} \tag{2.17}$$

Here the $\frac{1}{\sqrt{N!}}$ is a normalization factor due to the increased number of wave functions. Applying this procedure ensures Ψ will be antisymmetric under exchange. A more convenient notation for the total wave function uses the antisymmetrizing operator $\widehat{A}$.

$$\Psi = \widehat{A}[\psi_1(\overrightarrow{r}_1;\sigma_1)\psi_2(\overrightarrow{r}_2;\sigma_2)\dots\psi_N(\overrightarrow{r}_N;\sigma_N)] = \widehat{A}\prod_{\alpha=1}^{N}\psi_\alpha(\overrightarrow{r}_\alpha;\sigma_\alpha) \tag{2.18}$$

with,

$$\widehat{A} = \frac{1}{\sqrt{N!}}\sum_p (-1)^p \widehat{P} = \frac{1}{\sqrt{N!}}\left[1 - \sum_{ij}\widehat{P}_{ij} + \sum \widehat{P}_{ijk} - \cdots\right] \tag{2.19}$$

where $\widehat{P}$ is the permutation operator. $\widehat{P}_{ij}$ permutes the coordinates of electron i and electron j. If an even number of permutations occurs the term is positive and if odd, the term is negative. The total energy of a system of fermions can then be determined using the Schrödinger equation.

$$\varepsilon = \sum_p (-1)^p \left\langle \prod_{\alpha=1}^{N}\psi_\alpha(\overrightarrow{r}_\alpha;\sigma_\alpha)\middle|\widehat{H}\middle|\widehat{P}\prod_{\beta=1}^{N}\psi_\beta(\overrightarrow{r}_\beta;\sigma_\beta)\right\rangle \tag{2.20}$$

2.2.3 Single Particle Contributions

When using a properly anti-symmetrized wave function a large number of combinations of terms arise. The contribution to the total energy from the kinetic T, and nuclear Coulomb V_{NE}, energies would appear to have many combinations.

$$(T + V_{NE}) = \sum_p (-1)^p \left\langle \prod_{\alpha=1}^{N}\psi_\alpha(\overrightarrow{r}_\alpha;\sigma_\alpha)\middle| - \sum_{i=1}^{N}\frac{\overrightarrow{\nabla}_i^2}{2m} - \sum_{i=1}^{N}\frac{Z}{r_i}\middle|\widehat{P}\prod_{\beta=1}^{N}\psi_\beta(\overrightarrow{r}_\beta;\sigma_\beta)\right\rangle \tag{2.21}$$

Since each spin orbital is orthogonal, most combinations are zero. What survives is the term in which each combination of spin orbitals on each side of the operator are the same. This can then be written as a simple sum over single particle states.

$$(T + V_{NE}) = \sum_{i=1}^{N} \left\langle \psi_i(\overrightarrow{r};\sigma_i) \right| -\frac{\overrightarrow{\nabla}^2}{2m} - \frac{Z}{r} \left| \psi_i(\overrightarrow{r};\sigma_i) \right\rangle \tag{2.22}$$

The kinetic and nuclear Coulomb energy of a particular electron should not have direct dependence on the other electrons. Since the only remaining terms are those with the same spin orbitals the condition of like spin is satisfied.

2.2.4 Two Particle Contributions

The anti-symmetrizing of the total wave function has a more complex consequence in regards to the *e-e* Coulomb interactions. The *e-e* operator is defined as the inverse distance between two charged particles. This inherently involves more than one particle.

$$V_{ee} = \sum_{p} (-1)^p \left\langle \prod_{\alpha=1}^{N} \psi_\alpha(\overrightarrow{r}_\alpha;\sigma_\alpha) \right| \sum_{i=1}^{N} \sum_{j>1}^{N} \frac{1}{r_{ij}} \left| \widehat{P} \prod_{\beta=1}^{N} \psi_\beta(\overrightarrow{r}_\beta;\sigma_\beta) \right\rangle \tag{2.23}$$

The number of combinations that remain is N times as many as the number of single particle terms, where N is the total number of particles. Two of the spin orbitals in the product are operated on with $\frac{1}{|\overrightarrow{r}_i - \overrightarrow{r}_j|}$, which has the same value when the coordinates are switched. What survives are those integrals involving both the spin orbitals that have been operated on and a set of integrals where those orbitals have switched coordinates. The first is called the direct *e-e* Coulomb energy.

$$V_{ee}^{d} = \sum_{i=1}^{N} \sum_{j>i}^{N} \left\langle \psi_i(\overrightarrow{r}_1;\sigma_i)\psi_j(\overrightarrow{r}_2;\sigma_j) \right| \frac{1}{r_{12}} \left| \psi_j(\overrightarrow{r}_2;\sigma_j)\psi_i(\overrightarrow{r}_1;\sigma_i) \right\rangle \tag{2.24}$$

The second differs by a minus sign and a swapping of coordinates between two spin orbital states. This is called the exchange *e-e* Coulomb energy.

$$V_{ee}^{ex} = -\sum_{i=1}^{N} \sum_{j>i}^{N} \left\langle \psi_i(\overrightarrow{r}_1;\sigma_i)\psi_j(\overrightarrow{r}_2;\sigma_j) \right| \frac{1}{r_{12}} \left| \psi_j(\overrightarrow{r}_1;\sigma_j)\psi_i(\overrightarrow{r}_2;\sigma_i) \right\rangle \tag{2.25}$$

The direct term can be thought of as the regular Coulomb interaction between two electrons. It is positive and counters an electron's affinity to being bound to a nucleus while other electrons are also bound. The exchange energy is negative and aids in lowering the total energy of the system. This exchange effect can be justified by the fact that if two electrons have the same spin, there is a non-zero probability that they can switch states. A system will not switch states unless the outcome lowers the total energy, so the effect of exchange must lower the energy. This exchange energy is at most half the direct Coulomb energy but usually much less. Hartree-Fock takes into account the effect of exchange completely by fully anti-symmetrizing the total wave function.

As for the spin of an electron, the direct term already satisfies the condition of like spins. The number of non-zero exchange terms is more limited due to the condition that $\sigma_i = \sigma_j$. The delta function $\delta_{\sigma_i\sigma_j}$ from the spin of each orbital means $|V_{ee}^{d}| > |V_{ee}^{ex}|$. In integral form the expectation value of the Hamiltonian, in a completely anti-symmetrized state is [15]

$$\langle\Psi|\widehat{H}|\Psi\rangle = \sum_{i=1}^{N}\int d\overrightarrow{r}\Big[-\phi_i^*(\overrightarrow{r})\frac{\overrightarrow{\nabla}^2}{2m}\phi_i(\overrightarrow{r}) - \frac{Z}{r}|\phi_i(\overrightarrow{r})|^2\Big] + \sum_{i=1}^{N}\sum_{j>i}^{N}\int\int d\overrightarrow{r}_1 d\overrightarrow{r}_2 \frac{1}{r_{12}}\Big[|\phi_i(\overrightarrow{r}_1)|^2|\phi_j(\overrightarrow{r}_1)|^2 - \phi_i^*(\overrightarrow{r}_1)\phi_j^*(\overrightarrow{r}_2)\phi_j(\overrightarrow{r}_1)\phi_i(\overrightarrow{r}_2)\delta_{\sigma_i\sigma_j}\Big] \tag{2.26}$$

2.2.5 Variational Principle and the Schrödinger Equation

To make the expectation value equal to an extremum of the energy and the Fock equations, variations will be made to the wave functions [13][11]. Suppose a functional is defined in terms of the expectation value of the Hamiltonian and is subject to the constraint $\langle\Psi|\Psi\rangle = 1$. Each of these equalities will hold true.

$$F_H\{\Psi\} = \langle\Psi|\widehat{H}|\Psi\rangle = \frac{\langle\Psi|\widehat{H}|\Psi\rangle}{\langle\Psi|\Psi\rangle} \tag{2.27}$$

Extremum of $F_H\{\Psi\}$ will be from the extremum of Ψ. The easiest proof is to assume $\langle\Psi|$ and $|\Psi\rangle$ are independent functions. Setting the variation in $F_H\{\Psi\}$ with respect to $\langle\Psi|$ to zero is the condition for finding extremum. When this is done it is seen that this also satisfies the Schrödinger equation.

$$\frac{\partial}{\partial\langle\Psi|}F_H\{\Psi\} = \frac{\partial}{\partial\langle\Psi|}\frac{\langle\Psi|\widehat{H}|\Psi\rangle}{\langle\Psi|\Psi\rangle} = \frac{\widehat{H}|\Psi\rangle}{\langle\Psi|\Psi\rangle} - |\Psi\rangle\frac{\langle\Psi|\widehat{H}|\Psi\rangle}{\langle\Psi|\Psi\rangle^2} = 0 \tag{2.28}$$

$$\widehat{H}|\Psi\rangle = \varepsilon|\Psi\rangle, \quad with \quad \varepsilon = \frac{\langle\Psi|\widehat{H}|\Psi\rangle}{\langle\Psi|\Psi\rangle} \tag{2.29}$$

This shows that the variational procedure applied to the expectation of of the Fock operator, with a properly anti-symmetrized wave function, is equivalent in form to the Schrödinger equation. The energy that is obtained is then an extremum of the system.

2.2.6 Hartree-Fock Equations

The Hamiltonian is considered to be Hermitian so that ε is real and therefore a state in which $\widehat{H}$ is diagonal must exist. Finally this brings us to the Hartree-Fock equation for the i^{th} particle.

$$\widehat{F}_i\phi_i(\overrightarrow{r}) = -\frac{\nabla^2}{2m}\phi_i(\overrightarrow{r}) - \frac{Z}{r}\phi_i(\overrightarrow{r}) + \sum_{j=1}^{N}\int d\overrightarrow{r}'\frac{\phi_j^*(\overrightarrow{r}')\phi_j(\overrightarrow{r}')}{|\overrightarrow{r} - \overrightarrow{r}'|}\phi_i(\overrightarrow{r}) \tag{2.30}$$

$$-\sum_{j=1}^{N}\int d\overrightarrow{r}'\frac{\phi_j^*(\overrightarrow{r}')\phi_j(\overrightarrow{r})}{|\overrightarrow{r} - \overrightarrow{r}'|}\phi_i(\overrightarrow{r}')\delta_{\sigma_i\sigma_j} = \varepsilon_i\phi_i(\overrightarrow{r})$$

The Hartree-Fock equations thus form a set of pseudo-eigenvalue equations. They are a non-linear set of coupled integro-differential equations. A specific spin orbital cannot be determined until all other orbitals are known. In general the method to finding the lowest energy is iterative. Make a guess of the spin orbitals, calculate the energy, improve the guess and repeat. Once a guess yields the same energy back as the previous the orbitals are said to constitute a *Self-Consistent Field* (SCF). The energy can then be calculated from this SCF and the solution can be checked for validity.

2.3 Basis State Expansion

Until this point each spin orbital has not been defined and has been considered a single function. If the best function were known this approach would be sufficient. Since each spin orbital is not known they will be expanded into a set of known basis functions.

$$\phi_i(\overrightarrow{r};\sigma_i) = \sum_{\beta=1}^{M} c_{i\beta}\varphi_\beta(\overrightarrow{r};\sigma_i) \tag{2.31}$$

Here M is the maximum number of basis states β. In theory increasing the number of basis states should increase the degrees of freedom of the problem and could lower the energy. The effect of this will be explored due to large basis sets costing more computational time.

The Hartree-Fock equation for a spin orbital now expands to the following.

$$\begin{aligned}\varepsilon_i \sum_{\beta}^{M} c_{i\beta}\varphi_\beta(\overrightarrow{r}) &= \Big[-\frac{\nabla^2}{2m} - \frac{Z}{r}\Big]\sum_{\beta}^{M} c_{i\beta}\varphi_\beta(\overrightarrow{r}) \\ &+ \sum_{j=1}^{N}\sum_{\gamma\varrho}^{M} c^*_{j\gamma}c_{j\varrho}\int d\overrightarrow{r}\,'\frac{\varphi^*_\gamma(\overrightarrow{r}\,')\varphi_\varrho(\overrightarrow{r}\,')}{|\overrightarrow{r}-\overrightarrow{r}\,'|}\sum_{\beta}^{M} c_{i\beta}\varphi_\beta(\overrightarrow{r}) \\ -\sum_{j=1}^{N}\sum_{\gamma\varrho}^{M} c^*_{j\gamma}c_{j\varrho}\int d\overrightarrow{r}\,'\frac{\varphi^*_\gamma(\overrightarrow{r}\,')\varphi_\varrho(\overrightarrow{r})}{|\overrightarrow{r}-\overrightarrow{r}\,'|}\sum_{\beta}^{M} c_{i\beta}\varphi_\beta(\overrightarrow{r}\,') &= \widehat{F}_i\sum_{\beta}^{M} c_{i\beta}\varphi_\beta(\overrightarrow{r})\end{aligned} \tag{2.32}$$

This is the set of equations used to solve the system. Often orthogonal basis states are used, but that is not the case in this work. The angular portion of each basis state will be a spherical harmonic that requires like l and m quantum numbers. Small overlaps can be found between unlike n quantum numbers with the non-orthogonal radial basis states. When non-orthogonal sets are used, solutions are found using the techniques for a generalized eigenvalue problem.

$$\widehat{F}_i\sum_{\beta}^{M} c_{i\beta}\varphi_\beta(\overrightarrow{r}) = \varepsilon_i\sum_{\beta}^{M} c_{i\beta}\varphi_\beta(\overrightarrow{r}) \tag{2.33}$$

The matrix notation written below includes all of the spin orbitals.

$$\mathbb{FC} = \mathbb{SC}\varepsilon \tag{2.34}$$

$\mathbb{F}$ is the Fock matrix which contains all of the interaction energy terms, $\mathbb{S}$ is the overlap matrix of the α and β basis states and $\mathbb{C}$ is the coefficient matrix that contains the information about how much each particle is projected onto a particular basis state.

$$F_{\alpha\beta} = \langle\varphi_\alpha|\widehat{F}|\varphi_\beta\rangle, \quad and \quad S_{\alpha\beta} = \langle\varphi_\alpha|\varphi_\beta\rangle \tag{2.35}$$

The system is converged when the change in the spin orbital projections are very small. In practice what constitutes small enough depends on the desired precision. The choice of basis set is tremendously important with regards to convergence time and the value of the converged total energy. Along with this the basis can have an effect on how smooth the procedure converges and to what converged precision. It is for these reasons many basis sets should be explored.

The choice of basis sets is, in principle, arbitrary. This does not mean a wise choice is not beneficial. Atoms are, in general, a cloud of electron probability decreasing as you move away from their center. For this reason using a set functions that consist of an ever increasing power of r to model the probability density would not be the wisest choice. The worse the choice of basis set, the more terms are required to get precise convergence. The computation time runs like M^4 so increasing the basis set is not desirable.

One reasonable choice of basis set could be the states of the hydrogen atom, Eq. (2.7). Generally, the heavier the atom the less its electron's wave function resembles that of the hydrogen atom. Another common basis set that is used in Hartree-Fock theory was posed by Slater[14]. Here are the radial functions that are called Slater type orbitals.

$$R_n(r) = Nr^{n-1}e^{-Çr} \quad where \quad N = (2Ç)^n\sqrt{\frac{2Ç}{(2n)!}} \tag{2.36}$$

In this equation n is a number comparable to the principal quantum number and N is the normalization constant from enforcing Eq. 2.2. Ç is a damping constant that Slater envisioned representing the amount of Coulomb *shielding* the core electrons produced between outer shell electrons and the nucleus. Slater-type orbitals commonly use spherical harmonics for the angular wave function basis set.

2.3.1 Radial Wave Functions

One shortcoming of Hartree Fock theory is the large computational times required for a large number of basis states. The computer must perform many integrals and generate the matrix terms of a Hamiltonian. A goal of this work is to show that by using a basis set consisting of previously converged Density Functional Theory (DFT) states, the number of basis states required in HF is minimized. The DFT program, that is used to solve the ground state density of a free atom, was created by Dr. Henri Jansen. The program allows any electron occupation to be defined and the ground state wave function for each orbital to be generated. The DFT program is spherically symmetric and thus only radial wave functions can be determined. Each spin basis set will be identical and so all spin dependence will be accounted for in the context of Hartree-Fock Theory.

2.3.1.1 Density Functional Theory

Hohenberg and Kohn posed the idea that the potential of a system, up to an overall constant, should be dependent only on the electron density of the ground state [16][17]. This potential includes all of the interaction potentials into one. It is assumed that all of the information of the many-body wave function is encased in this electron density.

$$n(\overrightarrow{r}) = \sum_{i=1}^{N} |\Psi_i(\overrightarrow{r})|^2 \tag{2.37}$$

Here the electron density $n(\overrightarrow{r})$, is a sum over spin orbital wave functions.

The potential of the ground state is unique to a particular electron density. To prove this, assume there are two Hamiltonians that come from two potentials, $\mathcal{H}_1$ and $\mathcal{H}_2$, that yield the same ground state density. The ground state energy from $\mathcal{H}_1$ is produced from Ψ_1, so Ψ_2 is not the ground state of $\mathcal{H}_1$.

$$\varepsilon_1 = \langle \Psi_1 | \mathcal{H}_1 | \Psi_1 \rangle < \langle \Psi_2 | \mathcal{H}_1 | \Psi_2 \rangle \tag{2.38}$$

By adding and subtracting $\mathcal{H}_2$ to $\mathcal{H}_1$ the inequality in the above equation becomes

$$\varepsilon_1 < \langle \Psi_2 | \mathcal{H}_2 | \Psi_2 \rangle + \langle \Psi_2 | (\mathcal{H}_1 - \mathcal{H}_2) | \Psi_2 \rangle \tag{2.39}$$

The Hamiltonian of a system with the same number of electrons can only differ by their potentials and these potentials were said to be uniquely defined by the electron density.

$$\varepsilon_1 < \varepsilon_2 + \int d\overrightarrow{r}\, n(\overrightarrow{r})[\mathcal{U}_1(\overrightarrow{r}) - \mathcal{U}_2(\overrightarrow{r})] \tag{2.40}$$

The indices of each system could be swapped because they were both assumed to be from the same ground state density.

$$\varepsilon_2 < \varepsilon_1 + \int d\overrightarrow{r}\, n(\overrightarrow{r})[\mathcal{U}_2(\overrightarrow{r}) - \mathcal{U}_1(\overrightarrow{r})] \tag{2.41}$$

Adding Equation (2.40) and (2.41) yields an inequality that cannot be true.

$$\varepsilon_1 + \varepsilon_2 < \varepsilon_1 + \varepsilon_2 \tag{2.42}$$

Thus the ground state density and potential are unique to each other.

The non-degenerate ground state density $n(\overrightarrow{r})$ and potential $\upsilon(\overrightarrow{r})$ exist and are assumed. These are in principle impossible to know but in practice possible to approximate. The portions of the potential that cannot be accounted for exactly are the exchange υ_x and correlation υ_c potentials. A Local Density Approximation (LDA) uses an exchange-correlation potential based on the local change in energy as a function of density.

$$\upsilon([n]; \overrightarrow{r}) \equiv \frac{\delta E_{xc}[n]}{\delta n(\overrightarrow{r})}\bigg|_{n_o} = \epsilon_{xc}[n(\overrightarrow{r})] + n(\overrightarrow{r})\frac{\delta \epsilon_{xc}[n(\overrightarrow{r})]}{\delta n(\overrightarrow{r})} \tag{2.43}$$

Setting $\upsilon([n]; \overrightarrow{r})$ to zero requires the system move towards a minimum change in the functional $\delta\epsilon_{xc}[n(\overrightarrow{r})]$ with respect to the local density. The addition to the total electronic energy from the exchange-correlation potential can be calculated by the following integral.

$$E_{xc} = \int d\overrightarrow{r}\, n(\overrightarrow{r})\epsilon_{xc}[n(\overrightarrow{r})] \tag{2.44}$$

Basis states to be used in HF spin orbital expansions are generated by defining a desired electronic configuration in the DFT program. This DFT ground state densities can be found through iterative convergence. These converged DFT eigenstates densities are used for the radial basis states $R_{n,\ell}(r)$ in the HF approach. An example for a set of basis states generated for carbon is shown in Figure 2.1. Notice the similarity to the radial solutions of the hydrogen atom. The heavier the atom the further the electronic states match those of a hydrogen atom.

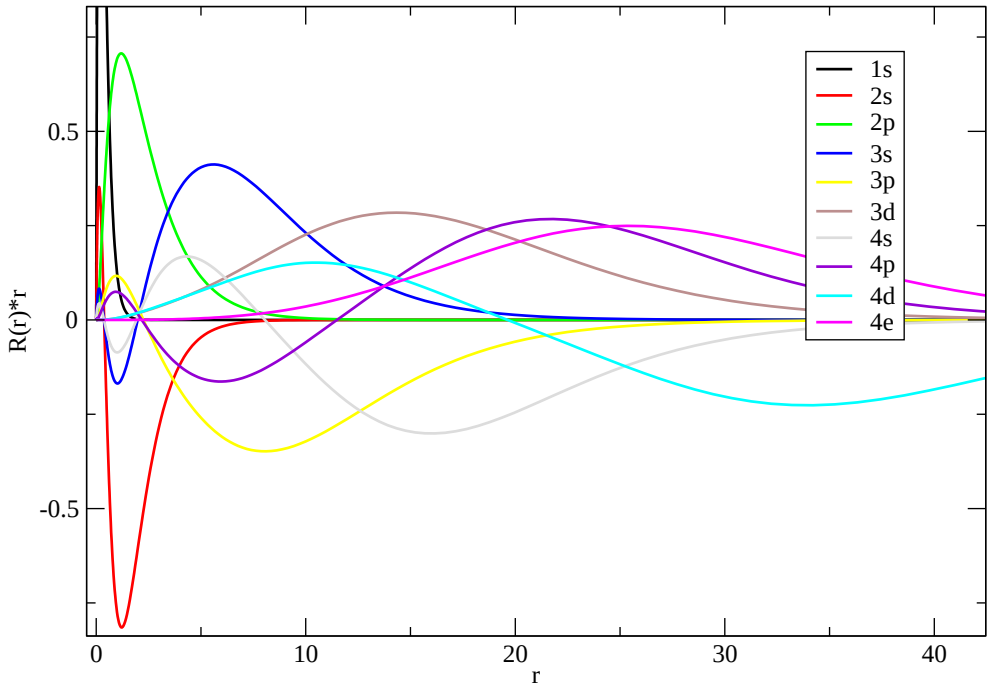

FIGURE 2.1: Example of converged DFT states used for the HF basis of carbon. Radial distances r, are measure in units of Bohr radii.

The number of particles present in the DFT program is arbitrary and has no integer requirement. To generate wave functions for virtual orbits, a fraction of an electron is excited into that state. This will not only generate a wave function for the virtual state, it

provides a way of generating different basis sets. The basis set above is for the minimum allowed fractionally excited occupation. This would be assumed to be the best basis set for a HF model of the ground state of an atom.

2.3.1.2 Electron Occupation

The larger fraction an electron is excited into a higher energy state, the more that state is expressed in all states. This feature will be explored in modelling ground and excited states. More accurate HF energies of excited states may be found from a basis set generated from a high fractional occupation into DFT excited states.

An example of the difference in the wave functions generated for various fractional occupations is plotted in Figure 2.2. These wave functions are for the n=3 virtual states of Carbon.

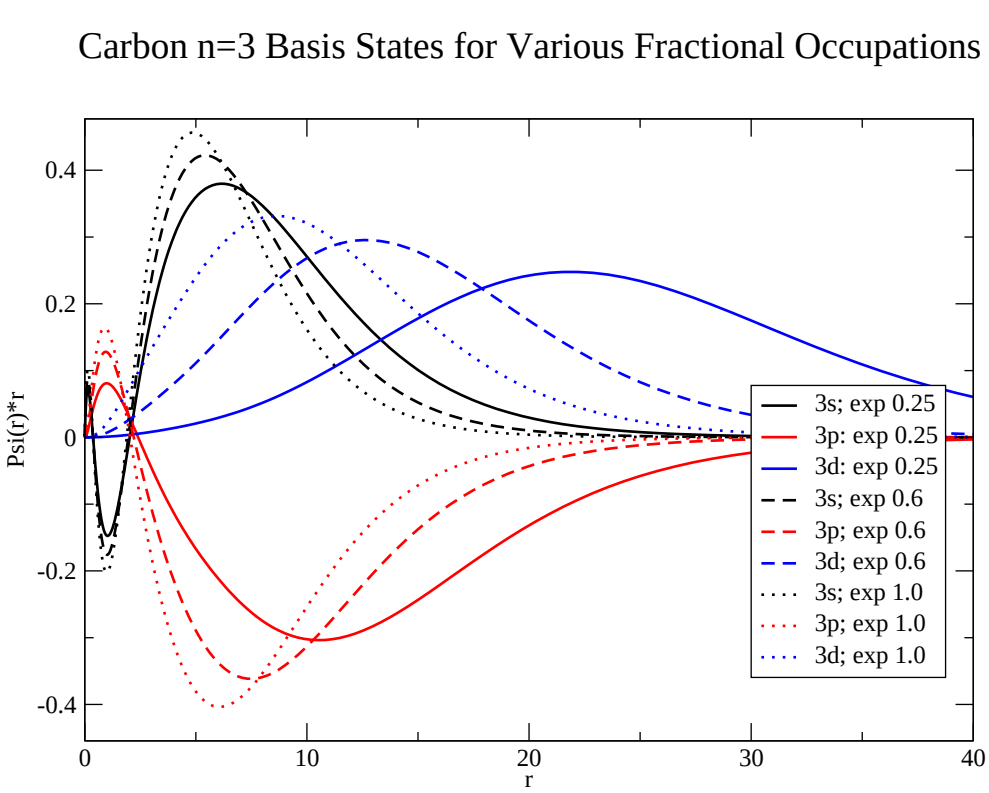

FIGURE 2.2: Carbon 3s, 3p and 3d basis states with different fractional occupations. The fraction is expressed by "exp 0.25".

As more of the charge is forced into a higher energy state the density of that state is pulled into the nucleus. The screening effect is reduced. As a result the smaller amount of charge in the lower energy state makes room for a smaller average excited state radius. The HF ground state for a given electron configuration will have an ideal location for the charge of the n=3 virtual states. This is why comparisons are done for ground state energies as a function of basis state fractional occupation.

2.3.2 Angular Wave Functions: Spherical Harmonics

In general electrons surrounding an atom are attracted to the central nucleus more than they are repelled by each other. The repulsion from the *e*-*e* Coulomb interaction

is not negligible but is still much less than the Coulomb attraction to the nucleus. Its then reasonable to use the angular solutions to a central potential problem for the angular basis of an electron bound to an atom. The basis sets angular wave functions will be the Spherical Harmonics (SH) which are solutions to the Laplace equation and the hydrogen atom (section 2.1.2).

$$Y_{\ell m}(\theta,\phi) \equiv \sqrt{\frac{2\ell+1}{4\pi}\frac{(\ell-m)!}{(\ell+m)!}} P_\ell^m(\cos\theta) e^{im\phi} \tag{2.45}$$

The functions are dependent on the magnitude and direction of an electrons angular momentum vector through the quantum numbers ℓ and m respectively. The $P_\ell^m(z)$ is an associated Legendre polynomial.

2.4 Numerical Implementation

Solving the Hartree Fock equations can only be done numerically. Each integral in the Fock matrix must be calculated for each combination of basis states. In practice each integral is stored in arrays that are then reused during the self consistent iterations. Once the complete Fock matrix has been generated from these arrays and the original coefficients guess, a singular value decomposition is done to fine the eigenvalues and eigenvectors. The new eigenvectors can be mixed with the original, which assigns new basis set coefficients for each spin orbital. Using the integrals stored in arrays and the new coefficients the process repeats until convergence. This process is at the core of all the work presented here.

2.4.1 Kinetic Energy

The kinetic energy terms in the Fock matrix, before they are expanded into a basis set, are only along the diagonal. The basis set chosen in this work is not completely orthogonal. For this reason terms involving states of unlike n but like l and m values are

not zero. The kinetic contribution to the Fock matrix is:

$$T_{\alpha\beta} = -\int \varphi_\alpha^*(\overrightarrow{r})\frac{\nabla^2}{2}\varphi_\beta(\overrightarrow{r})d\overrightarrow{r} \tag{2.46}$$

The Laplacian operating in spherical coordinates on φ can be expressed as follows.

$$\nabla^2\varphi(\overrightarrow{r}) = \nabla^2(R_{nl}(r)Y_{lm}(\theta,\phi)) = \left(\frac{d^2R_{nl}(r)}{dr^2} + \frac{2}{r}\frac{dR_{nl}(r)}{dr} - \frac{l(l+1)}{r^2}R_{nl}(r)\right)Y_{lm}(\theta,\phi) \tag{2.47}$$

The assumption that φ can be divided into two separate functions has been made. The radial portion is R_{nl} and the angular is the spherical harmonics Y_{lm}. The final kinetic energy term is now

$$T_{\alpha\beta} = \frac{1}{2}\int R^*_{n_\alpha l_\alpha}(r)\left(r^2\frac{d^2R_{n_\beta l_\beta}(r)}{dr^2} + 2r\frac{dR_{n_\beta l_\beta}(r)}{dr} - l(l+1)R_{n_\beta l_\beta}(r)\right)dr\ \delta_{l_\alpha l_\beta}\delta_{m_\alpha m_\beta} \tag{2.48}$$

2.4.2 Nuclear Coulomb Energy

The Coulomb attraction between the protons in the nucleus and the electrons is the source of the binding in an atom. The contribution to the Fock matrix from this negative energy is:

$$V^{NE}_{\alpha\beta} = -\int \varphi_\alpha^*(\overrightarrow{r})\frac{Z}{r}\varphi_\beta(\overrightarrow{r})d\overrightarrow{r} = -Z\int R^*_{n_\alpha l_\alpha}(r)R_{n_\beta l_\beta}(r)rdr\ \delta_{l_\alpha l_\beta}\delta_{m_\alpha m_\beta} \tag{2.49}$$

This simple term may lack luster but the central attraction of electrons is due to this interaction. Becoming an atom or forming a star or planet all rely on a central attraction similar to that above.

2.4.3 *e-e* Coulomb Energy

The most interesting terms in the Fock matrix are those that arise from the Coulomb interaction of electrons. The coupling amongst particle spin orbitals is from the $\frac{1}{|r-r'|}$ Coulomb potential that lies in these terms. The direct term looks like

$$V^d_{\alpha\beta} = \sum_{\gamma\varrho}^{M} c^*_{j\gamma}c_{j\varrho}\int\int d\overrightarrow{r}d\overrightarrow{r'}\varphi^*_\alpha(\overrightarrow{r})\frac{\varphi^*_\gamma(\overrightarrow{r'})\varphi_\varrho(\overrightarrow{r'})}{|\overrightarrow{r}-\overrightarrow{r}'|}\varphi_\beta(\overrightarrow{r}) \tag{2.50}$$

The Coulomb potential is the inverse of the absolute distance between two position vectors. This is inherently a three-dimensional problem. A natural solution to this problem is an expansion that separates the radial from the angular, spherical harmonic part [18].

$$\frac{1}{|\overrightarrow{r} - \overrightarrow{r'}|} = \sum_{l=0}^{\infty} \sum_{m=-l}^{l} \frac{4\pi}{2l+1} \frac{r_<^l}{r_>^{l+1}} Y_{lm}^*(\theta;\phi) Y_{lm}(\theta';\phi') \tag{2.51}$$

The radial integrals become:

$$\Lambda^d_{\alpha\gamma\varrho\beta} = \int\int R^*_{n_\alpha l_\alpha}(r) R^*_{n_\gamma l_\gamma}(r') \frac{r_<^l}{r_>^{l+1}} R_{n_\varrho l_\varrho}(r') R_{n_\beta l_\beta}(r) r^2 r'^2 dr dr' \tag{2.52}$$

The angular portion is now not as simple as an integral over two orthogonal spherical harmonics. Each angular term involves three spherical harmonics. These integrals show up often in many-body theory and are closely related to the Wigner 3j expressions [7].

$$\left\{ \begin{smallmatrix} l_\alpha^* & l & l_\beta \\ m_\alpha^* & m & m_\beta \end{smallmatrix} \right\} = \int\int Y^*_{l_\alpha m_\alpha}(\theta,\phi) Y_{lm}(\theta,\phi) Y_{l_\beta m_\beta}(\theta,\phi) sin(\theta) d\theta d\phi \tag{2.53}$$

Together this yields the contribution to the Fock matrix from the direct *e*-*e* Coulomb interaction.

$$V^d_{\alpha\beta} = \sum_{j=1}^{N} \sum_{\gamma\varrho}^{M} \sum_{l=0}^{\infty} \sum_{m=-l}^{l} c^*_{j\gamma} c_{j\varrho} \frac{4\pi}{2l+1} \Lambda^d_{\alpha\gamma\varrho\beta} \left\{ \begin{smallmatrix} l_\alpha^* & l & l_\beta \\ m_\alpha^* & m & m_\beta \end{smallmatrix} \right\} \left\{ \begin{smallmatrix} l_\gamma^* & l^* & l_\varrho \\ m_\gamma^* & m^* & m_\varrho \end{smallmatrix} \right\} \tag{2.54}$$

In practice the sums of γ and ϱ are over all of the basis states. The basis follows the rules of the quantum numbers of the hydrogen atom.

$$\sum_{\gamma\varrho}^{M} = \sum_{n_\gamma=1}^{\wp} \sum_{l_\gamma=0}^{n\gamma-1} \sum_{m_\gamma=-l_\gamma}^{l_\gamma} \sum_{n_\varrho=1}^{\wp} \sum_{l_\varrho=0}^{n_\varrho-1} \sum_{m_\varrho=-l_\varrho}^{l_\varrho}$$

This shows the reason Hartree-Fock is computationally taxing as the number of basis states goes up. Generating the direct and exchange Fock terms have *fifteen* nested loops, counting the *six* new loops from α and β.

One piece of good news, at least for the free atom, is the single basis set. Only a single radial integral array has to be generated and the effect of swapping coordinates for the exchange integral can be a swap of indices.

$$\Lambda^{ex}_{\alpha\gamma\varrho\beta} = \int\int R^*_{n_\alpha l_\alpha}(r) R^*_{n_\gamma l_\gamma}(r') \frac{r_<^l}{r_>^{l+1}} R_{n_\varrho l_\varrho}(r) R_{n_\beta l_\beta}(r') r^2 r'^2 dr dr' = \Lambda^d_{\alpha\gamma\beta\varrho} \tag{2.55}$$

This will not be possible when the basis states of the bound electrons are coupled with that of the free electrons in a gas. The basis set used for free electrons will be different from that used for bound electrons.

All together the contribution to the Fock matrix from the *e*-*e* Coulomb interaction is

$$V^d_{\alpha\beta} + V^{ex}_{\alpha\beta} = \sum_{j=1}^{N}\sum_{\gamma\varrho}^{M}\sum_{l=0}^{\infty}\sum_{m=-l}^{l} c^*_{j\gamma}c_{j\varrho}\frac{4\pi}{2l+1}$$

$$\left[\Lambda^d_{\alpha\gamma\varrho\beta}\begin{Bmatrix} l^*_\alpha & l & l_\beta \\ m^*_\alpha m & & m_\beta \end{Bmatrix}\begin{Bmatrix} l^*_\gamma & l^* & l_\varrho \\ m^*_\gamma m^* & & m_\varrho \end{Bmatrix} - \Lambda^{ex}_{\alpha\gamma\varrho\beta}\begin{Bmatrix} l^*_\alpha & l & l_\varrho \\ m^*_\alpha m & & m_\varrho \end{Bmatrix}\begin{Bmatrix} l^*_\gamma & l^* & l_\beta \\ m^*_\gamma m^* & & m_\beta \end{Bmatrix}\delta_{\sigma_i\sigma_j}\right] \tag{2.56}$$

The Fock matrix $\mathbb{F} \equiv F_{\alpha\beta} = T_{\alpha\beta} + V^{NE}_{\alpha\beta} + V^d_{\alpha\beta} + V^{ex}_{\alpha\beta}$ can now be generated.

2.4.4 Unrestricted Hartree-Fock

Now that the Fock matrix is known, the interaction of the spin can be accounted for. Two separate Fock matricies are made, one for each spin [12]. Each will be solved separately and when each spin orbital is assigned a new set of coefficients, the appropriate spin eigenvector will be chosen.

The sum over particles is first performed on the coefficients $c_{i\alpha}$. The resulting matrix $\mathbb{C}$ is a density matrix that holds the information about how much each particle is projected into each basis state.

$$C^{\uparrow}_{\alpha\beta} = \sum_{i=1}^{N_{up}} c_{i\alpha}c_{i\beta} \quad and \quad C^{\downarrow}_{\alpha\beta} = \sum_{i=N_{up}+1}^{N} c_{i\alpha}c_{i\beta} \tag{2.57}$$

The delineation between the two spin equations is from the exchange interaction. The spin-up Fock matrix is below and the spin requirement is applied through the $\mathbb{C}$'s.

$$F^{\uparrow}_{\alpha\beta} = T_{\alpha\beta} + V^{NE}_{\alpha\beta} + \sum_{\gamma\varrho}^{M}\sum_{l=0}^{\infty}\sum_{m=-l}^{l} c^*_{j\gamma}c_{j\varrho}\frac{4\pi}{2l+1}$$

$$\left[(\mathbf{C}^{\uparrow}_{\gamma\varrho} + C^{\downarrow}_{\gamma\varrho})\Lambda^d_{\alpha\gamma\varrho\beta}\begin{Bmatrix} l^*_\alpha & l & l_\beta \\ m^*_\alpha m & & m_\beta \end{Bmatrix}\begin{Bmatrix} l^*_\gamma & l^* & l_\varrho \\ m^*_\gamma m^* & & m_\varrho \end{Bmatrix} - C^{\uparrow}_{\gamma\varrho}\Lambda^{ex}_{\alpha\gamma\varrho\beta}\begin{Bmatrix} l^*_\alpha & l & l_\varrho \\ m^*_\alpha m & & m_\varrho \end{Bmatrix}\begin{Bmatrix} l^*_\gamma & l^* & l_\beta \\ m^*_\gamma m^* & & m_\beta \end{Bmatrix}\right] \tag{2.58}$$

The spin-down Fock matrix $F^{\downarrow}_{\alpha\beta}$ is the same except for a $C^{\downarrow}_{\alpha\beta}$ with the exchange integrals. The requirement of like spins decreases the effect of exchange. The separate Fock equations to solve are:

$$\mathbb{F}^{\uparrow}\mathbb{C}^{\uparrow} = \varepsilon^{\uparrow}\mathbb{S}\mathbb{C}^{\uparrow} \quad and \quad \mathbb{F}^{\downarrow}\mathbb{C}^{\downarrow} = \varepsilon^{\downarrow}\mathbb{S}\mathbb{C}^{\downarrow} \tag{2.59}$$

with,

$$S_{\alpha\beta} = \int R^{*}_{n_\alpha l_\alpha}(r) R_{n_\beta l_\beta}(r) r^2 dr \quad \delta_{l_\alpha l_\beta}\delta_{m_\alpha m_\beta} \tag{2.60}$$

Unrestricted Hartree-Fock (UHF) breaks spin symmetry and the degeneracies associated with those symmetries.

2.4.5 Generalized Eigenvalue Problem

The fact that the basis states are not completely orthogonal means that the Fock equation is a *generalized* eigenvalue problem. Solving the generalized eigenvalue problem is done by reformulating it into a standard eigenvalue problem [9]. The following procedure will accomplish this by defining,

$$\mathbb{F}\mathbb{C} = \varepsilon\mathbb{G}\mathbb{G}^{T}\mathbb{C}$$

with $\mathbb{S} = \mathbb{G}\mathbb{G}^{T}$. Now the matrix equation can be rearranged into a regular eigenvalue equation.

$$\mathbb{F}'\mathbb{C}' = \varepsilon\mathbb{C}'$$

where the transformed Fock matrix is $\mathbb{F}' = \mathbb{G}^{-1}\mathbb{F}\mathbb{G}^{-T}$ and the transformed vector space is $\mathbb{C}' = \mathbb{G}^{T}\mathbb{C}$. Once the eigenvector solutions are found they must be transformed back into the original basis.

The eigenvalue problem is solved with a single value decomposition (SVD) procedure. A linear algebra package JAMA for Sun's universal programming language *Java* is used. Diagonalizing matrices works well with JAMA with the understanding that the ordering of the eigenvalue and eigenvector can switch position from iteration to iteration. Simple logic allows following of this switching.

The eigenvalues are a way to interpret the difference in energies of single particle electron states. Using the eigenvalues to populate the new eigenvectors could be possible but for only light atoms. Atoms with greater numbers electrons will have more energy bands that have evermore closer energies. Deciphering which eigenvalue is associated with which state becomes difficult. Observing the eigenvalues during convergence can still be very useful in determining the cause of instabilities.

Via the eigenvectors the major state of an electron is followed from iteration to iteration. Each eigenvector is comprised of a list of coefficients that represent how much each electron is projected onto a particular basis state. If the i^{th} electron is defined to be in the n=2, l=1, m=1 state, then it is initially set to be *one hundred percent* in the φ_{211} basis state. This is accomplished by initially setting, $c_{i211} = 1$ and all other c_{i***} to zero. The expectation is that after the Fock matrix is solved one eigenvector will have the largest projection still in the 211 basis and that will be defined as the 211 eigenvector solution. In general this works very well but some electron configurations will have eigenvectors move towards degenerate states. Problems with convergence are due to this quasi-degeneracy in the eigenvectors and eigenvalues.

2.4.6 Self-Consistent Field

After the eigenvectors have been solved for and been assigned to the appropriate electron, the iteration process begins. The new eigenvectors are mixed with the old and a new guess of the spin orbital states is ready for the process to repeat. This process continues until the eigenvector solutions are close to the same from one iteration to the next. At this point the system is said to be converged and the *self-consistent field* (SCF) refers to this converged state. A flow-chart of the HF process is in Figure 2.3.

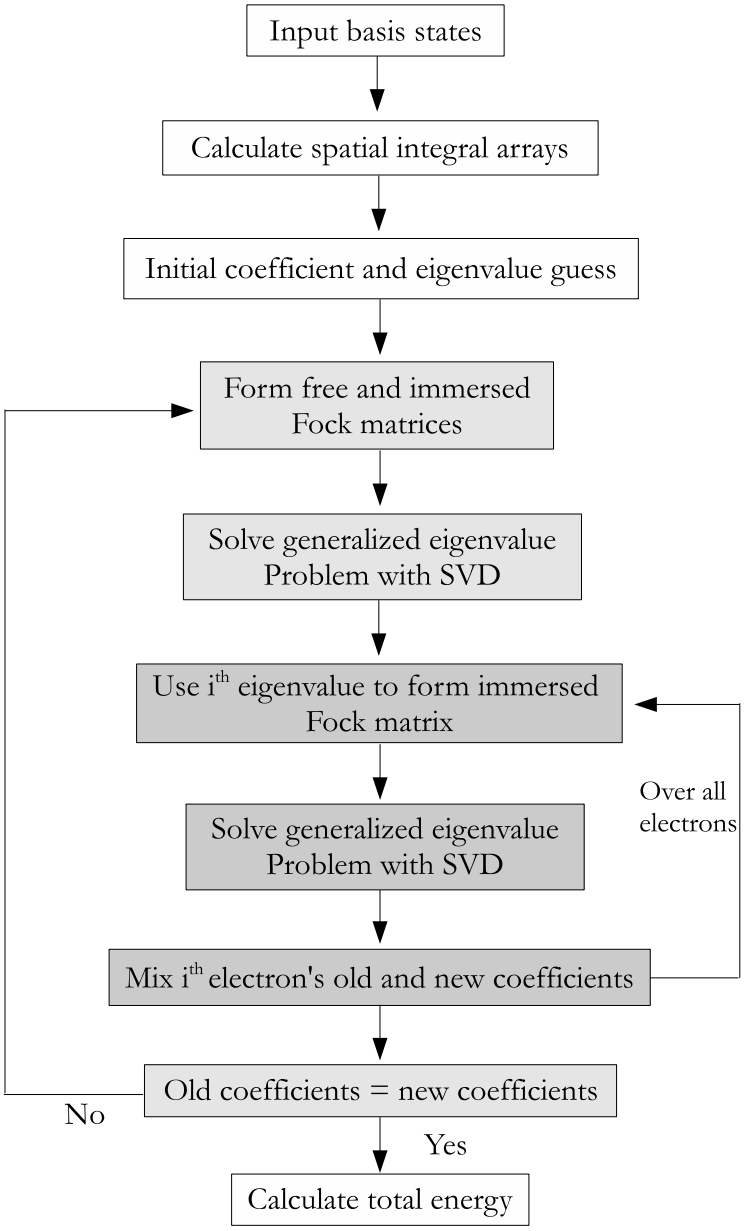

FIGURE 2.3: Flow chart of iterative HF scheme. Immersed atoms have an extra loop to form the immersed Fock matrix from each states previous eigenvalue.

2.4.7 Computational Details

All computational codes created for this work are written in Java. Numerous versions of the free atom code exist. Of those, two are complete. One applies direct calculation of the kinetic energy integrals. The other indirectly generates the kinetic energy terms by use of the converged DFT total potential and eigenvalues. Integrals are performed by a Simpson's rule method, applied to a logarithmic mesh [19]. The only code not generated from scratch is the linear algebra package JAMA for Java. The code used to generate the DFT basis states was created by Dr. Jansen and is written in Fortran.

The second program created was an angular momentum coupling algorithm. This really was three different codes for coupling two, three, and four electrons. This code requires an input file of uncoupled energies. Combining the free atom code and the coupling code could be a project for the future.

The last program created is an extension of the free atom code to include the effects of the immersion. This code is backwards compatible as the immersion can be turned off. The adjustable parameters are: particle number, max number of basis states (nmax), iterations or convergence condition, coefficient mixing ratio, separate angular and radial meshes, maximum number of power expansions for the plane waves (smax), maximum number of angular momentum coupling between bound and free states (lkmax), and the Fermi wave vector. The core of the code generates all the integral arrays. This can be stored in a file and different electron configurations can be calculated without having to re-calculate these arrays. If the basis sets do not change than these arrays do not change.

2.5 Post Hartree-Fock

UHF accounts for the exchange of particles exactly but fails to include the effects of correlation [11]. The difference in energy between the HF limit and the exact solution to

the non-relativistic Schrödinger equation is the correlation energy. The switch from non-relativistic Schrödinger to relativistic Dirac will lower the energy even more. Post Hartree-Fock methods attempt to account for correlation in a variety of ways. The common feature among each post HF method is using combinations of electronic configurations. Appropriately expanding your space to many configurations provides for an approximation to the correlation between each configuration. This should lower the energy of the system, getting closer to the exact energy as shown in Figure 2.4.

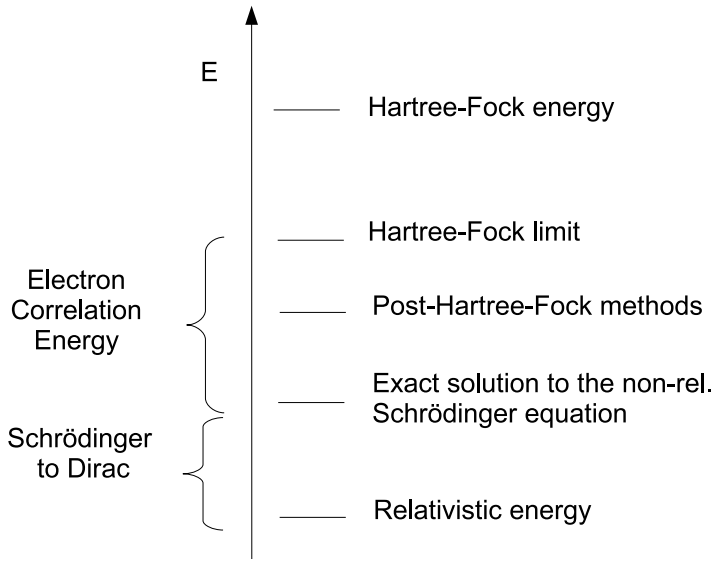

FIGURE 2.4: The energy decreases as correlation effects are accounted for. Exact solutions to the relativistic Dirac equation yields the lowest Hartree-Fock energies.

How a particular post HF method treats the interaction of different electron configurations depends on the system being modelled. HF is commonly used for modelling molecules and many atom clusters. For these systems the cause of the greatest correlation may differ, warranting a number of different modelling techniques. A few of these techniques are featured in this section.

2.5.1 Configuration Interaction

A single Slater determinant for a given electronic configuration results a Configurational State Function (CSF). The breaking of spherical and spin symmetry in UHF results in many CSF for a given total angular (L^2) and spin (S^2) momentum. To exactly solve the non-relativistic Schrödinger equation the total wave function must be an eigenstate of the Hamiltonian. Since the Hamiltonian commutes with L^2 and S^2 using a total wave function that is comprised of all CSF, for a given total angular and spin symmetry, is a full Configurational Interaction (CI) approach [20].

To get a CI total wave function a linear combination of CSFs is used.

$$\Psi = \sum_{i=0} c_i \Phi_i = c_0\Phi_0 + c_1\Phi_1 + c_2\Phi_2 + ... \tag{2.61}$$

Here Φ_i is a CSF and c_i is a variational parameter determined by the by the L^2 and S^2 symmetry. These terms are to be in order of excitations from the ground state. The zeroth term is the single Slater determinant of the ground state. The first is a single excitation from a spin orbital to a virtual orbital. The second term is if two spin orbitals are excited. In practice the series must be truncated due to large computational times.

2.5.2 Multi-Configurational Hartree-Fock

A common post HF technique for including correlation effects involves expanding the total wave function as a linear combination of orthogonal CSFs. This expands the active space and allows correlations that CI ignores.

$$\Psi(LS) = \sum_{i=1}^{M} c_i \Phi_i(LS) \tag{2.62}$$

The expression for the energy is now

$$E(LS) = \sum_{i=1}^{M}\sum_{j=1}^{M} c_i c_j H_{ij} = \sum_{i=1}^{M} |c_i|^2 H_{ii} + 2\sum_{i<j}^{M} c_i c_j H_{ij} \tag{2.63}$$

where

$$H_{ij} = \langle \Phi_i(LS)|\widehat{H}|\Phi_j(LS)\rangle. \tag{2.64}$$

The $|c_i|^2$ term in equation **??** is the energy of each CSF that satisfies a given symmetry and CI contribution. The additional $c_i c_j$ cross term allows *mixing coefficients* of different CSFs. This energy of this mixing is the approximations to the correlation energy. This would then need to be applied during the self-consistent iteration procedure. The final converged spin orbitals would be generated with correlations between different CSFs and is considered an Multi-Configurational Hartree-Fock (MCHF)approach [21],[22].

Configuration Interaction accounts for symmetries of a system and in the process uses addition of angular momentum to average the energy if different CSFs. What CI fails to do is allow the wave functions of a given spin orbital to change during this coupling process. Correlation is then accounted for from a static set of CSFs. What MCHF does is allow the spin orbitals to change through the mixing of coefficients of different CSFs [12]. If the radial functions are optimized during the iterative process due to mixing of different CSFs the method is MCHF.

3. SINGLE ATOM ELECTRONIC CONFIGURATIONS

The Schrödinger equation in the context of Hartree-Fock relies on a variational principle that minimizes the energy. Once this is applied the resultant eigenvalue problem provides a method to find solutions for the given set of spin orbitals. The application of the variational principle also has the feature of driving the system to a minimum during the iteration process. At convergence, variations in the wave function do not lower the energy. Thus, Hartree-Fock is a method for finding the lowest energy of a many-body system.

Once the system reaches *self-consistency* the total contribution to the electron energy can be calculated. These energies are important in understanding ground state electronic configurations and interactions between states. There is no restriction to what electronic configuration is modelled. This means excited states can also be explored. The error in the energy is increases as the configuration moves away from the ground state.

Many tools can be used to analyze the features of a given system. Configurations with closely lying states will have difficulty converging. Analyzing the eigenvalues, eigenvectors, and total energy during convergence can shed light on the mechanism for system instability. Ground state energies and interesting electronic configurations of a free atom are presented in this chapter.

3.1 Electronic Configurations

The electronic configuration refers to the states each electron is in for a single converged Slater determinant. As the atoms increase in number of electrons so does the number of possible interesting electronic configurations and number of degeneracies. The

total energy for a single electron configuration will be denoted by:

$$E[n_1 l_1 m_1 \sigma_1; n_2 l_2 m_2 \sigma_2; ....; n_N l_N m_N \sigma_N;] \tag{3.1}$$

Filling of orbital shells in general obeys Hund's rules. Those rules will be tested and excited states will be explored. For larger atoms a shorthand notation for all of the closed shells will be used. For example: carbon has six electrons, two close the 1s subshell, two more close the 2s subshell and the last two reside in the 2p subshell. The last two electrons in the 2p shell are of most interest as they can be put into many different m states and the energies be compared. If both 2p electrons are spin up and one is the m=0 state and the other in the m=1, the shorthand notation would be:

$$E[(2s); 210\uparrow; 211\uparrow] \tag{3.2}$$

Nine distinct configurations maintain two electrons in 2p state and the energy difference between these are very small or zero.

Degeneracies will occur often due to the polar, up or down, nature of spin. A atom such as boron has five electrons. Four close the first two shells. The fifth electron then can be viewed as being added to a spherically symmetric system. The spin of the fifth electron does not affect the total energy. Another example would be nitrogen with the last two electrons in the same two m states. The energy is degenerate if the spin of each are both up or both both down. Degeneracies occur when all the valence electrons switch spin.

$$E[(2s); 210\uparrow; 211\uparrow; 210\downarrow] = E[(2s); 210\downarrow; 211\downarrow; 210\uparrow] \tag{3.3}$$

Spin coupling occurs in the the exchange Coulomb interaction but coupling of different m states is applied in both Coulomb terms. Integrals over three spherical harmonics, Equation 2.53, have the requirement that $m_\alpha = m + m_\beta$. The sum over m is done for a given α and β. The consequence of this is that multiple β states will couple to the same

α state. Each term will be degenerate with $m_\alpha = m + m_\beta$ satisfied because the value of the integral is the same for any permutation of the same three m's.

More degeneracies are expected with the spin and m state symmetries. One example is carbon in the states below.

$$E[(2s); 210\uparrow; 211\uparrow] = E[(2s); 210\uparrow; 21-1\uparrow] \tag{3.4}$$

Here the last electron is coupling to two closed shell orbitals and a 2p electron in the m=0 state. Coupling to m=1 and m=-1 is symmetric. Another example is nitrogen in the following states.

$$E[(2s); 21-1\downarrow; 211\uparrow; 210\downarrow] = E[(2s); 21-1\downarrow; 211\uparrow; 210\uparrow] \tag{3.5}$$

With three electrons of interest many degeneracies are found. This particular example has two of the electrons remaining in the same $m = -1, \downarrow$ and $m = 1, \uparrow$ states. Now the spin of the third electron doesn't matter, providing its in the m=0 state.

3.2 Eigenvalues, Eigenvectors and Total Energy

During the iterative process the Fock matrix is created and then diagonalized via a single value decomposition. The system eigenvalues and eigenvectors result from this procedure. Observing the behavior of each of these quantities provides a way of tracking the system.

The eigenvalues are approximate energies of each spin orbital state. Since each electron is bound there should the same number of negative eigenvalues as there are electrons. This can be seen in the eigenvalues of oxygen, shown in Figure 3.1.

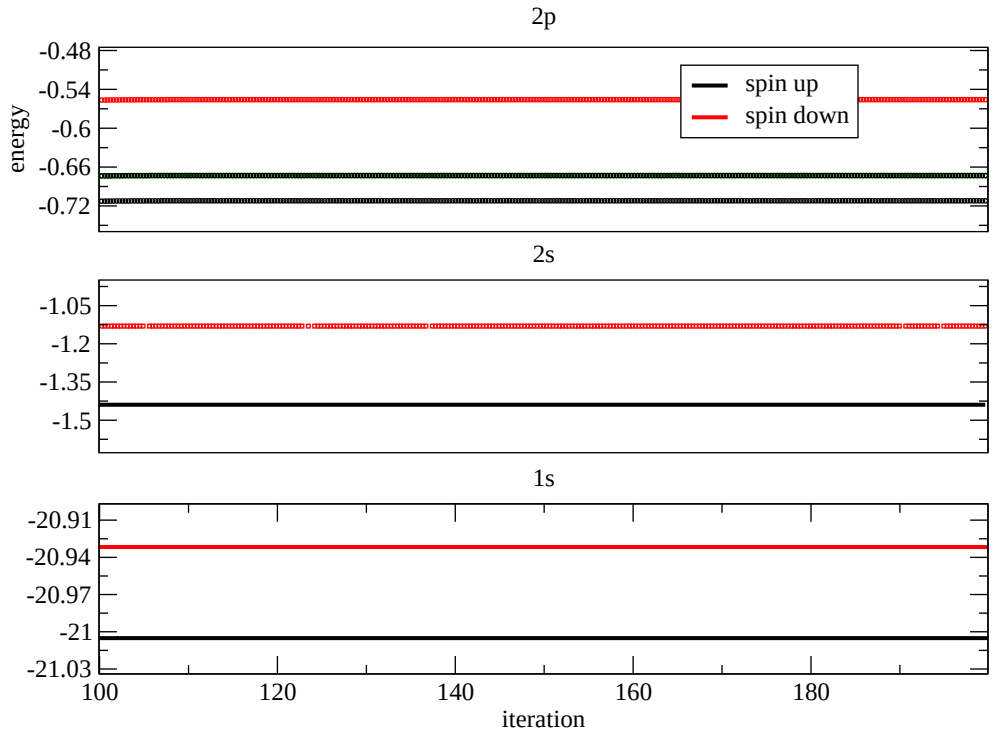

FIGURE 3.1: Eigenvalues for oxygen in the ground state electron configuration $E[(2s); 21-1\uparrow, 210\uparrow, 211\uparrow, 21-1\downarrow]$ with nmax=3. The lowest 2p state is occupied by the 210 spin up electron, the middle 2p state is degenerate among the 21-1 and 211 spin up electrons.

There may appear to be only seven eigenvalues but a degeneracy exists. The symmetry of having a closed spin up 2p shell causes the degeneracy among the m=-1 and m=1 states.

The eigenvalues of the system not only provide information about convergence behavior, they also describe how much each spin orbit is projected into each basis state. This can be used to understand the resulting charge density and state mixing. Unstable systems result from nearly degenerate states but truly understanding how these states interfere must be done by following the eigenvectors.

During the iteration process the total energy can be calculated and observed for smooth convergence. The first iteration requires each electron to be completely in one

basis state. If the DFT converged density produced states that complete Fock space than the system wouldn't mix coefficients and the total energy would not change. Since the states created through DFT are not eigenstates of the Fock matrix mixing occurs to lower the energy.

3.2.1 Ground State Total Energy

The ground state total energy of an atom can depend on many factors. Generating the DFT basis states relied on parameters to adjust charge density, integral mesh and, although not explored in this work, spin dependence and relativistic effects. Each of these can have small effects on the final HF energy. The number of basis states used can also affect the final energy. Each of these change the degree of completeness of the basis set used for a given electronic configuration. Along with this the electronic configuration itself must also be explored. This becomes increasingly important as more angular and spin symmetries are broken.

First observed through spectroscopic data, *Hund's Rules* predict the ground state electron configuration of an atom [5]. A closed atomic shell has no contribution to L and S. For this reason these rules apply to the filling of any incomplete shell.

Hund's First Rule: The first priority in filling an incomplete shell is to maximize the total spin S. Electrons of like spin are repelled by the Pauli-Exclusion Principle and thus stay further away from each other, lowering their Coulomb energy.

Hund's Second Rule: The second priority in filling an incomplete shell is to maximize the total angular momentum L. Still a Coulomb effect, this can be thought of classically as the advantage of two electrons spinning in the same direction around the same axis. If they spun opposite each other they would encounter each other twice per revolution.

Hund's Third Rule: The final priority is to split the states by the spin-orbit interaction. For shells that are less than half full the preferred state is $J = |L - S|$ and for shells that are over half full $J = |L + S|$ is preferred.

In principle the true constant of motion is $J = L + S$, but in practice the interaction between L and S is small for the light atoms modelled here. Hund's rules are based on an assumed separation of L and S. The heavier an atom becomes the more it can interact with its own magnetic field because the larger number of electrons with spin. For this reason L and S coupling increases for heavier atoms and Hund's rules are violated. The HF approximation also breaks the total wave function into separate spatial and spin states. Therefore HF would be expected to obey Hund's rules for light atoms. For many atoms Hund's rule predicted the ground state electron configuration. For other atoms with large numbers of electronic configurations that are nearly degenerate, these rules are sometimes violated as shown in the energies presented in section 3.3. This feature was also observed when solving the spin dependent DFT problem with broken spherical symmetry. The violation found in HF can be understood by the missing correlation energy. If a set of nearly degenerate configurations exist and the difference in their energies is on the order of the correlation energy, the ground state configuration cannot be predicted.

The ground state total electronic energy for many light atoms is listed in Table 3.1.

TABLE 3.1: Total energy for many light atoms calculated, by direct and indirect treatments of the kinetic energy. These are compared to the exact, complete basis set, Roothaan-Hartree-Fock (RHF)energies. Basis set generated up to nmax=3. The energy difference is tabulated under indirect-Rooth.

Atom	HF(KE_{direct})	HF($KE_{indirect}$)	Roothaan HF	indirect-Rooth
Helium	-2.85809	-2.85917	-2.86168	0.00251
Lithium	-7.43244	-7.42996	-7.43273	0.00269
Beryllium	-14.57391	-14.57016	-14.57302	0.00293
Boron	-24.53079	-24.52637	-24.52906	0.00269
Carbon	-37.68770	-37.68625	-37.68862	0.00237
Nitrogen	-54.715	-54.41200	-54.40093	-0.01107
Oxygen	-75.31368	-74.81924	-74.80940	-0.00984
Fluorine	-100.19073	-99.46000	-99.40935	-0.05065
Neon	....	-128.60000	-128.54710	-0.05290
Sodium	....	-162.40000	-161.85891	-0.54109

Atoms helium through carbon have been carefully and completely converged. More work could find more complete basis sets for heavier atoms. Instability during and at convergence could also be more controlled by more active techniques like variable coefficient mixing between iterations.

The difficulties in numerically performing second derivatives in the kinetic energy (KE_{direct}), resulted in slightly less precise data. Indirectly calculating the kinetic energy from the DFT total potential and eigenvalues appeared reliable for helium through carbon. The total energy, calculated by this work, is within millihartees of those found by using Roothaan-Hartree-Fock wave functions [23],[24].

As the number of electrons surrounding the nucleus increases the binding energy of the innermost electrons increases. The electron is deeper in the potential well. This effect

can be seen in the eigenvalue of a 1s electron as atoms become heavier, shown in Figure 3.2.

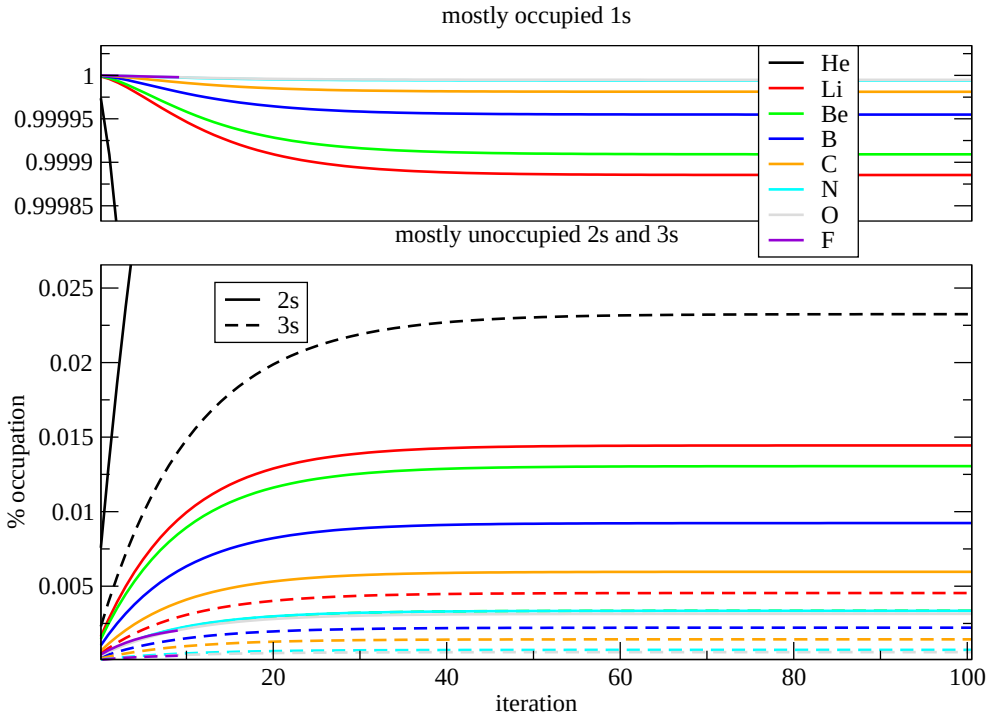

FIGURE 3.2: Eigenvalue of the 1s spin-up electron for helium through oxygen.

The eigenvector can tell more of the story of a given electron's charge density as you move up the periodic table. Spin symmetry breaks the 1s eigenvalue degeneracy for a number of configurations. An example showing this for a number of atoms is in Figure 3.3 were the plot shows the eigenvector coefficients of the deepest eigenvalue electron.

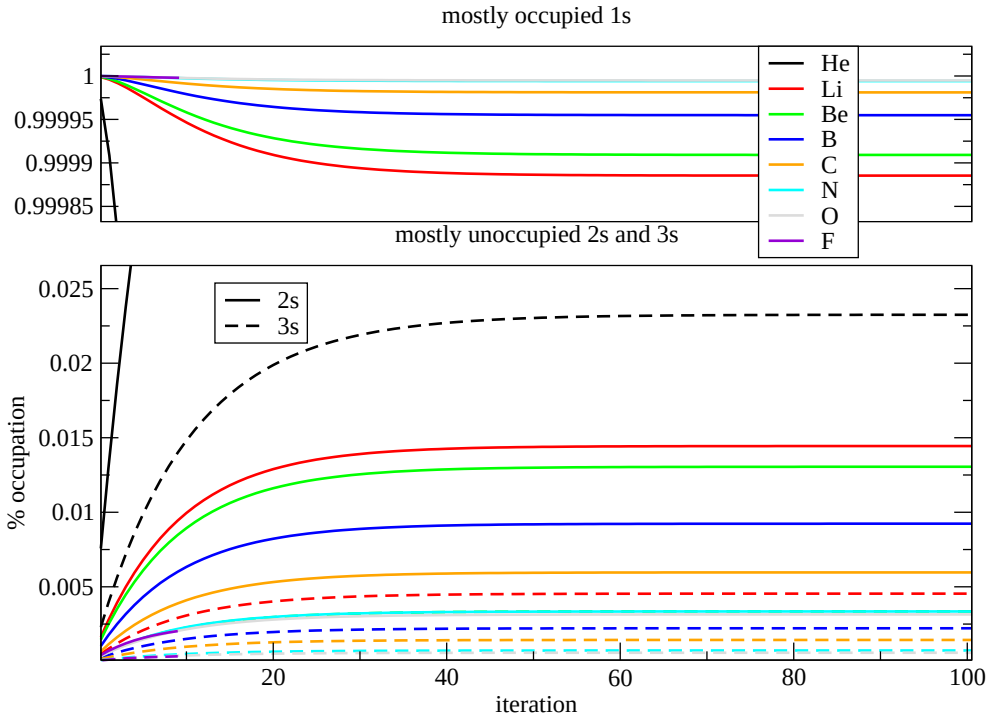

FIGURE 3.3: The mostly occupied 1s and mostly unoccupied 2s and 3s eigenvector coefficients for helium to fluorine

The mixing between the inner and outer shell basis states decrease as more electrons surround the core. The 1s eigenvector spreads less into the 2s and 3s basis states as the atom increases in mass. The innermost electron is pulled in towards the nucleus more for heavier atoms.

3.2.2 Helium

Helium is the first atom in the periodic table that requires a many-body approach to quantifying interactions. With only two electrons each is able to reside in the lowest energy level, provided they are opposite in spin. The electron configuration for the ground state is thus $1s^2$. With a full principal quantum number shell, helium is a noble gas. The energies calculated for helium are compared to Roothaan HF in Table 3.2.

TABLE 3.2: Total energy of helium, for different basis sets, compared to Roothaan HF. *Basis* refers to the fractional charge excitation in the DFT basis set generation.

$Basis$	$nmax = 4$	$nmax = 3$	$nmax = 2$	$RoothaanHF$	$\triangle E(nmax = 3)$
1.0	-2.8489	-2.8495	-2.8512	-2.8617	0.0122
0.8	-2.8522	-2.8526	-2.8538	-	0.0079
0.6	-2.8552	-2.8554	-2.8561	-	0.0056
0.4	-2.8577	-2.8577	-2.8579	-	0.0037
0.2	-2.8592	-2.8592	-2.8592	-	0.0025

The lower the fractional charge excitation, used in generating the basis sets from DFT, the lower the total HF energy. This is understood by the fact that moving more charge to higher energy levels, when generating the basis, results in wave functions that are more spread out from the nucleus. These basis sets then increase the energy when used in HF.

Another important feature of this data is the relatively small difference in total energy from nmax=2 to nmax=4. For the most complete set, that with smallest fractional occupation (0.2), the energy difference is negligible. That has important consequences on computational times. The number of basis functions for nmax=2 is *five* , nmax=3 is *fourteen*, and nmax=4 is *thirty*. Respectively, computational times run on the order of a minute, to many minutes, to many hours.

The eigenvalues of helium during and at convergence can also be shown. These values are plotted in Figure 3.4 for a specific nmax=3 case.

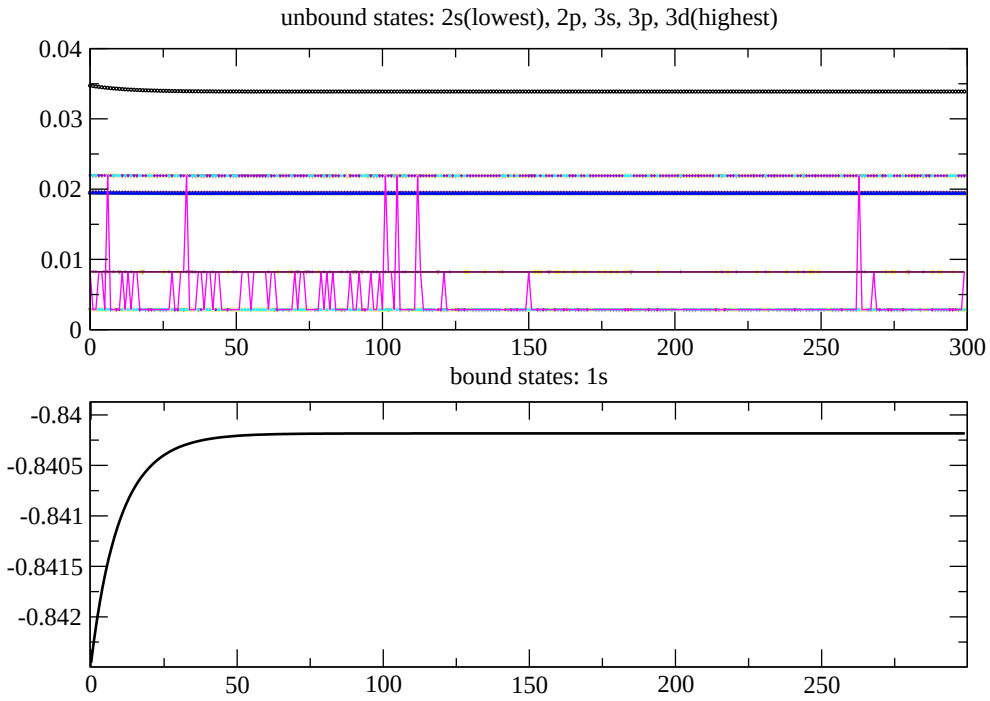

FIGURE 3.4: Helium eigenvalues for nmax=3 with a basis set generated with the lowest fractional occupation. Switching of eigenvalues is shown with the vertical lines of one of the sets.

As expected the bound eigenvalue is degenerate among unlike spins. Helium is a very smooth converging system, as shown by the 1s eigenvalue convergence. The unbound states also converge nicely. The JAMA, linear algebra package used to perform the SVD would mix which output index corresponds to which eigenvalue. Data lines are used on one of the series to show this behavior.

As the fractional charge occupation to excited states increased in the basis set generation, the amount of the 1s spin orbitals projection in the 1s state decreased. This can be observed in Figure 3.5 were the eigenvector of the 1s spin orbital changes more for basis sets generated with a greater excitation fraction.

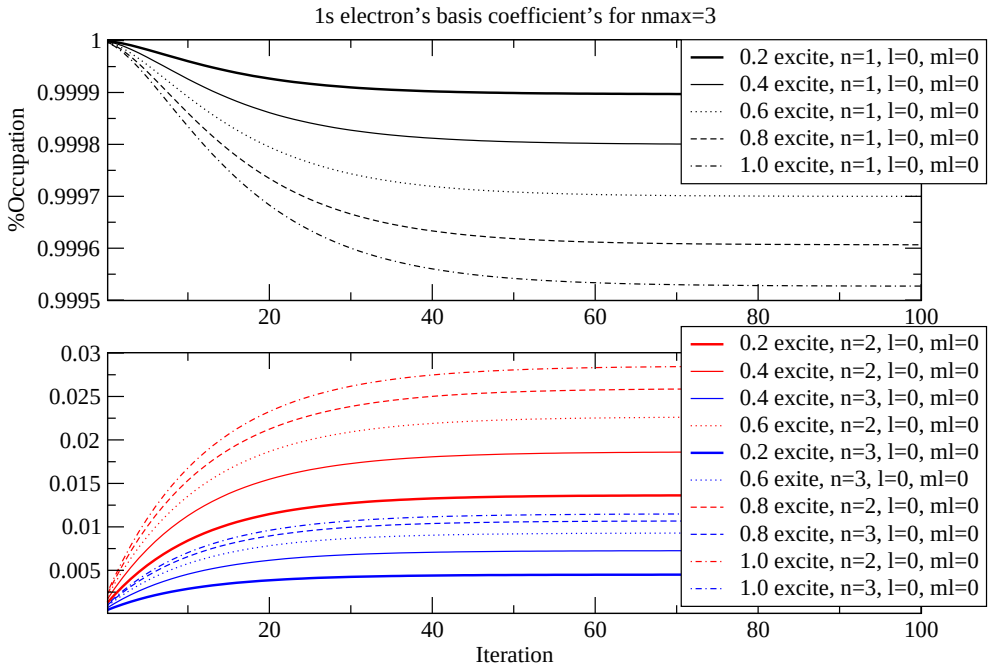

FIGURE 3.5: Helium 1s eigenvector for various fractional charge excitations in DFT basis set generation. nmax=3.

The more charge is moved out of the 1s state the more accurate the excited states become in DFT. The HF system then spreads more of the spin orbital into those states. When this is done the energy is increased, as shown in table **??**.

3.2.3 Lithium

In the ground state lithium is the first atom to occupy states with a principal quantum number greater then one. The first two electrons occupy a closed 1s angular momentum shell while the third resides in the 2s. Having only one electron out of closed shells means no spin is preferred. The electron configuration for the ground state is thus $1s^2 2s$. Lithium is an alkali metal due to the open 2s subshell. The energy for various basis sets is listed below in Table 3.3.

TABLE 3.3: Total energy of lithium, for different basis sets, compared to Roothaan HF. *Basis* refers to the fractional charge excitation in the DFT basis set generation.

$Basis$	$nmax = 4$	$nmax = 3$	$nmax = 2$	$RoothaanHF$	$\triangle E(nmax = 3)$
1.0	-7.42953	-7.42955	-7.42996	-7.43273	0.00269
0.8	-7.42955	-7.42957	-	-	0.00317
0.6	-7.42968	-7.42970	-	-	0.00315
0.4	-7.42984	-7.42984	-	-	0.00289
0.2	-7.42998	-7.42997	-	-	0.00276

Lithium has electrons in both n=1 and n=2 shells. When generating the basis states from the DFT program, fractional excitations are used to generate virtual, unoccupied orbitals. The 2p states are different for each basis set but the 2s spin orbital does not couple to them. Since the 1s and 2s basis states are the same all of the energies are the same for nmax=2.

The most complete basis set for lithium is 0.2 fractional excitation occupation set for an nmax=4. What is interesting is for basis sets generated with higher fractional occupation, increasing the basis up to greater nmax actually raises the energy. This means size of the basis is less important than how close the DFT was to the ground state. Again the differences are small enough that shorter computational time would outweigh a 5^{th} decimal place difference in energy.

The data shows the total converged energy increases as the basis set is generated from an increased difference from the ground state. A plot of the total energy during convergence in Figure 3.6 shows how good the initial guess of coefficients are. Initially each spin orbital is completely in a given basis state. During convergence the coefficients spread out to those states that couple. The final energy can either be less than the original guess, or, in the case of a highly excited basis set, greater.

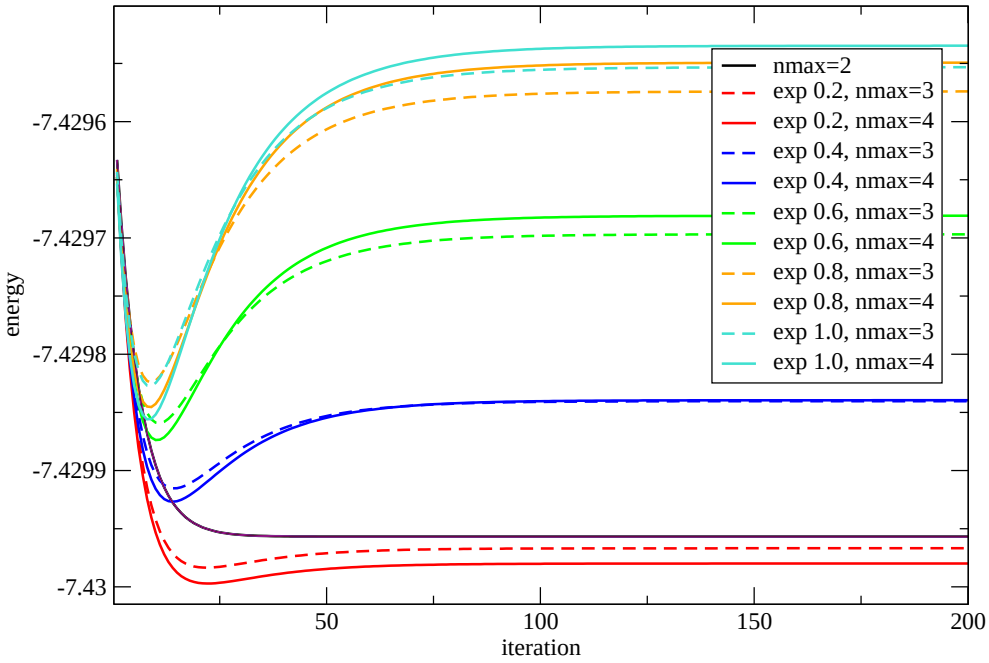

FIGURE 3.6: Lithium total energy, during convergence, for different basis sets (exp 0.2 to 1.0).

Figure 3.7 shows the 1s eigenvalues of lithium splitting due to the loss of spin symmetry. With two of the electrons spin up and one spin down the 1s states of the spin up electron are lower in energy.

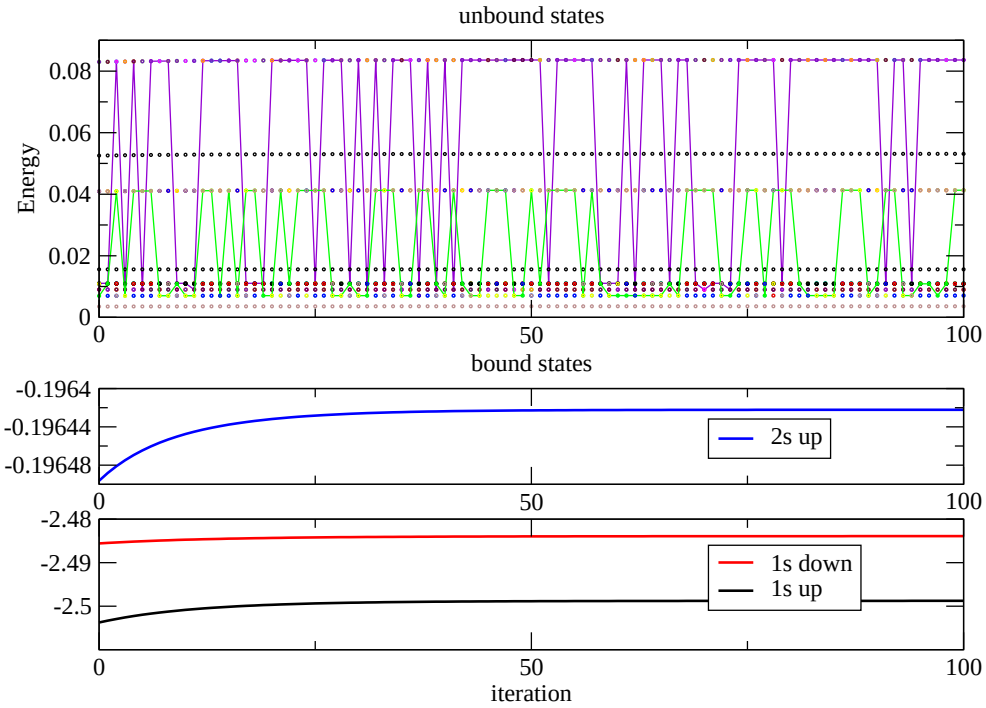

FIGURE 3.7: Lithium eigenvalues for nmax=3 with a basis set generated with the lowest fractional occupation.

The extra exchange interaction between like spins results in a negative shift in energy. Including exchange not only lowers the total energy of the system it also lowers the eigenvalues of electrons that experience the most exchange interaction. Since 1s and 2s states can mix this is seen above.

3.2.4 Beryllium

In the ground state beryllium has a closed 1s and 2s shell giving it an electron configuration of $1s^2 2s^2$. Beryllium is an alkali earth metal due to the small difference in energy between the 2s and 2p states. Free electrons in a metal have a large enough Fermi energy to excite a 2s electron into the 2p state and make conduction possible. Table 3.4 has a list of the energies calculated for beryllium with various basis sets.

TABLE 3.4: Total energy of beryllium, for different basis sets, compared to Roothaan HF. *Basis* refers to the fractional charge excitation in the DFT basis set generation.

$Basis$	$nmax = 4$	$nmax = 3$	$nmax = 2$	$RoothaanHF$	$\triangle E(nmax = 3)$
1.0	-14.57145	-14.57116	-14.56985	-14.57302	0.00187
0.8	-14.57107	-14.57083	-	-	0.00219
0.6	-14.57070	-14.57053	-	-	0.00250
0.4	-14.57036	-14.57026	-	-	0.00276
0.25	-14.57016	-14.57010	-	-	0.00293

The most complete sets are for nmax=4 but are not for the lowest fractional excitation during the basis set generation. Still the energy differences are small and weighing the advantages to shorter computational times must be made.

A look at the total energy in Figure 3.8 during convergence shows that the initial guess of the coefficients is consistently not the best choice. If it was the energy would not change from iteration to iteration.

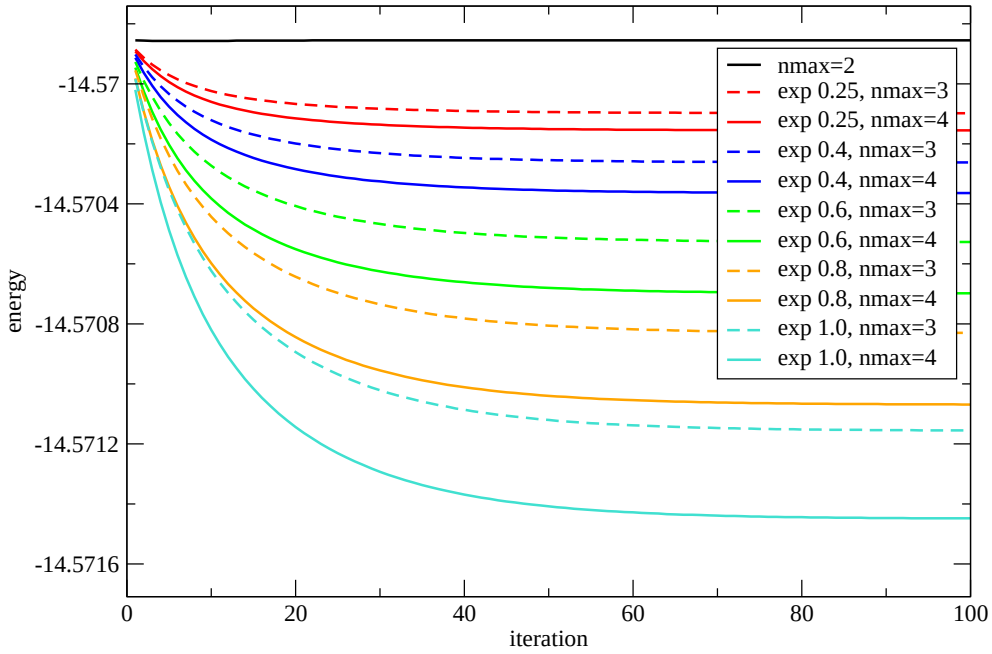

FIGURE 3.8: Beryllium total energy, during convergence, for different basis sets (exp 0.2 to 1.0).

Every basis set has an energy advantage to mixing. The mixing is best seen by a plot of the eigenvectors during convergence. Figure 3.9 is a plot of the outer shell 2s spin orbital's projection onto the 1s, 2s and 3s state.

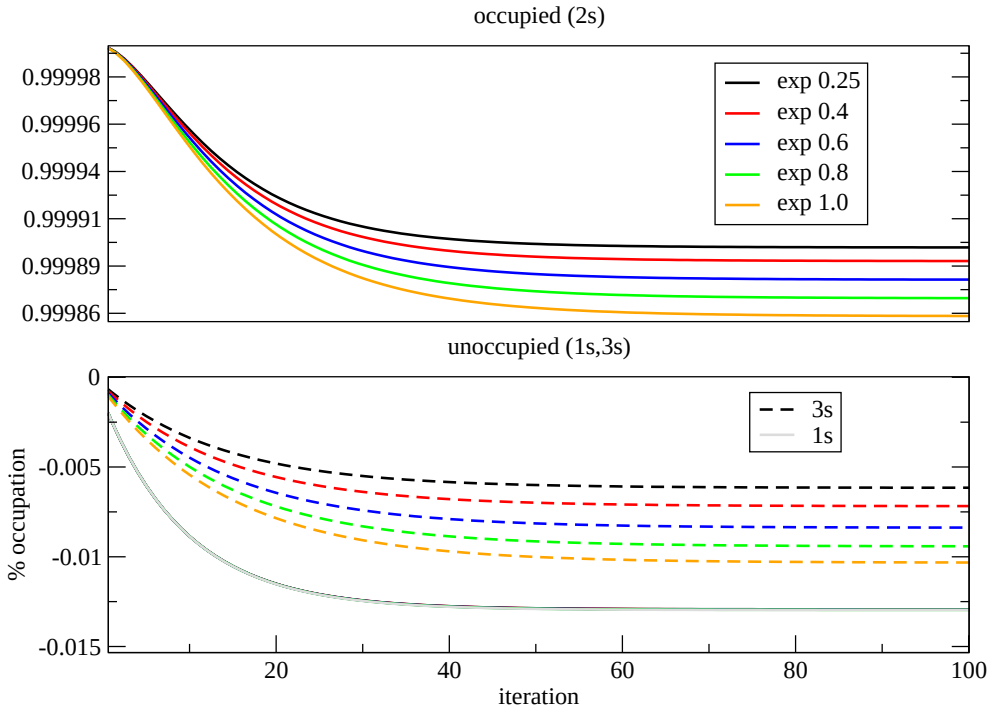

FIGURE 3.9: Beryllium with nmax=3. 2s spin orbit eigenvector for a number of fractionally excited basis sets.

As the generated basis set is expanded into higher fractional occupations the amount of the spin orbit in the 2s basis state is decreased. The mixing of the 2s state is not as strong with the 1s as it is with the 3s. The HF ground state prefers to project more of the 2s spin orbital in the 3s state as basis set is extended away from the nucleus.

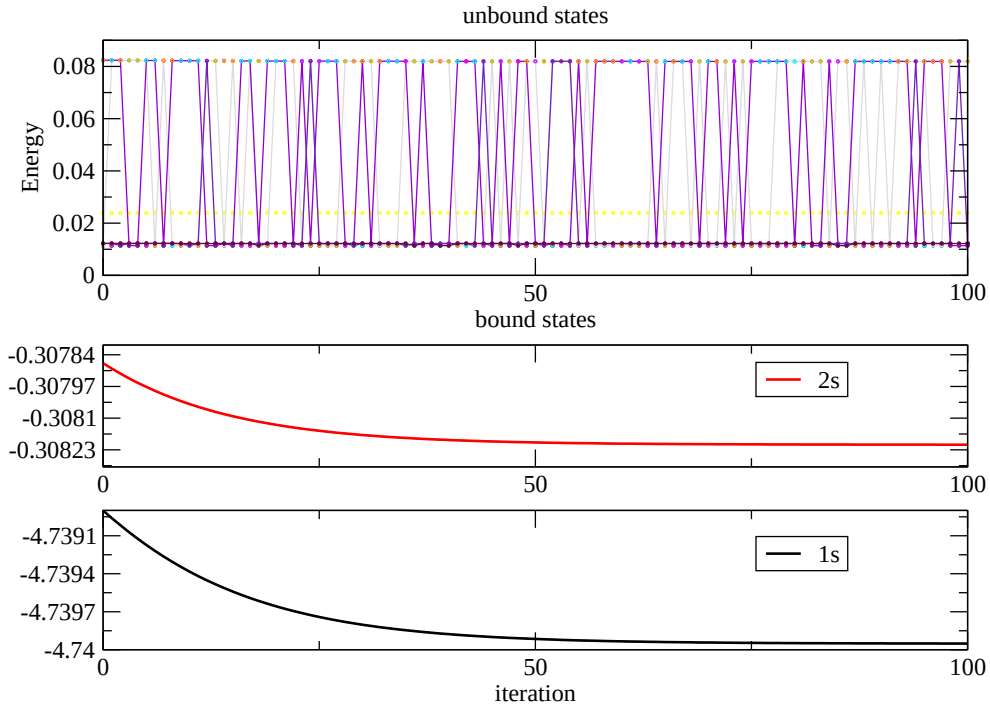

FIGURE 3.10: Beryllium eigenvalues for nmax=3 with a basis set generated with the lowest fractional occupation.

Both angular momentum shells are closed resulting in degeneracy between unlike spin states. This is shown in Figure 3.10 were both 1s and 2s states are separately degenerate. Convergence for beryllium is smooth and complete.

3.2.5 Boron

Boron has a ground state with one electron out of closed angular momentum shells. This electron resides in a 2p state, thus boron is the first atom to explore the consequences of having a non-zero angular momentum. Boron is never found as a free element in nature because this lone, out of closed shells electron, will bond well with other atoms. Boron, a semi-metal, is often used as a dopant for the semi-conductor industry. The electron configuration for the ground state is $1s^2 2s^2 2p^1$ and the energies are listed in Table 3.5.

TABLE 3.5: Total energy of boron, for different basis sets, compared to Roothaan HF. *Basis* refers to the fractional charge excitation in the DFT basis set generation.

$Basis$	$nmax = 4$	$nmax = 3$	$nmax = 2$	$RoothaanHF$	$\triangle E(nmax = 3)$
1.0	-24.52325	-24.52352	-24.52631	-24.52906	0.00554
0.8	-24.52406	-24.52432	-	-	0.00474
0.6	-24.52494	-24.52511	-	-	0.00395
0.4	-24.52575	-24.52581	-	-	0.00326
0.25	-24.52620	-24.52619	-	-	0.00287

For boron, expanding the basis set out to higher $\langle r \rangle$ results in an increase in total energy. The HF lowest energy is for the basis set from the ground state of DFT. More interesting is expansion to greater nmax actually increases the energy. The mixing of the 2p electron with higher 2p states raises the total energy. A plot of each basis set during convergence shows this feature in Figure 3.11. The only initial coefficient guess that remains unchanged is that for nmax=2. This is also the lowest of all the final converged energies.

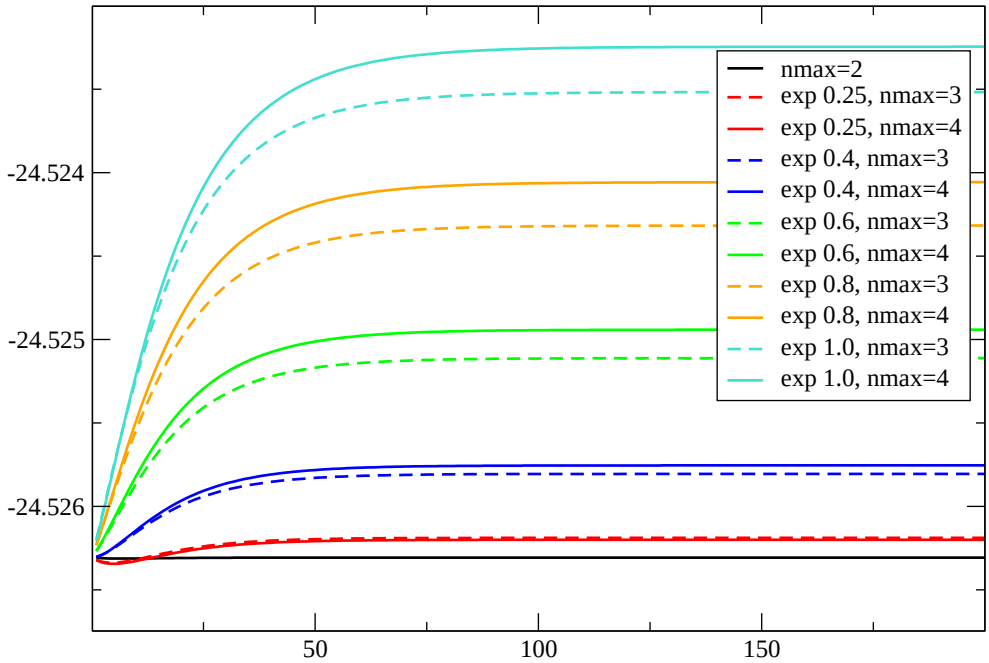

FIGURE 3.11: Boron total energy, during convergence, for different fractional excitation basis sets (exp 0.2 to 1.0).

Boron is especially interesting because of the closely lying 2s and 2p states. Breaking spin degeneracy allows all five bound states to been seen separately. Figure 3.12 is a plot of Boron's eigenvalues.

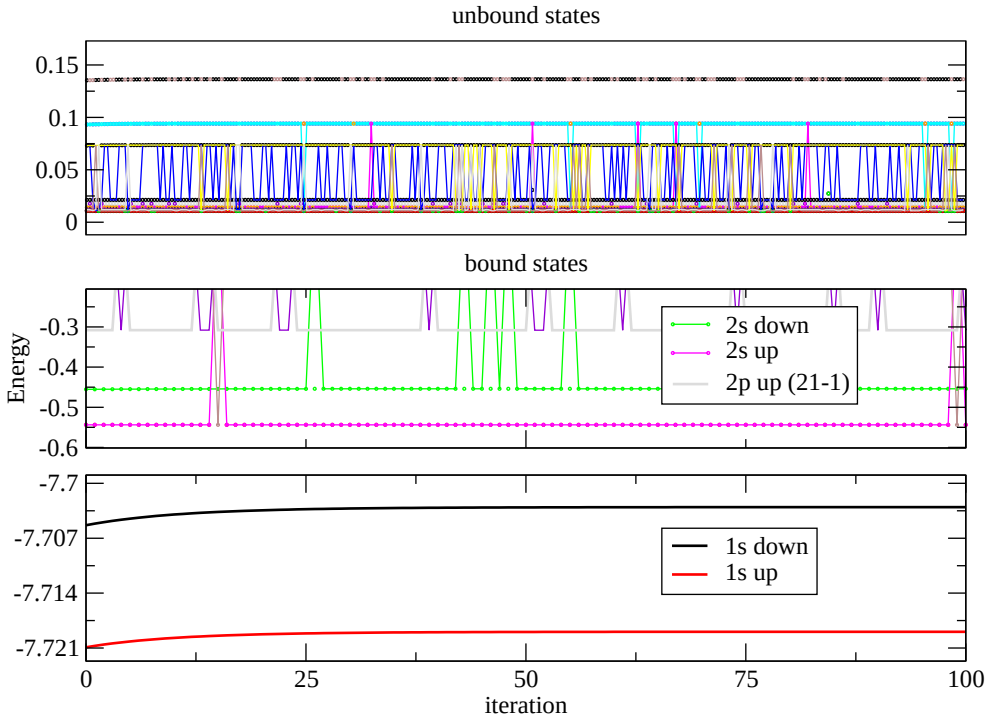

FIGURE 3.12: Boron eigenvalues for nmax=3 with a basis set generated with the lowest fractional occupation.

The closely lying n=2 states show the most bound is that of the 2s spin up state. This is also due to the exchange interaction between like spins. The separation between eigenvalues is not as large for the nmax=2 case because of the lack of mixable higher 2p states. This strong mixing increased the overall energy of boron.

3.3 A Detailed Example: Carbon

Carbon's ground state electron configuration is $1s^2 2s^2 2p^2$. With two electrons in the p state, studying the effects of the interaction between two non-spherically symmetric spin orbitals is possible. Differences in energy for different configurations allow studying the obeyance of Hund's rules. These differences can be as small as in the seventh decimal place, as is the case when putting one 2p electron in the $m_\ell = -1$ state and the other in

either the $m_\ell = 0$ or $m_\ell = 1$ state. This tetravalent p shell makes carbon ideal for covalent bonding. Carbon is a non-metal and essential to the semi-conductor industry and many sciences. The energies are listed in Table 3.6.

TABLE 3.6: Total energy of carbon, for different basis sets, compared to Roothaan HF. *Basis* refers to the fractional charge excitation in the DFT basis set generation.

$Basis$	$nmax = 4$	$nmax = 3$	$nmax = 2$	$RoothaanHF$	$\triangle E(nmax = 3)$
1.0	-37.67762	-37.67915	-37.68643	-37.68862	0.00946
0.8	-37.68052	-37.68159	-	-	0.00703
0.6	-37.68319	-37.68375	-	-	0.00487
0.4	-37.68531	-37.68543	-	-	0.00319
0.25	-37.68630	-37.68625	-	-	0.00237

To better understand the workings of UHF, carbon will be used for a more detailed discussion. Many features that arise from our model system can be found by a thorough study of carbon. What makes it an important example is it is the lightest atom with two electrons in an open valence shell. With complete symmetry breaking the interaction of these two electrons can be studied. Four electrons close the 1s and 2s shells and the last two want to maximize the total spin and total angular momentum. There are five unique energies with the valence electrons occupying the 2p subshell. Here are the energies for these configurations with a basis set with the maximum principal quantum number of three. Various basis sets have been generated by the method of fractional occupation and the energies are listed in Table 3.7.

TABLE 3.7: Total energy of carbon, for electron configurations with the same L, for different basis sets.

$e-configuration$	$basis$ 0.25	$basis$ 0.4	$basis$ 0.6	$basis$ 0.8	$basis$ 1.0
$E[(2s); 21-1\uparrow; 210\uparrow]$	-37.686253	-37.685429	-37.683748	-37.681593	-37.679154
$E[(2s); 21-1\uparrow; 211\uparrow]$	-37.686253	-37.685431	-37.683757	-37.681623	-37.679221
$E[(2s); 21-1\uparrow; 210\downarrow]$	-37.658568	-37.657904	-37.656656	-37.655173	-37.653619
$E[(2s); 21-1\uparrow; 211\downarrow]$	-37.631087	-37.630644	-37.629863	-37.628982	-37.628100
$E[(2s); 210\uparrow; 210\downarrow]$	-37.603665	-37.603497	-37.603272	-37.603105	-37.603037

It is expected that electrons with like spin will have a stronger interaction due to the Pauli Exclusion principle. This results in lower energies as is the case above and throughout all the atoms modelled. What's surprising is that Hund's rule predicts the ground state should maximize the absolute value of the total spin and orbital angular momentum. The ground state thus should be $E[(2s); 21-1\uparrow; 210\uparrow]$ which is not the case here. This trend is not uncommon within the context of UHF due to not properly accounting for correlation.

The ground state of carbon is well behaved during convergence, as is most all the light atoms. Figure 3.13 is a plot of the total energy during convergence for the ground state Hund's rule would predict.

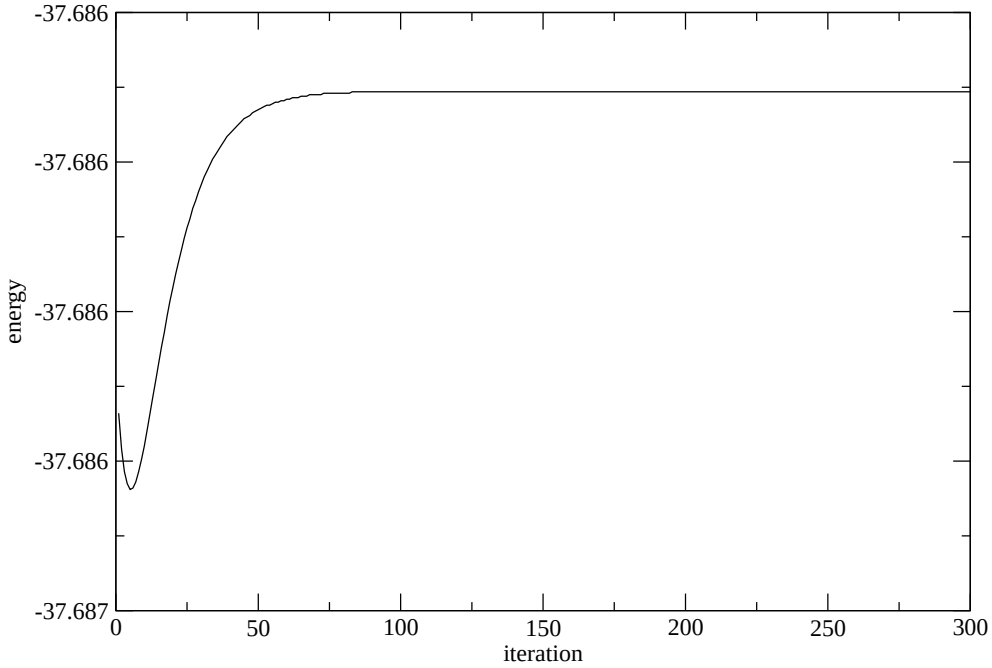

FIGURE 3.13: Total Hund's rule predicted ground state energy of carbon during convergence for nmax=3 and 0.25 fractional excitation.

Ease of convergence and state mixing can be shown by examining the eigenvectors in Figure 3.14. The plot is of the $(n = 2, \ell = 1, m_\ell = -1, m_s = \uparrow)$ valence spin orbital projection into each non-zero basis state. Systems that experience convergence difficulties will not display this smooth change in eigenvector coefficients.

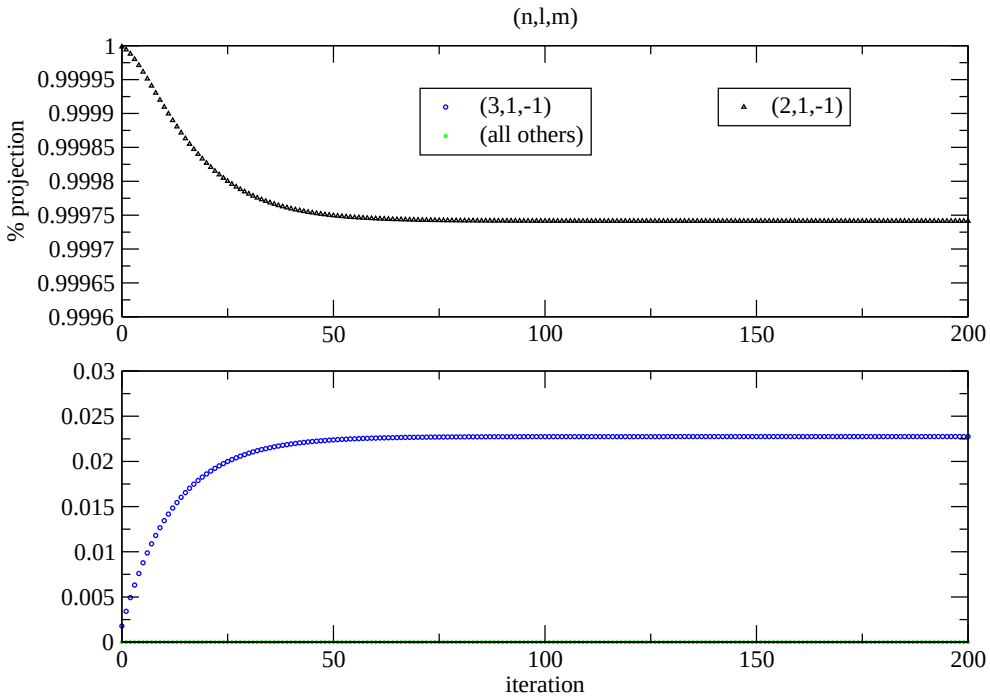

FIGURE 3.14: Eigenvector of the 2p(m=-1) spin orbital of carbon during convergence. The basis states were generated with 0.25 fractional excitation and has nmax=3.

To cause convergence problems in carbon an excited state with large coupling between angular states is required. To achieve this strong coupling the spins of many p orbital electrons needs to be the same. Figure 3.15 shows an example of such a state. The 1s shell is closed and all of the remaining four electrons are spin up. The electronic configuration is thus $E[(1s); 200\uparrow; 21-1\uparrow; 210\uparrow; 211\uparrow]$.

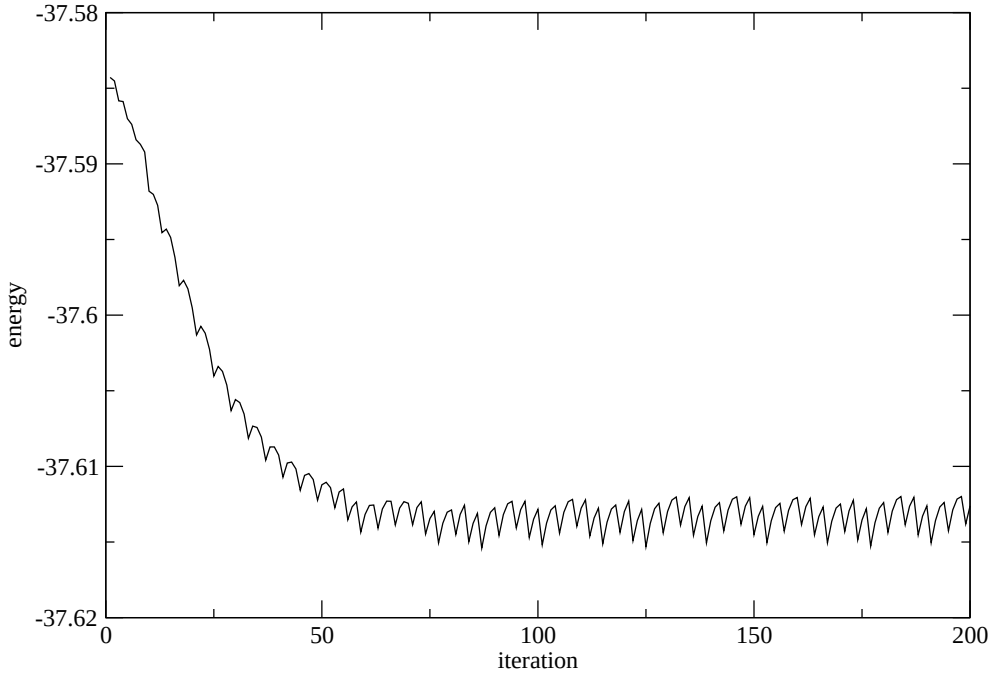

FIGURE 3.15: Total energy of an excited $E[(1s); 200\ \uparrow, 21-1\ \uparrow, 210\ \uparrow, 211\ \uparrow]$ state of carbon during convergence instabilities. The basis states were generated with 0.25 fractional excitation and has nmax=3.

The eigenvalues for each iteration shed some light onto the cause. Figure 3.16 shows the eigenvalues of the four spin up valence electrons. What is important is the switching between eigenvalues. The 2p degeneracies have been lifted and coupling is strong between them. What is the fourth eigenvalue one iteration can become third the next. This dynamic switching, when not tracked properly, can cause additional instabilities not related to fundamental problem of the system.

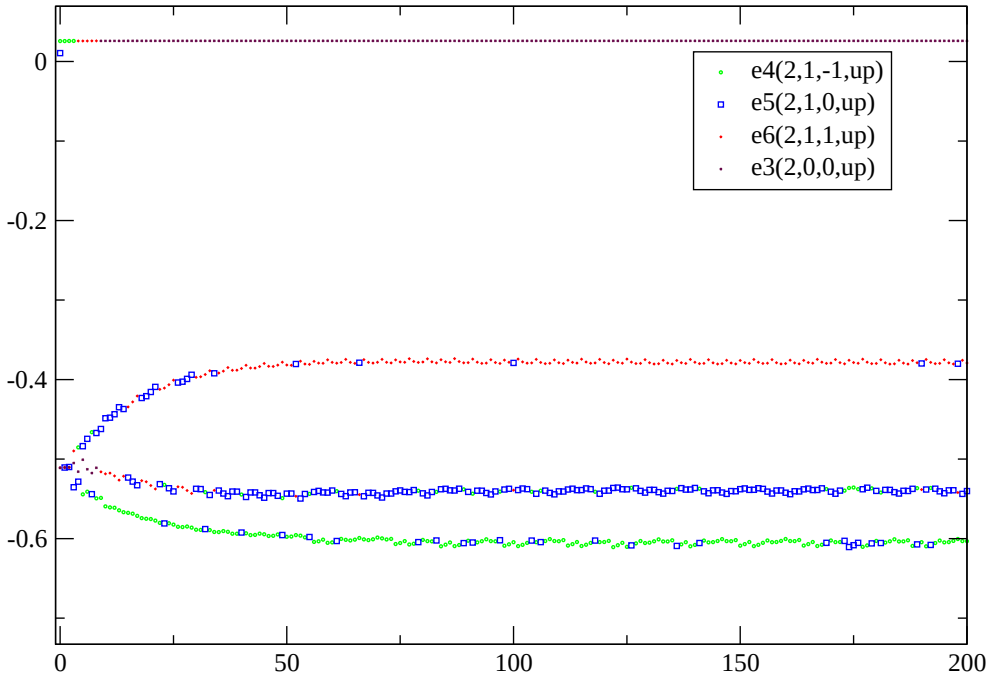

FIGURE 3.16: 2p spin-up degenerate eigenvalues lifted for an excited $E[(1s); 200\uparrow, 21-1\uparrow, 210\uparrow, 211\uparrow]$ state of carbon. The basis states were generated with 0.25 fractional excitation and has nmax=3.

Another tool for examining poor convergence is to look at the eigenvector of each electron from iteration to iteration. Figure 3.17 is a plot of all three 2p spin orbit projections into each 2p basis state. Each is mostly in its respectively set state with a non-zero portion in each of the other 2p states. The mixing is heavy and the coarse switching of each projection is seen. This was done with a coarse convergence mixing term. Smaller mixing ratios from iteration to iteration can damp this behavior but never eliminate it.

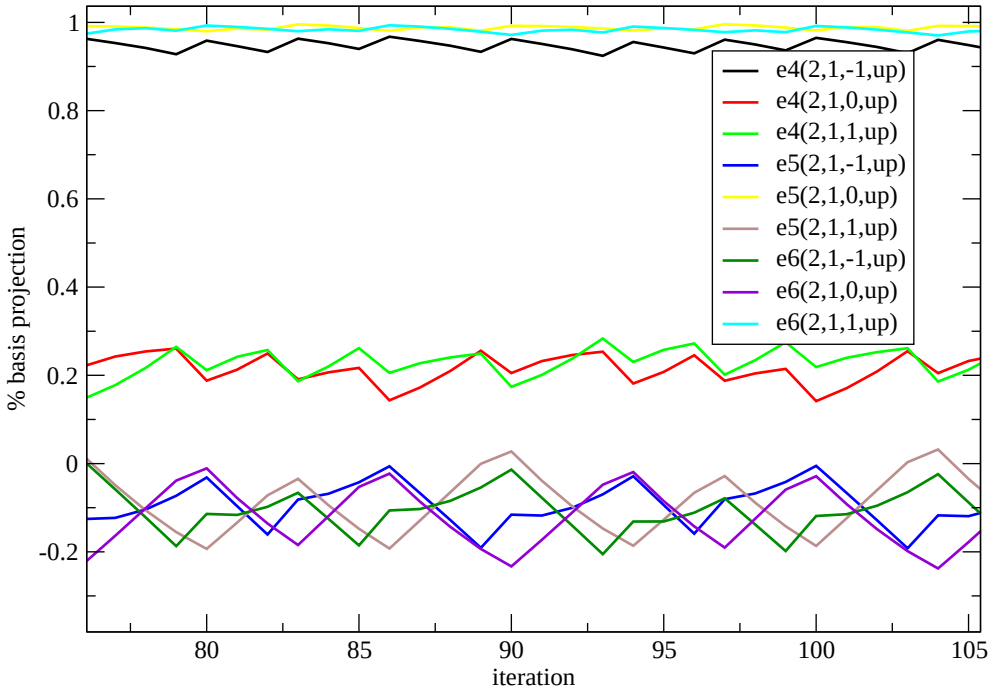

FIGURE 3.17: 2p spin orbit eigenvector for an excited $E[(1s); 200\uparrow, 21-1\uparrow, 210\uparrow, 211\uparrow]$, non-convergent, state of carbon. The basis states were generated with 0.25 fractional excitation and has nmax=3.

Symmetry

Breaking spherical symmetry and using spin unrestricted Hartree-Fock still results in electronic configurational degeneracies. Kinetic and nuclear potentials are single particle operators that result in equal contributions to the total Fock matrix of each spin. The electron-electron interaction is where the true coupling of the orbital and spin angular momentum occur. The direct electrostatic interaction involves this coupling, but like the kinetic and nuclear potentials the contribution is the same, for each spin, to the total Fock matrix. The breaking of spin symmetry occurs in the exchange electrostatic term. This term arose when the total wave function was required to be antisymmetric under exchange of particle. It would seem natural that the ease of exchanging a particle would be dependent on if the spins are the same or different. The data in Table 3.8 shows this symmetry. In this case the first of the two valence electrons is in the $(n = 2, \ell = 1, m_\ell =$

$-1, m_s = \uparrow$) state. For a second electron of the same spin the energy is degenerate for $m_\ell = \pm 1$. For a second electron of different spin this degeneracy is broken. Notice these differences are at the fifth or sixth decimal place.

TABLE 3.8: Total energy of carbon with an electron excited into n=3 states. Broken symmetries allow for the large number of unique configurations.

n, ℓ, m_ℓ, m_s	*Energy*	n, ℓ, m_ℓ, m_s	*Energy*
3,1,-1,↑	-37.326118	3,1,-1,↓	-37.324271
3,1,0,↑	-37.325540	3,1,0,↓	-37.325253
3,1,1,↑	-37.324867	3,1,1,↓	-37.324271
3,2,-2,↑	-37.286028	3,2,-2,↓	-37.286018
3,2,-1,↑	-37.286080	3,2,-1,↓	-37.286074
3,2,0,↑	-37.286096	3,2,0,↓	-37.286093
3,2,1,↑	-37.286076	3,2,1,↓	-37.286074
3,2,2,↑	-37.286021	3,2,2,↓	-37.286018

Configurations with electrons of like spin consistently have a lower energy than those with opposite spin. Those configurations with an l=1 angular momentum form a band of closely lying energies that is separate from the band of energies for the l=2 states. These energies represent all the unique configurations for exciting the one valence electron into either a 3p or 3d state.

3.4 Basis Set Completeness

To explore the effects of generating different basis sets boron will be studied. Boron is good to explore this effect because of the lone, out of closed subshells, electron. Generating these basis sets was done by filling the 1s and 2s subshells. The remaining electron

must then fractionally occupy higher states if a density for that higher state is to be determined. For each of these basis states 90% of remaining electron is in the labelled state below. The remaining 10% is then populated into higher states to yield densities and thus wave functions for those states. This effectively changes the state each basis set emphasizes.

TABLE 3.9: Boron energies with different basis sets and electronic configurations. The lowest energy configuration is $E[(2s); 210 \uparrow]$ and the most complete basis is generated with excitations into the 3s state.

e configuration	2p	3s	3p	3d
$E[(2s); 21 \pm 1 \uparrow]$	-24.7083294	-24.97204287	-24.96048109	-24.97137308
$E[(2s); 210 \uparrow]$	-24.7083295	-24.97217379	-24.96062186	-24.97151478
$E[(2s); 300 \uparrow]$	-24.3720293	-24.45812448	-24.45650109	-24.46245391
$E[(2s); 31 \pm 1 \uparrow]$	-24.3334285	-24.34764089	-24.35110004	-24.36335369

The first observation of the data in Table 3.9 is that lowest energy electron configuration, regardless of basis set, is when the fifth electron is in the n=2, m=0 state. The next interesting feature is the basis set that emphasized the 2p states are not the lowest energy basis set. The 3s basis set is consistently the lowest energy set. This is due to the large coupling between the 1s, 2s and 3s states. As the degrees of freedom for the fifth electron increase the energy should decrease. When the 3s basis set is used more of that electron spreads into the higher, virtual orbitals. Specifically the eigenvector is not entirely in the (210) state but is distributed partially into the 3s state. This increases the degrees of freedom and decreases the energy.

4. EXPERIMENTAL VERIFICATION

Finding the total energy of an atom is valuable for theoretical analysis but comparison to experimental data is limited. Experimentally finding the total energy of an atom requires stripping one electron off at a time and adding up the total energy required to completely ionize all electrons from the atom. This is possible for only very light atoms as the technical difficulties of stripping electrons, one at a time, from a heavy atom are much more difficult. The more electrons an atom has the closer the higher energy states lie. The uncertainty in which electron you've experimentally probed becomes relevant and the total energy cannot be precisely determined.

What can be determined is the difference between stable electronic states. Exciting an electron into a higher energy configuration will result in a relaxation back to the ground state. The energy of the photon released during this relaxation can be measured and compared to differences in HF electronic configurations. This is the theory behind spectroscopy and extensive data, for almost all atoms, can be found at the National Institute for Standards and Technology (NIST) website [25].

Spectroscopic experiments can only determine the difference in energy between states of total angular momentum L and total spin S. The freedom to break all spatial symmetries in HF means the energies calculated are for a specific uncoupled electronic configuration. Degeneracy is broken for different m states. Many electronic configurations have the same total L and S. The uncoupled energies must be averaged appropriately to get a total L and S energy to compare to experiment. The coupling of angular momentum is used to find an appropriate coupled state in terms of uncoupled states. A coupled state comprised of all CSF that posses the appropriate symmetry is called a full Configuration Interaction state [20].

4.1 Addition of Angular Momentum

For a full Configuration Interaction, coupling of all electron configurations that satisfy a given total orbital angular momentum and total spin vector must be made.

$$\overrightarrow{L} = \sum_{i}^{N} \overrightarrow{l}_i \quad and \quad \overrightarrow{S} = \sum_{i}^{N} \overrightarrow{s}_i$$

Closed shells have total $|\overrightarrow{L}| = 0$ and $|\overrightarrow{S}| = 0$. Only electrons out of closed shells will be coupled together. The state for a given electronic configuration is a tensor product of both the total spin and orbital angular momentum wave function.

$$\Psi \equiv |L, M_l\rangle \otimes |S, M_s\rangle \tag{4.1}$$

Many different m_l and m_s combinations maintain the symmetry of the same total L and S state.

First consider the coupling of two electrons [26]. The angular momentum coupled state $|l, m_l\rangle$ can be expanded into all the combinations of uncoupled states$|\ell_1, m_{\ell_1}; \ell_2, m_{\ell_2}\rangle$.

$$|\ell, m_\ell; \ell_1, \ell_2\rangle = \sum_{m_{\ell_1}}^{\ell_1} \sum_{m_{\ell_2}}^{\ell_2} \mathcal{C}^{\ell, m_\ell}_{\ell_1, m_{\ell_1}, \ell_2, m_{\ell_2}} |\ell_1, m_{\ell_1}; \ell_2, m_{\ell_2}\rangle \tag{4.2}$$

Each uncoupled state has a coefficient $\mathcal{C}$ that represents the strength of the coupling between the uncoupled and coupled states. These are the well known Clebsch-Gordan coefficients and are defined as the overlap of three spherical harmonics.

$$\mathcal{C}^{l, m_l}_{\ell_1, m_{\ell_1}, \ell_2, m_{\ell_2}} = \langle l_1, m_{\ell_1}; l_2, m_{\ell_2} | l, m\rangle \tag{4.3}$$

A feature of the Clebsch-Gordan coefficients is that if $m_\ell \neq m_{\ell_1} + m_{\ell_2}$ than $\mathcal{C} = 0$. This can be applied as a delta function $\delta(m_\ell = m_{\ell_1} + m_{\ell_2})$ to avoid computations of zero. Coupling two electrons is nice but many important configurations involve coupling three or more electrons.

The coupling of three electrons will illustrate the richness of the physics of properly coupled states while avoiding the drudgery of coupling four or more electrons. To couple three electron's angular momentum you first couple two as shown above. Then the third is coupled to the first two's coupled state.

$$|L, M_L; \ell_1, \ell_2, \ell_3\rangle = \sum_{m_\ell}^{\ell} \sum_{m_{\ell_3}}^{\ell_3} \mathcal{C}^{L,M_L}_{\ell,m_\ell,\ell_3,m_{\ell_3}} |\ell, m_\ell; \ell_3, m_{\ell_3}\rangle \tag{4.4}$$

As expected to couple a fourth electron the procedure is simply repeated. Spin adds like orbital angular momentum vectors so the procedure is also the same for spin. The resulting total coupled spin state for three electrons, in terms of uncoupled spin states, is below.

$$|S, M_S; s_1, s_2, s_3\rangle = \sum_{m_s}^{s} \sum_{m_{s_3}}^{s_3} \mathcal{C}^{S,M_S}_{s,m_s,s_3,m_{s_3}} |s, m_s; s_3, m_{s_3}\rangle \tag{4.5}$$

The same requirement of the angular momentum quantum numbers must be satisfied for the spin, $m_s = m_{s_1} + m_{s_2}$ and $m_S = m_s + m_{s_3}$.

Expanded out the total tensor product of the spatial and spin coupled states is below. The order of electron one coupled to electron two, then that coupled to the third has been assumed. The properly coupled total wave function for a set of three bosons is below.

$$|L, M_L; \ell_1, \ell_2, \ell_3\rangle \otimes |S, M_S; s_1, s_2, s_3\rangle = \tag{4.6}$$
$$\sum_{m_\ell, m_{\ell_3}}^{all} \sum_{m_{\ell_1}, m_{\ell_2}}^{all} \sum_{m_s, m_{s_3}}^{all} \sum_{m_{s_1}, m_{s_2}}^{all} \kappa^{m_{\ell_1}, m_{\ell_2}, m_{\ell_3}}_{m_{s_1}, m_{s_2}, m_{s_3}} |\Psi^{m_{\ell_1}, m_{\ell_2}, m_{\ell_3}}_{m_{s_1}, m_{s_2}, m_{s_3}}\rangle$$

Here the combination of Clebsch-Gordan coefficients is denoted as,

$$\kappa^{m_{\ell_1}, m_{\ell_2}, m_{\ell_3}}_{m_{s_1}, m_{s_2}, m_{s_3}} = \mathcal{C}^{L,M_L}_{\ell,m_\ell,\ell_3,m_{\ell_3}} \mathcal{C}^{\ell,m_\ell}_{\ell_1,m_{\ell_1},\ell_2,m_{\ell_2}} \mathcal{C}^{S,M_S}_{s,m_s,s_3,m_{s_3}} \mathcal{C}^{s,m_s}_{s_1,m_{s_1},s_2,m_{s_2}} \tag{4.7}$$

with the product of uncoupled spatial and spin states

$$|\Psi^{m_{\ell_1}, m_{\ell_2}, m_{\ell_3}}_{m_{s_1}, m_{s_2}, m_{s_3}}\rangle = |\ell_1, m_{\ell_1}; \ell_2, m_{\ell_2}; \ell_3, m_{\ell_3}\rangle \otimes |s_1, m_{s_1}; s_2, m_{s_2}; s_3, m_{s_3}\rangle \tag{4.8}$$

The order implies the relations: $m_\ell = m_{\ell_1} + m_{\ell_2}$, $M_L = m_\ell + m_{\ell_3}$, $m_s = m_{s_1} + m_{s_2}$ and $M_S = m_s + m_{s_3}$.

4.2 Many-Fermion Angular Coupling

The total wave function for a set of electronic configurations must remain antisymmetric under particle exchange. This is due to the fermion nature of electrons. To enforce this condition a new array $\mathcal{A}$ is defined to be an anti-symmetrized version of the κ array. The first condition is when two electrons are in the same state.

$$\left\{ \begin{array}{llllll} n_1 = n_2, & \ell_1 = \ell_2, & m_{\ell_1} = m_{\ell_2}, & m_{s_1} = m_{s_2} & \Rightarrow & \mathcal{A}^{m_{\ell_1},m_{\ell_2},m_{\ell_3}}_{m_{s_1},m_{s_2},m_{s_3}} = 0 \\ n_1 = n_3, & \ell_1 = \ell_3, & m_{\ell_1} = m_{\ell_3}, & m_{s_1} = m_{s_3} & \Rightarrow & \mathcal{A}^{m_{\ell_1},m_{\ell_2},m_{\ell_3}}_{m_{s_1},m_{s_2},m_{s_3}} = 0 \\ n_3 = n_2, & \ell_3 = \ell_2, & m_{\ell_3} = m_{\ell_2}, & m_{s_3} = m_{s_2} & \Rightarrow & \mathcal{A}^{m_{\ell_1},m_{\ell_2},m_{\ell_3}}_{m_{s_1},m_{s_2},m_{s_3}} = 0 \end{array} \right\} \tag{4.9}$$

The next configuration that must be considered is where multiple electrons occupy the same n and ℓ state. If each electron have the same m_ℓ state then this violates the pauli exclusion principle and that configuration is not allowed. The condition of like spin will follow the same as for like m_ℓ and will be omitted for now, to more clearly show the antisymmetrizing method. A permutation operator will be used to enforce the pauli exclusion principle.

$$p_{i,j,k} = -1^{(\eta_{i,j,k})} \tag{4.10}$$

Here is the case for each pair of electrons that share the same principal and orbital angular quantum number.

$$\left\{ \begin{array}{lll} n_1 = n_2, & \ell_1 = \ell_2 \Rightarrow & A^{m_{\ell_1},m_{\ell_2},m_{\ell_3}}_{m_{s_1},m_{s_2},m_{s_3}} = \frac{1}{2}(\kappa^{m_{\ell_1},m_{\ell_2},m_{\ell_3}}_{m_{s_1},m_{s_2},m_{s_3}} p_{1,2,3} + \kappa^{m_{\ell_2},m_{\ell_1},m_{\ell_3}}_{m_{s_2},m_{s_1},m_{s_3}} p_{2,1,3}) \\ n_1 = n_3, & \ell_1 = \ell_3 \Rightarrow & A^{m_{\ell_1},m_{\ell_2},m_{\ell_3}}_{m_{s_1},m_{s_2},m_{s_3}} = \frac{1}{2}(\kappa^{m_{\ell_1},m_{\ell_2},m_{\ell_3}}_{m_{s_1},m_{s_2},m_{s_3}} p_{1,2,3} + \kappa^{m_{\ell_3},m_{\ell_2},m_{\ell_1}}_{m_{s_3},m_{s_2},m_{s_1}} p_{3,2,1}) \\ n_2 = n_3, & \ell_2 = \ell_3 \Rightarrow & A^{m_{\ell_1},m_{\ell_2},m_{\ell_3}}_{m_{s_1},m_{s_2},m_{s_3}} = \frac{1}{2}(\kappa^{m_{\ell_1},m_{\ell_2},m_{\ell_3}}_{m_{s_1},m_{s_2},m_{s_3}} p_{1,2,3} + \kappa^{m_{\ell_1},m_{\ell_3},m_{\ell_2}}_{m_{s_1},m_{s_3},m_{s_2}} p_{1,3,2}) \end{array} \right\} \tag{4.11}$$

For each combination of like m_ℓ's the term in $\mathcal{A}$ array will be zero.

The most degenerate case is when all three electrons occupy the same n and ℓ state. The permutation operator again insures terms that are symmetric under exchange are set to zero.

$$\left\{ \begin{array}{ll} n_1 = n_2, & n_1 = n_3 \\ \ell_1 = \ell_2, & \ell_1 = \ell_3 \end{array} \right\} \Rightarrow A^{m_{\ell_1},m_{\ell_2},m_{\ell_3}}_{m_{s_1},m_{s_2},m_{s_3}} = \frac{1}{6} \left(\begin{array}{ll} \kappa^{m_{\ell_1},m_{\ell_2},m_{\ell_3}}_{m_{s_1},m_{s_2},m_{s_3}} p_{1,2,3} & +\kappa^{m_{\ell_1},m_{\ell_3},m_{\ell_2}}_{m_{s_1},m_{s_3},m_{s_2}} p_{1,3,2} \\ +\kappa^{m_{\ell_2},m_{\ell_1},m_{\ell_3}}_{m_{s_2},m_{s_1},m_{s_3}} p_{2,1,3} & +\kappa^{m_{\ell_2},m_{\ell_3},m_{\ell_1}}_{m_{s_2},m_{s_3},m_{s_1}} p_{2,3,1} \\ +\kappa^{m_{\ell_3},m_{\ell_2},m_{\ell_1}}_{m_{s_3},m_{s_2},m_{s_1}} p_{3,2,1} & +\kappa^{m_{\ell_3},m_{\ell_1},m_{\ell_2}}_{m_{s_3},m_{s_1},m_{s_2}} p_{3,1,2} \end{array} \right) \tag{4.12}$$

Finally if none of the states are the same then symmetry under exchange is not an issue and the term remains the same.

$$A^{m_{\ell_1},m_{\ell_2},m_{\ell_3}}_{m_{s_1},m_{s_2},m_{s_3}} = \kappa^{m_{\ell_1},m_{\ell_2},m_{\ell_3}}_{m_{s_1},m_{s_2},m_{s_3}} \tag{4.13}$$

Applying the same method to electrons of like spin the fully anti-symmetrized coupled state is defined. This state can now be used to find the total coupled energy. This is a Configuration Interaction function because it is a linear combination of single Slater determinants. It is an eigenstate of the square of angular momentum $\widehat{L}^2$ and spin operator $\widehat{S}^2$.

$$|L, M_L, S, M_S\rangle = \sum_{m_\ell,m_{\ell_3}}^{all} \sum_{m_{\ell_1},m_{\ell_2}}^{all} \sum_{m_s,m_{s_3}}^{all} \sum_{m_{s_1},m_{s_2}}^{all} A^{m_{\ell_1},m_{\ell_2},m_{\ell_3}}_{m_{s_1},m_{s_2},m_{s_3}} |\Psi^{m_{\ell_1},m_{\ell_2},m_{\ell_3}}_{m_{s_1},m_{s_2},m_{s_3}}\rangle \tag{4.14}$$

Since the system is now in an eigenstate of the non-relativistic Schrödinger equation the energies obtained are comparable to experiment. The energy is calculated as follows:

$$E_{L,M_L,S,M_S} = \langle L, M_L, S, M_S | \epsilon \left[\begin{array}{cccc} n_1 & \ell_1 & m_{\ell_1} & m_{s_1} \\ n_2 & \ell_2 & m_{\ell_2} & m_{s_2} \\ n_3 & \ell_3 & m_{\ell_3} & m_{s_3} \end{array} \right] |L, M_L, S, M_S\rangle \tag{4.15}$$

Where $\epsilon[\ ]$ is the energy of the uncoupled CSF produced by the UHF program. The final coupled energy is now a sum over uncoupled energies multiplied by the square of an anti-symmetrized coupling array.

$$E_{L,M_L,S,M_S} = \sum_{m_\ell,m_{\ell_3}}^{all} \sum_{m_{\ell_1},m_{\ell_2}}^{all} \sum_{m_s,m_{s_3}}^{all} \sum_{m_{s_1},m_{s_2}}^{all} \epsilon \begin{bmatrix} n_1 & \ell_1 & m_{\ell_1} & m_{s_1} \\ n_2 & \ell_2 & m_{\ell_2} & m_{s_2} \\ n_3 & \ell_3 & m_{\ell_3} & m_{s_3} \end{bmatrix} |A^{m_{\ell_1},m_{\ell_2},m_{\ell_3}}_{m_{s_1},m_{s_2},m_{s_3}}|^2 \tag{4.16}$$

4.3 Results: Boron

To see the results of configuration interaction calculations compared with spectroscopic data boron will be used [25]. Boron's ground state has the 1s and 2s subshells closed. A closed subshell has zero total orbital angular momentum and spin. That means only one electron contributes to the total L and S. The electronic configuration of the ground state is thus $1s^2 2s^1 2p^1$ and with the p electron in $m_\ell = 0$ state the energy is -24.972 hartrees.

Once you excite a 2s electron into the p state, three electrons contribute to the total L and S. Boron makes a good example because its ground state requires no coupling but the excited states of $1s^2 2s^1 2p^2$ require coupling of at least three electrons and it's just complicated enough for an example. The total angular momentum of the excited 2p states can be $L = 0, 1, 2$ and the total spin can be $S = \frac{1}{2}, \frac{3}{2}$. Even in the coupled state a configuration can still have different M_L and M_S. These coupled energies are averaged to give a theoretical energy of a L and S state. Table 4.1 shows those energies and the difference from the ground state.

TABLE 4.1: Configuration interaction energies for boron L, S, M_l, M_s states. Comparison to experiment for the first excited state of boron differs by millihartrees.

L	S	M_L	M_S	E	*Average E*	ΔE	*Exp. E*
1	$\frac{3}{2}$	0	$\pm\frac{3}{2}$	-24.885387	-24.839842	0.132158	0.1315415
1	$\frac{3}{2}$	±1	$\pm\frac{3}{2}$	-24.885302			
1	$\frac{3}{2}$	±1	$\pm\frac{1}{2}$	-24.797284			
1	$\frac{3}{2}$	0	$\pm\frac{1}{2}$	-24.788495			
2	$\frac{1}{2}$	±2	$\pm\frac{1}{2}$	-24.799605	-24.803175	0.168825	0.2180522
2	$\frac{1}{2}$	±1	$\pm\frac{1}{2}$	-24.812803			
2	$\frac{1}{2}$	0	$\pm\frac{1}{2}$	-24.791061			
0	$\frac{1}{2}$	0	$\pm\frac{1}{2}$	-24.795333	-24.795333	0.176667	0.2896036
1	$\frac{1}{2}$	±1	$\pm\frac{1}{2}$	-24.781765	-24.780305	0.191695	0.3304385
1	$\frac{1}{2}$	0	$\pm\frac{1}{2}$	-24.777386			

For the first excitation the difference in energy between experiment and HF theory with DFT basis states is in millihartrees. Further comparison shows the accuracy of the model decreases as the excitation increases. This is expected because the basis sets are those best suited to the ground state. The accuracy of the first excited state provides evidence for the validity of the HF model.

5. IMMERSED ATOM

The system of an impurity atom in a metal can be posed as an approximately solvable many-body problem [27][28][3][4][1][29]. What makes many-body problems difficult are the larger number of simultaneous equations. Solutions are possible through iterative approximations but the computation time required increases rapidly with an increased number of equations. HF is especially guilty of these large computation times because of its M^4 basis size scaling. The saving features of a metal are that the atoms only interact slightly with the free electrons and free electrons can be modelled well as a electron gas.

Large conductivities found in metals are due to small free electron scattering off the atomic lattice [6]. The background electron gas is only a small perturbation on the bound atomic electrons. Such a system is nice because the free and bound electrons are almost isolated systems. Solutions to a free electron gas are well known and result in simple plane wave basis states. The assumption is that if an electron gas separates two atoms, and the gas has little effect on each atom, then each atom should have an even less effect on each other. This is a bold claim that must be tested. If true, a rather complicated many-many-body problem can be reduced to a much more simple many-body problem. Such a system includes a single atom immersed into a free electron gas. The density of free electrons in a metal is an experimentally obtainable and is what connects this model to the real world.

5.1 Theory Overview

Immersing an atom into an electron gas could be done a number of different ways. One possible way would be to expand your space to include all electronic states in the gas. For a free atom with nmax=3, the state space is on the order of *fourteen*. Computational

convergence time for my HF code is many minutes. Increasing to an nmax=4 increases state space to order *thirty*, but increased the computational time to many hours. A brute force increase in state space to include a continuous energy electron gas is not currently possible. The goal of the immersion theory presented here is to couple a free atom to an electron gas without extending state space to unrealistic sizes.

Keeping the order of the Hamiltonian small will be done by folding the plane wave state space into the bound electron space. This will achieve coupling the large number of free electron states into a Hamiltonian space no larger than that of the atom. A perturbation technique by Löwdin accomplishes this feat. Derivation for a new perturbed Fock matrix is then implemented into the HF iterative scheme. The system then converges with the influence of the gas on the free atom, without increasing state space. Shifts in the total energy and charge density can then be used to understand the effects of the immersion.

5.1.1 Basis State Extensions

A step towards immersing an atom into a free electron gas was to explore the effects of extending the basis states to greater radii. The question to be answered was whether or not compressing or extending the charge density would lower the energy of the system. Immersed DFT calculations have shown the energy decreases as atoms are immersed into jellium [3],[4]. This is due to the increased degrees of freedom the system obtains when coupling the free to the bound electrons. The coupling between each system will only occur if the interaction lowers the energy. Since the system still has the state of the free atom, the coupling will at worst not change the energy. The expectation is it will actually lower the energy.

To simulate this effect each wave function was modified by a multiplicative function that spreads out the charge. This basis set could then be explored for completeness. The function that spreads out the charge must be one that once multiplied to the wave function

will keep the result continuous and smooth. With the goal of only spreading out the tail of each function the cosh function was chosen.

$$if\ r < R; \qquad R'_{nl}(r) = R_{nl}(r) \tag{5.1}$$

$$if\ r \geq R; \qquad R'_{nl}(r) = R_{nl}(r)\cosh(\mathsf{C}\sqrt{\varepsilon_{nl}}(r-R))$$

The parameter R is the radius where the extension will occur. The resulting function will remain continuous because $\cosh(r-R) = 1\big|_{r=R}$ and smooth because $\frac{d}{dr}\cosh(r-R) = 0\big|_{r=R}$. Various extension radii R, were explored to learn about the effect on the total energy. The coefficient C is typically a number between zero and one providing the ability to strengthen and weaken the extension. The pre-factor $\sqrt{\varepsilon_{nl}}$ is a number to scale the effect by how bound a state is. The eigenvalues of the converged DFT provided these numbers.

Once this is done the new more dispersed wave function is re-normalized according to Eq. 2.2. Figure 5.1.1 is a plot of the 1s electronic state of carbon with progressively more extension into the free electron gas. The original 1s was generated with a fractionally low excitation occupation.

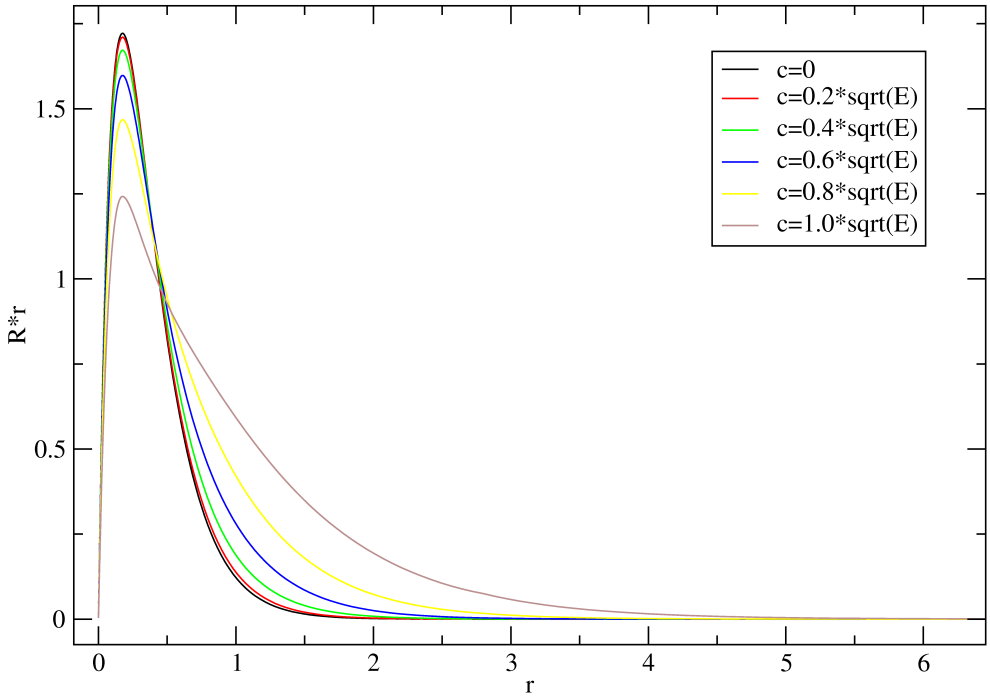

FIGURE 5.1: 1s basis state of carbon as it is dispersed away from the nucleus by $R_{new}(r) = R_{old}(r) r \cosh(c\sqrt{E}(r - R))$.

The dispersion occurs past the inflection point but the re-normalization lowers the charge density near the nucleus while increasing it further away.

To see the effects of extending the wave functions away from the nucleus the total converged energy is in Table 5.1.

TABLE 5.1: Total energy for carbon, with various dispersions out from the nucleus with the equation $R_{new}(r) = R_{old}(r)r\cosh(c\sqrt{E}(r-R))$. This is compared to many different basis states.

C	$R=1$	$R=2$	$R=3$	$R=10$	$R=1stpeak$	$R=lastpeak$
0.2	-37.458	-37.472	-37.477	-37.480	-37.439	-37.443
0.4	-37.377	-37.444	-37.468	-37.479	-37.164	-37.197
0.6	-37.189	-37.384	-37.449	-37.477	-36.148	-36.232
0.8	-36.798	-37.257	-37.415	-37.474	-33.384	-33.301
1.0	-36.011	-36.968	-37.342	-37.469	-27.228	-26.152

This shows the energy increases as the basis set extension increases. A plot of these energies in Figure 5.2 shows how extending the basis set more increases the total energy.

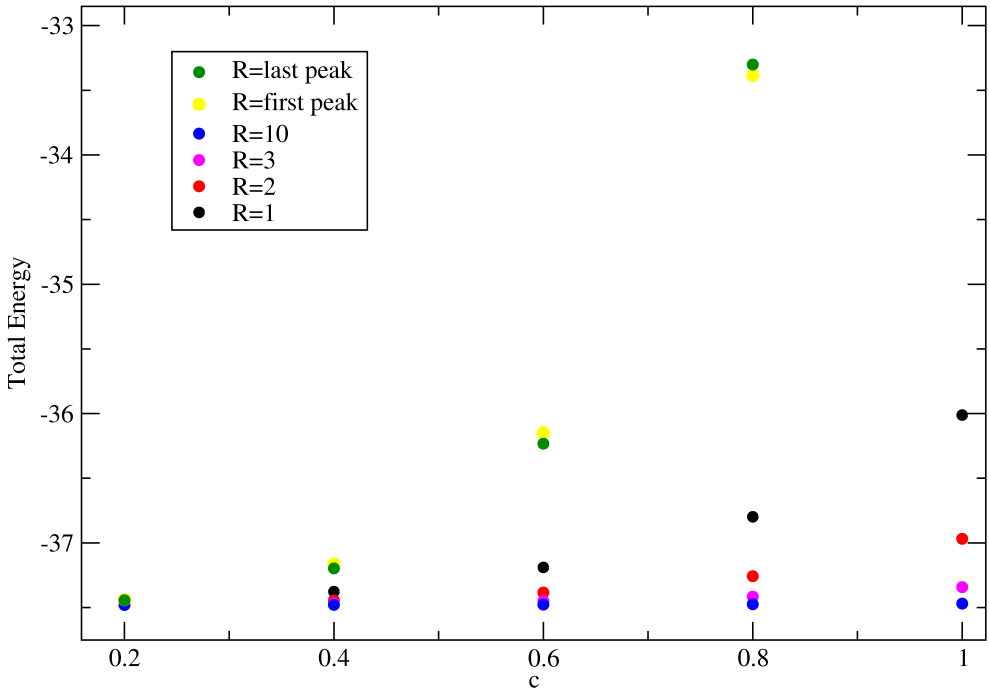

FIGURE 5.2: Energy of carbon with basis states extended out from the nucleus with $R_{new}(r) = R_{old}(r)r\cosh(c\sqrt{E}(r-R))$. The electronic state is $E[(2s); 210\uparrow; 211\uparrow]$.

This can be understood by the fact that simply spreading out the charge, of the same number of basis states, doesn't increase any degrees of freedom. The energy could then be greater because the original basis set, from converged DFT, represented a fairly complete set when compared to exact Roothaan HF. If the charge is spread far enough away the electrons are no longer bound and the total energy of the system has increased to positive values.

Conversion for this set of states is can take up to 300 iterations. The 2p electrons are coupled to each other and mixing between each other occurs. The (210) electron's projection into the 210 state is almost identical to the (211) electron's projection into the 211 state. This effect is shown on the top half of Figure 5.3.

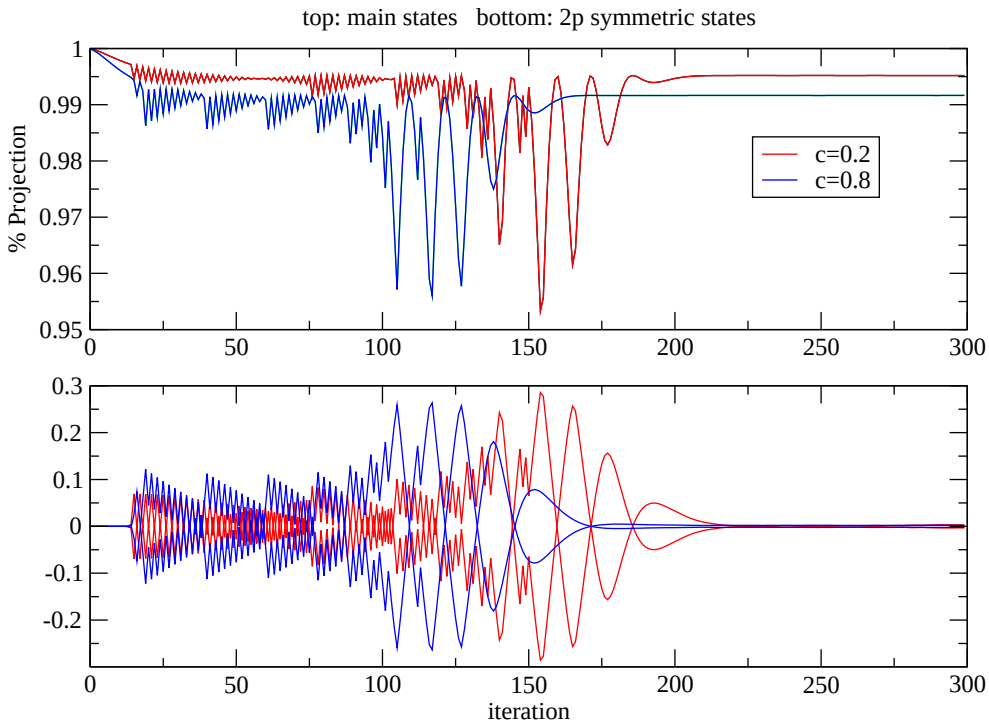

FIGURE 5.3: 2p eigenvector coefficients for carbon with dispersed states. Electron configuration is $E[(2s); 210\uparrow; 211\uparrow]$.

The bottom half of the plot shows the coupling between the different electrons basis

states. Here the different electrons minority projections are not the same. The (210) electron's projection into the 211 state is different then the (211) electron's projection into the 210 state.

The other feature of the convergence is the difference between the extended states. The wave functions that are spread out away from the nucleus converge quicker. The smaller, earlier oscillations are larger for the more dispersed states while the larger, later oscillations are smaller for more dispersed states.

5.1.2 Löwdin

The Schrödinger equation is well suited for perturbation expansions. The Hamiltonian can be perturbed by a potential energy V and $H = H_o + V$. The perturbation potential is expanded as a power series of some parameter λ. A different approach to the perturbation of the Schrödinger equation was posed by Löwdin [8]. This method separates the unperturbed states into two classes, A and B. Löwdin derived a set of linear equations, akin to those in Hartree-Fock, that describe A with the influence of B. The application to immersions is that a set of atomic states A, can be coupled to a set of electronic gas states B, through this perturbation.

The many-body HF Schrödinger equation is the starting point for deriving the perturbation. Here it is expressed as a linear set of equations for N states. The notation that follows is that of Löwdin [8].

$$\sum_{n=1}^{N}(H_{mn} - E\delta_{mn})c_n = 0, \quad m = 1, 2...N \tag{5.2}$$

Now separate the states into two classes A and B. The sum over the H_{mn} must also be separated into two sums, over each set of states. A slight rearrangement and this looks like:

$$(E - H_{mm})c_m = \sum_{n}^{A} H'_{mn}c_n + \sum_{n}^{B} H'_{mn}c_n \tag{5.3}$$

where the prime denotes only off-diagonal terms. Before performing the perturbation expansion a new notation is useful where $h'_{mn} = \frac{H'_{mn}}{(E-H_{mm})}$.

$$c_m = \sum_n^A h'_{mn} c_n + \sum_n^B h'_{mn} c_n \tag{5.4}$$

Next the B states are eliminated by recursively substituting equation **??**, for c_m, into the coefficient associated with the B states. B states are thus folded into the A states through a perturbation expansion.

$$c_m = \sum_n^A (h'_{mn} + \sum_\alpha^B h'_{m\alpha} h'_{\alpha n} + \sum_{\alpha\beta}^B h'_{m\alpha} h'_{\alpha\beta} h'_{\beta n} + ...) c_n \tag{5.5}$$

A necessary condition is the expansion parameter h'_{mn} must be much less than unity $|H'_{mn}/(E - H_{mn})| \ll 1$ to ensure convergence. Substituting back in h'_{mn} and adopting a new notation, the expansion to the unperturbed Hamiltonian matrix is found.

$$U^A_{mn} = H_{mn} + \sum_\alpha^B \frac{H'_{m\alpha} H'_{\alpha n}}{E - H_{\alpha\alpha}} + \sum_{\alpha\beta}^B \frac{H'_{m\alpha} H'_{\alpha\beta} H'_{\beta n}}{(E - H_{\alpha\alpha})(E - H_{\beta\beta})} + ... \tag{5.6}$$

The set of linear equations can now be expressed in terms of U^A_{mn}.

$$\sum_n^A (U^A_{mn} - E\delta_{mn}) c_n = 0, \quad m \; in \; (A) \tag{5.7}$$

This approach sets up an eigenvalue problem where two classes of states (A and B), are reduced to one class of states (A), with the influence of B on A accounted for through an expansion. The free atom Fock matrix will simply be replaced by the new perturbed matrix U^A_{mn}. Once the coefficients (c_n) to A are found, the coefficients (c_m) for B can also be found.

$$c_m = \sum_n^A \frac{U^A_{mn}}{E - H_{mm}} c_n, \quad m \; in \; (B) \tag{5.8}$$

Löwdin envisioned the method would be useful in MO-LCAO theory. The perturbation procedure shown above will be used in a similar way to model free atoms immersed in jellium.

5.1.3 Hydrogen Function Perturbation

To test the validity of Löwdin's perturbation theory a hydrogen atom is immersed into two plane wave states. The hydrogen and free electron wave functions are well known. The Hamiltonian can be solved exactly and compared to perturbation theory. The use of analytic equations lends well to using mathematical software. Maple is used for modelling these hydrogen systems.

The first system tested was a single 1s hydrogen wave function (α), immersed into two plane waves with wave vectors k and κ. The Hamiltonian matrix for this system can be determined and exact solutions exist at energies where the determinant to this matrix equals zero.

$$\mathcal{H}^3 = \begin{Vmatrix} H_{\alpha\alpha} - e & H_{\alpha k} & H_{\alpha\kappa} \\ H_{\alpha k} & H_{kk} - e & H_{\kappa k} \\ H_{\alpha\kappa} & H_{k\kappa} & H_{\kappa\kappa} - e \end{Vmatrix} \tag{5.9}$$

The superscript on $\mathcal{H}$ refers to three total states. With just one bound state α, equation 5.6 up to first order can be rearranged to following:

$$U^1 = (e - H_{kk})(e - H_{\kappa\kappa})\left(H_{\alpha\alpha} + \frac{H_{\alpha k}^2}{e - H_{kk}} + \frac{H_{\alpha\kappa}^2}{e - H_{\kappa\kappa}} - e\right) \tag{5.10}$$

Setting equation 5.10 equal to zero will satisfy equation 5.7. Extending this to second order and requiring U^2 equal zero yields an equation to compare the order of perturbation.

$$U^2 = (e - H_{kk})(e - H_{\kappa\kappa})\left(H_{\alpha\alpha} + \frac{H_{\alpha k}^2}{e - H_{kk}} + \frac{H_{\alpha\kappa}^2}{e - H_{\kappa\kappa}} + 2\frac{H_{\alpha k}H_{k\kappa}H_{\kappa\alpha}}{(e - H_{kk})(e - H_{\kappa\kappa})} - e\right) \tag{5.11}$$

Solutions to the system exist for each model when the det$\mathcal{H}^3 = 0$, $U^1 = 0$ and $U^2 = 0$. These quantities can be plotted as a function of energy for a given value of each electron gas's wave vector. For $k = 1$ and $\kappa = 2$ this plot is shown in Figure 5.4.

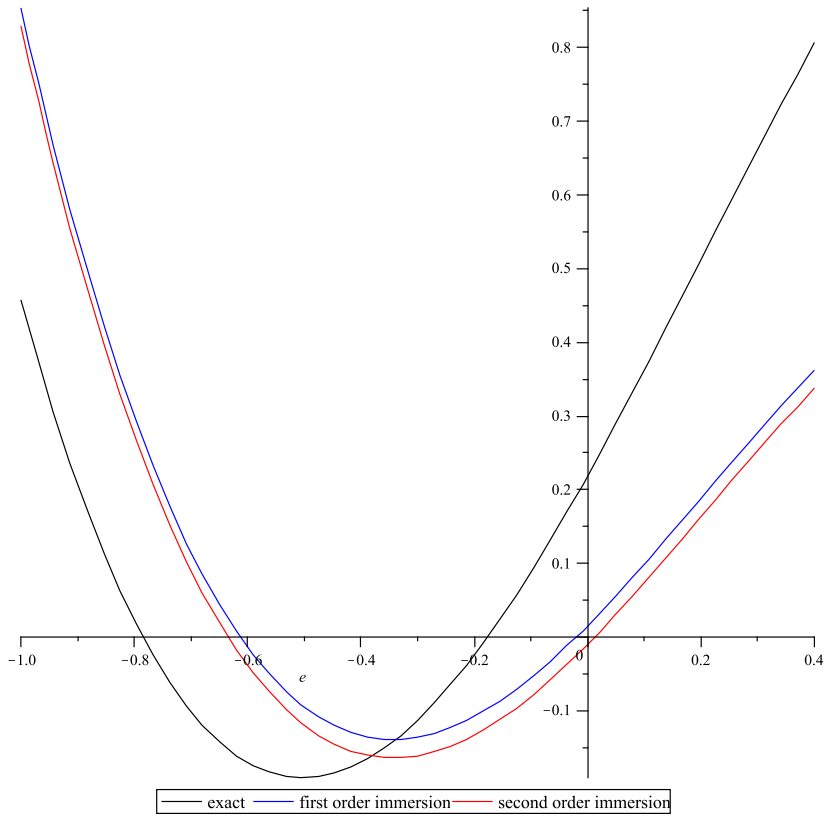

FIGURE 5.4: 1s hydrogen state coupled to two plane wave states with wave numbers k=1 and kappa=2. First and second order Löwdin perturbation is compared to the exact solution. The vertical axis is U^1, U^2 and the det[Hamiltonian].

Here the solutions are the zeros of each function. The free atom ground state energy is 0.5 hartrees. Each technique was successful in lowering the energy with the exact solution of the Hamiltonian matrix being the lowest. Extending the perturbation to second order has the effect of lowering the energy 0.02 hartrees more than first order. The window of the plot doesn't show the third solution, which is greater than 0.4 hartrees.

The next state to couple to a 1s hydrogen electron would be the 2s state. This simple model will now be extended to include the 2s state as an additional degree of freedom for

the bound hydrogen electron. The new exact Hamiltonian matrix will now be:

$$\mathcal{H}^4 = \left\| \begin{array}{cccc} H_{\alpha\alpha} - e & H_{\alpha\beta} & H_{\alpha k} & H_{\alpha\kappa} \\ H_{\beta\alpha} & H_{\beta\beta} - e & H_{\beta k} & H_{\beta\kappa} \\ H_{k\alpha} & H_{k\beta} & H_{kk} - e & H_{k\kappa} \\ H_{\kappa\alpha} & H_{\kappa\beta} & H_{\kappa k} & H_{\kappa\kappa} - e \end{array} \right\| \tag{5.12}$$

For the perturbation with two bound states, equation **??** expands to a set of two equations. The matrix whose determinant must be set to zero, up to first order is:

$$\mathcal{L}^1 = \left\| \begin{array}{cc} H_{\alpha\alpha} + \frac{H_{\alpha k}^2}{e - H_{kk}} + \frac{H_{\alpha\kappa}^2}{e - H_{\kappa\kappa}} - e, & H_{\alpha\beta} + \frac{H_{\alpha k} H_{k\beta}}{e - H_{kk}} + \frac{H_{\alpha\kappa} H_{\kappa\beta}}{e - H_{\kappa\kappa}} \\ H_{\beta\alpha} + \frac{H_{\beta k} H_{k\alpha}}{e - H_{kk}} + \frac{H_{\beta\kappa} H_{\kappa\alpha}}{e - H_{\kappa\kappa}}, & H_{\beta\beta} + \frac{H_{\beta k}^2}{e - H_{kk}} + \frac{H_{\beta\kappa}^2}{e - H_{\kappa\kappa}} - e \end{array} \right\| \tag{5.13}$$

The second order matrix $\mathcal{L}^2$ looks similar with the addition of $H_{\alpha k} H_{k\kappa} H\kappa\beta$ cross terms. Solutions to the perturbation system occur when the following equations are set to zero.

$$U^1 = (e - H_{kk})(e - H_{\kappa\kappa}) det(\mathcal{L}^1) \tag{5.14}$$

$$U^2 = (e - H_{kk})(e - H_{\kappa\kappa}) det(\mathcal{L}^2)$$

The plot of the det$\mathcal{H}^4$, U^1 and U^2 is in Figure 5.5. Here all three techniques lower the energy less than the free atom.

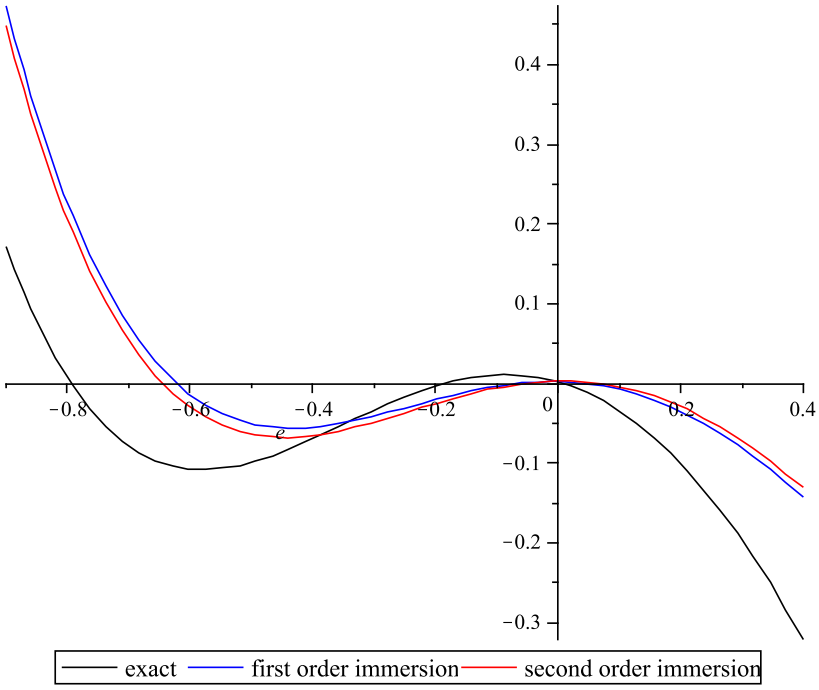

FIGURE 5.5: Two hydrogen states coupled to two plane wave states. First and second order Löwdin perturbation is compared to the exact solution. The vertical axis is U^1, U^2 and the det[Hamiltonian]

The lowering is much less than when just one bound state exists. The difference between the exact, first and second order is also greatly reduced.

Overall the method posed by Löwdin had the effect of lowering the energy of a hydrogen atom immersed into a two state gas. The general shape of Löwdin's equations follows that of the exact solution. These results justify an effort to extend this technique to heavier atoms with many different free electron wave vectors. The bound wave function will be found through the HF self consistent field method.

5.2 Numerical Implementation: First Order

To immerse an atom into the free-electron gas the perturbation theory suggested by Löwdin is used [8]. The free atom will be treated as the main system with the electron gas as a small perturbation. With a set of plane wave perturbation states the sum over states is a sum over wave vectors. Assuming the volume is large enough to warrant a continuous k-space the sum can be turned into an integral.

$$U_{\alpha\beta} = F_{\alpha\beta} + \sum_{k}^{k_f} \frac{H'_{\alpha k} H'_{k\beta}}{(E - H_{kk})} = F_{\alpha\beta} + \frac{1}{V_k} \int_0^{k_f} \frac{H'_{\alpha k} H'_{k\beta}}{(E - H_{kk})} k^2 d\overrightarrow{k} \tag{5.15}$$

$F_{\alpha\beta}$ is the regular Fock matrix, k the electron gas state, k_f is the Fermi wave vector, and E is an eigenvalue from the Fock matrix. The factor $\frac{1}{V_k}$ is required to maintain dimensionality when converting from a sum to an integral.

The goal of this derivation is to separate the spatial integrals in the Hamiltonian H from the wave vector integrals above. Then the spatial integrals can be calculated numerically, while the k-space integrals analytically.

5.2.1 Immersed Kinetic Energy Terms

In general, the terms of the immersed Fock matrix will look similar to those of the free atom. Complications arise when the electron gas plane wave states are expanded multiple times. The features of these expansions can easily be seen in single particle energy terms. The kinetic energy term that couples an atomic state α to a free electron is:

$$T_{\alpha k}(\overrightarrow{k}) = -\int \Phi^*_\alpha(\overrightarrow{r}) \frac{\nabla^2}{2} \Phi(\overrightarrow{r}, \overrightarrow{k}) d\overrightarrow{r} \tag{5.16}$$

The wave function for free electron states $\Phi(\overrightarrow{r}, \overrightarrow{k})$ are assumed to be infinite plane waves with normalization constant $\frac{1}{\sqrt{V}}$. $T_{\alpha k}$ is assumed to be hermitian, thus the kinetic energy operator can operate on either the atomic or free electron state. Operating on the plane wave simply returns a k^2 and the plane wave back again.

$$T_{\alpha k}(\overrightarrow{k}) = -\frac{1}{2\sqrt{V}} \int \Phi_{\alpha}^{*}(\overrightarrow{r}) \nabla^2 e^{i\overrightarrow{k}\cdot\overrightarrow{r}} d\overrightarrow{r} = -\frac{k^2}{2\sqrt{V}} \int \Phi_{\alpha}^{*}(\overrightarrow{r}) e^{i\overrightarrow{k}\cdot\overrightarrow{r}} d\overrightarrow{r} \tag{5.17}$$

To avoid the complexity of $\overrightarrow{k} \cdot \overrightarrow{r}$ the plane wave will be expanded into spherical Bessel functions [18]. The angular part of a spherical Bessel function is a spherical harmonic. This allows the angular and radial integrals to be separated.

$$e^{i\overrightarrow{k}\cdot\overrightarrow{r}} = 4\pi \sum_{\ell_k, m_k}^{\infty} (i)^{\ell_k} j_{\ell_k}(kr) Y_{\ell_k m_k}(\theta_r, \phi_r) Y_{\ell_k m_k}^{*}(\theta_k, \phi_k) \tag{5.18}$$

The angular integral equals a delta function that requires the angular quantum numbers of each state to be equal. In $T_{\alpha k}$ and Φ_{α}^{*}, α refers to a basis state with quantum numbers n_α, ℓ_α and m_ℓ. The sum is not collapsed so that both the kinetic and nuclear Coulomb terms are consistent with the electron-electron Coulomb energy terms. When the k-space integrals are performed analytically each energy term will have the same summation structure.

$$T_{n_\alpha l_\alpha m_\alpha}(\overrightarrow{k}) = -\frac{2\pi k^2}{\sqrt{V}} \sum_{l_k, m_k}^{\infty} (i)^{l_k} \int \varphi_{n_\alpha l_\alpha}^{*}(r) j_{l_k}(kr) r^2 dr Y_{l_k m_k}^{*}(\theta_k, \phi_k) \delta_{l_\alpha l_k} \delta_{m_\alpha m_k} \tag{5.19}$$

The radial Bessel functions are dependent on both k and r. At this point it is important to note that an alternate way of implementing Löwdin's theory would be to perform double numeric integrations over k and r. This was originally seen as introducing unnecessary error associated with double numeric integration. In hindsight the chosen expansion may restrict the range of the model more than the numerical error would have. This point should be tested in the future.

Since the bound states are not dependent on k, decoupling the spatial r and k-space k integrals will allow separate integrations. The expansion below will decouple a Bessel function into two separable equations [9].

$$j_{l_k}(kr) = \sum_{s=0}^{\infty} c_{s l_k} k^{2s+l_k} r^{2s+l_k}, \quad c_{s l_k} = \frac{2^{l_k}(-1)^s (s+l_k)!}{s!(2s+2l_k+1)!} \tag{5.20}$$

Now the radial integrals are reduced to powers of r multiplied by a bound state radial function. The summation index s, for a free electron state, now plays a role similar to the principal quantum number n of a bound state. This is in principle a fine expansion but in practice the maximum possible s value will have to be explored.

$$T_{n_\alpha l_\alpha m_\alpha}(\overrightarrow{k}) = -\frac{2\pi k^2}{\sqrt{V}} \sum_{l_k,m_k}^{\infty} (i)^{l_k} \sum_{s=0}^{\infty} c_{sl_k} k^{2s+l_k} \int \varphi^*_{n_\alpha l_\alpha}(r) r^{2s+l_k} r^2 dr Y^*_{l_k m_k}(\theta_k, \phi_k) \delta_{l_\alpha l_k} \delta_{m_\alpha m_k} \tag{5.21}$$

With the radial integrals reduced to a scalar array $\tau^s_{n_\alpha l_\alpha}$, concentration can be focused on the free electron wave vector contribution.

$$T_{n_\alpha l_\alpha m_\alpha}(\overrightarrow{k}) = \frac{1}{\sqrt{V}} \sum_{l_k,m_k}^{\infty} \sum_{s=0}^{\infty} (i)^{l_k} c_{sl_k} \tau^s_{n_\alpha l_\alpha} k^2 k^{2s+l_k} Y^*_{l_k m_k}(\theta_k, \phi_k) \delta_{l_\alpha l_k} \delta_{m_\alpha m_k} \tag{5.22}$$

$$\tau^s_{n_\alpha l_\alpha} = -2\pi \int \varphi^*_{n_\alpha l_k}(r) r^{2s+l_k} r^2 dr$$

5.2.2 Immersed Nuclear Energy Terms

The nuclear Coulomb potential follows quite similarly. In terms of the bessel functions the nuclear Coulomb energy term is:

$$V_{n_\alpha l_\alpha m_\alpha}(\overrightarrow{k}) = -\frac{4\pi Z}{\sqrt{V}} \sum_{l_k,m_k}^{\infty} (i)^{l_k} \int \varphi^*_{n_\alpha l_\alpha}(r) j_{l_k}(kr) r dr Y^*_{l_k m_k}(\theta_k, \phi_k) \delta_{l_\alpha l_k} \delta_{m_\alpha m_k} \tag{5.23}$$

The big difference between the nuclear and kinetic energy terms is the power of k. For the kinetic energy term the second order derivative left an additional k^2.

$$V_{n_\alpha l_\alpha m_\alpha}(\overrightarrow{k}) = -\frac{4\pi Z}{\sqrt{V}} \sum_{l_k,m_k}^{\infty} (i)^{l_k} \sum_{s=0}^{\infty} c_{sl_k} k^{2s+l_k} \int \varphi^*_{n_\alpha l_\alpha}(r) r^{2s+l_k} r dr Y^*_{l_k m_k}(\theta_k, \phi_k) \delta_{l_\alpha l_k} \delta_{m_\alpha m_k} \tag{5.24}$$

Leaving the summations in the same order as the kinetic energy term the single particle energy terms are *form similar* with the only difference in the power of k.

$$V_{n_\alpha l_k m_k}(\overrightarrow{k}) = \frac{1}{\sqrt{V}} \sum_{l_k,m_k}^{\infty} \sum_{s=0}^{\infty} (i)^{l_k} c_{sl_k} \upsilon^s_{n_\alpha l_\alpha} k^{2s+l_k} Y^*_{l_k m_k}(\theta_k, \phi_k) \delta_{l_\alpha l_k} \delta_{m_\alpha m_k} \tag{5.25}$$

$$\upsilon^s_{n_\alpha l_\alpha} = -4\pi Z \int \varphi^*_{n_\alpha l_\alpha}(r) r^{2s+l_k} r dr$$

5.2.3 Direct and Exchange Terms

The Coulomb interaction between the electrons bound to an atom and those free to move in an electron gas, can be modelled under the scheme of Hartree-Fock theory nicely. The HF direct *e*-*e* Coulomb contribution to the Hamiltonian, before many functions are expanded, was derived in section **??**.

$$J_\alpha(\overrightarrow{k}) = \sum_{\beta\gamma}^{M} c_{j\beta} c^*_{j\gamma} \int\int d\overrightarrow{r} d\overrightarrow{r'} \varphi^*_\alpha(\overrightarrow{r}) \frac{\varphi^*_\beta(\overrightarrow{r'}) \varphi_\gamma(\overrightarrow{r'})}{|\overrightarrow{r} - \overrightarrow{r}'|} \Phi(\overrightarrow{r}, \overrightarrow{k}) \tag{5.26}$$

Following the expansion of the Coulomb potential Eq(**??**) and the plane wave expansions, the direct *e*-*e* immersion term has a large number of detailed notations. The goal will be to simplify $J_\alpha(\overrightarrow{k})$ to an expression that separates dependence on k, like those derived for the kinetic and nuclear potential energy terms.

Using the expansion (ref equation))for $\frac{1}{|\overrightarrow{r_i} - \overrightarrow{r_j}|}$, the Bessel plane wave expansion (ref equation) and the separable equation expansions (ref eq), the expression for direct Coulomb interaction of a bound state with the gas becomes:

$$J_{n_\alpha l_\alpha m_\alpha}(\overrightarrow{k}) = \frac{1}{\sqrt{V}} \sum_{n_\beta l_\beta m_\beta}^{all} \sum_{n_\gamma l_\gamma m_\gamma}^{all} \sum_{l=0}^{\infty} \sum_{m=-l}^{l} \sum_{l_k m_k}^{\infty} \sum_{s=0}^{\infty} (i)^{l_k} c_{sl_k} k^{2s+l_k} Y^*_{l_k m_k}(\theta_k, \phi_k) \tag{5.27}$$

$$c^*_{i,n_\beta l_\beta m_\beta} c_{i,n_\gamma l_\gamma m_\gamma} \frac{4(2\pi)^4}{2l+1} \int\int \varphi^*_{n_\alpha l_\alpha}(r_1) \varphi^*_{n_\beta l_\beta}(r_2) \frac{r^l_<}{r^{l+1}_>} \varphi_{n_\gamma l_\gamma}(r_2) r_1^{2s+l_k} r_1^2 r_2^2 dr_1 dr_2$$

$$\int Y^*_{l_\alpha m_\alpha}(\theta_{r1}, \phi_{r1}) Y_{lm}(\theta_{r1}, \phi_{r1}) Y_{l_k m_k}(\theta_{r1}, \phi_{r1}) d\Omega_1$$

$$\int Y^*_{l_\beta m_\beta}(\theta_{r2}, \phi_{r2}) Y^*_{lm}(\theta_{r2}, \phi_{r2}) Y_{l_\gamma m_\gamma}(\theta_{r2}, \phi_{r2}) d\Omega_2$$

The first piece that can be defined as a scalar array is the set of radial integrals. Generating this array is very similar to that of the bound states with one of the four wave functions replaced with r to an integer power. One of the dangers in these expressions are those progressively higher powers of r. The combination of the other three wave functions $\varphi_{n_\gamma l_\gamma}(r_2)$ then must go to zero quickly enough to cancel out this rapid increase.

$$\iota^{n_\alpha n_\beta n_\gamma s}_{l_\alpha l_\beta l_\gamma l_k l} = \int\int \varphi^*_{n_\alpha l_\alpha}(r_1)\varphi^*_{n_\beta l_\beta}(r_2)\frac{r^l_<}{r^{l+1}_>}\varphi_{n_\gamma l_\gamma}(r_2) r_1^{2s+l_k} r_1^2 r_2^2 dr_1 dr_2 \tag{5.28}$$

The three spherical harmonic integrals can be condensed to another scalar array.

$$\{\begin{smallmatrix} l_\alpha & l & l_k \\ m_\alpha & m & m_k \end{smallmatrix}\} = \int Y^*_{l_\alpha m_\alpha}(\theta_r,\phi_r) Y_{lm}(\theta_r,\phi_r) Y_{l_k m_k}(\theta_r,\phi_r) d\Omega \tag{5.29}$$

A few additional steps will be made to simplify all the expression that doesn't involve the k-space integrals. Putting the radial together with the angular results in a single array for all the spatial integrals,

$$\varsigma\begin{bmatrix} n_\alpha & n_\beta & n_\gamma & s \\ l_\alpha & l_\beta & l_\gamma & l_k \\ m_\alpha & m_\beta & m_\gamma & m_k \end{bmatrix} = \frac{4(2\pi)^4}{2l+1} c^*_{i,n_\beta l_\beta m_\beta} c_{i,n_\gamma l_\gamma m_\gamma} \iota^{n_\alpha n_\beta n_\gamma s}_{l_\alpha l_\beta l_\gamma l_k l} \{\begin{smallmatrix} l_\alpha & l & l_k \\ m_\alpha & m & m_k \end{smallmatrix}\}\{\begin{smallmatrix} l_\beta & l & l_\gamma \\ m_\beta & m & m_\gamma \end{smallmatrix}\} \tag{5.30}$$

Now the sums not involving α or k states are done.

$$\varsigma^{s l_k m_k}_{n_\alpha l_\alpha m_\alpha} = \sum_{n_\beta l_\beta m_\beta}^{all} \sum_{n_\gamma l_\gamma m_\gamma}^{all} \sum_{l=0}^{\infty} \sum_{m=-l}^{l} \varsigma\begin{bmatrix} n_\alpha & n_\beta & n_\gamma & s \\ l_\alpha & l_\beta & l_\gamma & l_k \\ m_\alpha & m_\beta & m_\gamma & m_k \end{bmatrix} \tag{5.31}$$

Deceivingly the resulting expression allows calculations of wave vector integrals. The form is the same as those for the kinetic and nuclear energies. In term of the spatial integrals $\varsigma^{s l_k m_k}_{n_\alpha l_\alpha m_\alpha}$, the direct e-e Coulomb contribution to the immersed Hamiltonian is:

$$J_{n_\alpha l_\alpha m_\alpha}(\overrightarrow{k}) = \frac{1}{\sqrt{V}} \sum_{l_k m_k}^{\infty} \sum_{s=0}^{\infty} (i)^{l_k} c_{s l_k} k^{2s+l_k} Y^*_{l_k m_k}(\theta_k,\phi_k) \varsigma^{s l_k m_k}_{n_\alpha l_\alpha m_\alpha} \tag{5.32}$$

All of this procedure will repeat for the electron-electron Coulomb exchange term. The only difference will be a switch between γ states and k states.

$$\zeta^{sl_km_k}_{n_\alpha l_\alpha m_\alpha} = \sum_{n_\beta l_\beta m_\beta}^{all} \sum_{n_\gamma l_\gamma m_\gamma}^{all} \sum_{l=0}^{\infty} \sum_{m=-l}^{l} \varsigma \begin{bmatrix} n_\alpha & n_\beta & s & n_\gamma \\ l_\alpha & l_\beta & l_k & l_\gamma \\ m_\alpha & m_\beta & m_k & m_\gamma \end{bmatrix} \tag{5.33}$$

$$K_{n_\alpha l_\alpha m_\alpha}(\overrightarrow{k}) = \frac{1}{\sqrt{V}} \sum_{l_k m_k}^{\infty} \sum_{s=0}^{\infty} (i)^{l_k} c_{sl_k} k^{2s+l_k} Y^*_{l_k m_k}(\theta_k, \phi_k) \zeta^{sl_km_k}_{n_\alpha l_\alpha m_\alpha} \tag{5.34}$$

This is the expression for the exchange e-e Coulomb contribution to the immersed Hamiltonian.

5.2.4 *k*-space Integrations

All dependence in k must now be organized so that the integration in k-space can be performed. The denominator of equation 5.6 has a dependence on k due to the energy of a free electron. Derived in section 2.1.1, the energy of a free electron is simply the kinetic energy.

$$H_{kk} = T_{kk} = -\int e^{-i\overrightarrow{k}\cdot\overrightarrow{r}} \frac{\nabla^2}{2} e^{i\overrightarrow{k}\cdot\overrightarrow{r}} d\overrightarrow{r} = \frac{k^2}{2} \tag{5.35}$$

The Hamiltonian $H'_{n_\alpha l_\alpha m_\alpha}(\overrightarrow{k})$ will be simplified by grouping like powers of k. The kinetic energy term has an additional k^2 from the Laplacian, while each of the potential energies has the same power of k. From the separable equation expansion they each have a common $k^{2s+\ell_k}$.

$$H'_{n_\alpha l_\alpha m_\alpha}(\overrightarrow{k}) = \frac{1}{\sqrt{V}} \sum_{l_k, m_k}^{\infty} \sum_{s=0}^{\infty} (i)^{l_k} c_{sl_k} k^{2s+l_k} [k^2 \tilde{\tau}^s_{n_\alpha l_\alpha} + \varrho^{sl_km_k}_{n_\alpha l_\alpha m_\alpha}] Y^*_{l_k m_k}(\theta_k, \phi_k) \tag{5.36}$$

The spatial integrals with the delta functions not yet applied are defined below.

$$\varrho^{sl_km_k}_{n_\alpha l_\alpha m_\alpha} = \upsilon^s_{n_\alpha l_k m_k} \delta_{l_\alpha l_k} \delta_{m_\alpha m_k} + \varsigma^{sl_km_k}_{n_\alpha l_\alpha m_\alpha} + \zeta^{sl_km_k}_{n_\alpha l_\alpha, m_\alpha}, \quad \tilde{\tau}^s_{n_\alpha l_\alpha} = \tau^s_{n_\alpha l_\alpha} \delta_{l_\alpha l_k} \delta_{m_\alpha m_k} \tag{5.37}$$

Collapsing of the sums for the single particle terms angular delta functions will happen after the k integral. The $H'_{n_\beta l_\beta m_\beta}$ term looks the same with primes to denote different s, ℓ_k and m_k's.

$$H'_{n_\beta l_\beta m_\beta}(\overrightarrow{k}) = \frac{1}{\sqrt{V}} \sum_{l'_k, m'_k}^{\infty} \sum_{s'=0}^{\infty} (-i)^{l'_k} c^{s' l'_k} k^{2s'+l'_k} [k^2 \tilde{\tau}^{s'}_{n_\beta l_\beta} + \varrho^{s' l'_k m'_k}_{n_\beta l_\beta m_\beta}] Y^*_{l'_k m'_k}(\theta_k, \phi_k) \tag{5.38}$$

The numerator in the first order perturbation term can now be written with all the spatial information compressed into a simplified notation.

$$H'_{n_\alpha l_\alpha m_\alpha}(\overrightarrow{k})H'_{n_\beta l_\beta m_\beta}(\overrightarrow{k}) = \frac{1}{V}\sum_{l_k,m_k}^{\infty}\sum_{s=0}^{\infty}\sum_{s'=0}^{\infty} c^{sl_k}c^{s'l_k}k^{2s+2s'+2l_k}[\varepsilon_3 k^4 + \varepsilon_2 k^2 + \varepsilon_1] \quad (5.39)$$

Here $\delta_{l_k l'_k}\delta_{m_k m'_k}$ from the wave vector angular integral has now been applied. The spatial integral arrays are denoted with ε's to simplify the expression and to group like powers of k.

$$\varepsilon_3 \equiv \tilde{\tau}^{s}_{n_\alpha l_\alpha}\tilde{\tau}^{s'}_{n_\beta l_\beta}, \quad \varepsilon_2 \equiv \tilde{\tau}^{s}_{n_\alpha l_\alpha}\varrho^{s'l_k m_k}_{n_\beta l_\beta m_\beta} + \tilde{\tau}^{s'}_{n_\beta l_\beta}\varrho^{sl_k m_k}_{n_\alpha l_\alpha m_\alpha}, \quad \varepsilon_1 \equiv \varrho^{sl_k m_k}_{n_\alpha l_\alpha m_\alpha}\varrho^{s'l_k m_k}_{n_\beta l_\beta m_\beta} \quad (5.40)$$

Now the full first order element in the immersed contribution to the Fock matrix is three integrals over similar functions of k. These integrals over k-space can be done analytically. The total immersed Fock matrix $U_{\alpha\beta}$ is the addition of these immersed terms to those of the free atom Fock matrix.

$$U_{\alpha\beta} = F_{\alpha\beta} + \frac{1}{(2\pi)^3}\sum_{l_k,m_k}^{\infty}\sum_{s=0}^{\infty}\sum_{s'=0}^{\infty} c_{sl_k}c^{s'l_k}\int_0^{k_f}\frac{\varepsilon_3 k^{2s+2s'+2l_k+6} + \varepsilon_2 k^{2s+2s'+2l_k+4} + \varepsilon_1 k^{2s+2s'+2l_k+2}}{(E - \frac{k^2}{2})}dk \quad (5.41)$$

The extra k^2 comes from the all space integral over $d\overrightarrow{k}$. The pre-factor is from both real and wave vector space normalization, $\frac{1}{VV_k} = \frac{1}{(2\pi)^3}$ [6][13].

The first step in performing the integral is to rewrite the expression with a substitution $y = \frac{k}{\sqrt{2E}}$. Now the problem can be formulated as an arbitrary integer power of y, divided by one plus the square of y.

$$\int_0^{k_f}\frac{2k^{2n}}{(-2E - k^2)}dk = \int_0^{k_f}\frac{2k^{2n}}{-2E(1 + \frac{k^2}{2E})}dk = \frac{-\sqrt{2E}^{2n}}{E}\int_0^{k_f}\frac{y^{2n}}{1+y^2}\sqrt{2E}dy \quad (5.42)$$

$$= -2^{n+\frac{1}{2}}E^{n-\frac{1}{2}}\int_0^{k_f}\frac{y^{2n}}{1+y^2}dy, \quad n = s + s' + l_k$$

This integral can be done by recursively stepping down the power of the numerator. Each time this is done a simple power integral is produced with the addition of the same original

integral, only the power of the numerator is less by two. This can be done until the powers in the numerator are zero.

$$\int_0^{k_f} \frac{y^{2n}}{1+y^2}dy = \int_0^{k_f} \frac{y^{2n-2}(y^2+1-1)}{1+y^2}dy = \int_0^{k_f} y^{2n-2}dy - \int_0^{k_f} \frac{y^{2n-2}}{1+y^2}dy \tag{5.43}$$

$$= \int_0^{k_f} y^{2n-2}dy - \int_0^{k_f} y^{2n-4}dy + \int_0^{k_f} y^{2n-6}dy + ... + (-1)^{n-1}\int_0^{k_f} dy + (-1)^n \int_0^{k_f} \frac{1}{1+y^2}dy$$

$$= \left[\frac{y^{2n-1}}{2n-1} - \frac{y^{2n-3}}{2n-3} + \frac{y^{2n-5}}{2n-5} + ... + (-1)^{n-1}y + (-1)^n \arctan(y)\right]_0^{\frac{k_f}{\sqrt{E}}}$$

The integral has been performed and the result can be denoted as a sum over integers.

$$\int_0^{k_f} \frac{y^{2n}}{1+y^2}dy = \left[\sum_{j=0}^{n-1}(-1)^j \frac{y^{2n-2j-1}}{2n-2j-1} + (-1)^n \arctan(y)\right]_0^{\frac{k_f}{\sqrt{E}}} \tag{5.44}$$

$$= \sum_{j=0}^{n-1}(-1)^j \frac{1}{\sqrt{E}^{2n-2j-1}} \frac{k_f^{2n-2j-1}}{2n-2j-1} + (-1)^n \arctan(\frac{k_f}{\sqrt{E}})$$

After applying the limits of the integration the result can be multiplied by the constants that arose from the original y substitution in equation 5.42.

$$\int_0^{k_f} \frac{2k^{2n}}{(-2E-k^2)}dk = -\sum_{j=0}^{n-1}(-1)^j 2^{n+\frac{1}{2}} E^j \frac{k_f^{2n-2j-1}}{2n-2j-1} - (-1)^n 2^{n+\frac{1}{2}} E^{n-\frac{1}{2}} \arctan(\frac{k_f}{\sqrt{E}}) \tag{5.45}$$

The final step before putting all of this together is to write $U_{\alpha\beta}$ in a form that takes advantage of the integral solved above.

$$U_{\alpha\beta} = F_{\alpha\beta} + \frac{1}{(2\pi)^3}\sum_{l_k,m_k}^{\infty}\sum_{s=0}^{\infty}\sum_{s'=0}^{\infty} c_{sl_k}c^{s'l_k}\int_0^{k_f} \frac{\varepsilon_3 2k^{2(n+3)} + \varepsilon_2 2k^{2(n+2)} + \varepsilon_1 2k^{2(n+1)}}{(-2E-k^2)}dk \tag{5.46}$$

Here $n = s + s' + l_k$ to make each integral differ by only one integer.

Now the immersed Fock matrix is a series of nested sums over analytic expressions.

$$U_{\alpha\beta} = F_{\alpha\beta} + \frac{1}{(2\pi)^3}\sum_{l_k,m_k}^{\infty}\sum_{s=0}^{\infty}\sum_{s'=0}^{\infty} c_{sl_k}c^{s'l_k}\sum_{i=1}^{3}\varepsilon_i\Big[-\sum_{j=0}^{(n+i)-1}(-1)^j 2^{n+i+\frac{1}{2}} E^j \frac{k_f^{2(n+i)-2j-1}}{2(n+i)-2j-1} \tag{5.47}$$

$$-(-1)^{n+i}2^{n+i+\frac{1}{2}}E^{n+i-\frac{1}{2}}\arctan(\frac{k_f}{\sqrt{E}})\Big]$$

The value of the immersed matrix elements depends on the Fermi wave vector k_f and the energy E of the system. In principle the energy is not known but in practice it is assumed to be close to that of the free atom.

5.3 Immersed Self Consistent Field

The perturbation on the free atom Fock matrix must be done carefully. The system is highly unstable and solutions are only possible for a discrete set of parameters. One important parameter that must be within a limited range is E, the energy of the system. Along with this, each sum over plane wave *principal* indices s, must be truncated to a reasonable value. Finally all of this must be for a particular range of the Fermi wavevector k_f. Exploring parameter space will have to been done with caution and breakdowns of the system justified.

5.3.1 Immersed Energy Eigenvalues

The problem of having to know an unknown energy E is solved by slowly moving the system from a free atom to an immersed atom. To do this the first iteration is for that of a free atom. The energy solutions to the system are then the eigenvalues of the Fock matrix. Each eigenvalue should be a reasonable value for the energy if the perturbation is small. Each (*negative*) eigenvalue corresponds to a particular bound electron and will be used to generate new coefficients for that particular electron. The eigenvalue is used as the energy in the perturbation and the immersed Fock matrix is then solved. The eigenvector corresponding to that bound state is then used as the new coefficients. Mixing the old coefficients slowly with the new will ensure the energy is always approximately true.

5.3.2 Maximum Number of States

The system's ability to converge depended heavily on the maximum value of, not only s, but also by the maximum number of bound electron basis states. This can be seen by examining all of the locations $n = s + s' + l_k$ appears in equation **??**. Increasing the number of bound basis states increases the number of maximum possible angular momentum quantum numbers l_α. The plane wave quantum number l_k will have all states up to the allowed coupling to l_α. Increasing both the maximum number of bound states and the maximum number of free states will affect convergence heavily.

An example of a value in which the system will not converge is when the maximum principal bound quantum number is three and the maximum value for s is also three. These mean the maximum value for the index $n = s + s' + l_k$ is eight. The summation over j in equation 5.47 is applied to $(-1)^j$ and the stage is set for large subtractive cancellation. This is a purely numerical effect not the most likely candidate for the cause of the instability.

The most likely cause for problems in convergence lie in the expansion of the Bessel functions into increasing powers of r and that effect on the spatial integrals like equation 5.22 . The Bessel equation 5.20 is an asymptotic expansion whose validity is dependent on $k_f r \ll 1$. The average radius of 3s basis states can be as large as five or ten. This explains why large principal quantum numbers can break convergence.

One last condition, very much related to the previous, is when s_{max} is large. The higher the power of r that a Bessel function is expanded the less any tails to a basis state can exist. Even 2p basis states can have long tails in the wave function that extend to a radius of two or three. It is for each of these reasons that equation 5.47 is valid only for a limited range of parameters.

5.3.3 Fermi Wave Vector: k_f

The last parameter that can be varied is the Fermi wave vector k_f. This value is the connection to real world metals. If you were to place one electron in an empty box it would lie in the ground state. Another would as well but with opposite spin. The following electrons would, in two, fill progressively higher states. Real metals have Fermi wave vectors that connect this theory to experiment. The energy of the maximum energy level is the Fermi energy and is related to k_f by:

$$E_f = \frac{\hbar^2 k_f^2}{2m} \tag{5.48}$$

To relate k_f to the density of free electrons a summation over all available states, up the Fermi level, must be made. In general some function $G_{\overrightarrow{k}}$, describes the allowable wave vector states. As the electron density increases, the allowed k states become more continuous. Assuming the electron density is high enough the sum can be turned into an integral [13]. The symmetry used here is a spherical shell in k-space out to k_f.

$$N = \sum_{\overrightarrow{k}}^{k_f} G_{\overrightarrow{k}} = V \int_0^{k_f} D_{\overrightarrow{k}} d\overrightarrow{k} \tag{5.49}$$

Here $D_{\overrightarrow{k}} = \frac{2}{(2\pi)^3}$ is the density of electron states in three dimensions and V is the real space volume. Now the Fermi wave vector can be found in terms of the density $n = \frac{N}{V}$.

$$k_f = (3\pi^2 n)^{\frac{1}{3}} \tag{5.50}$$

5.4 Results

In many-body theory increasing the degrees of freedom for the problem should result in lowering the total energy. Immersing an atom in an electron gas increases the degrees of freedom because of the additional coupling between bound and free states.The immersion energies for various k_f are shown in Table 5.2.

TABLE 5.2: Immersed atom energies for helium through carbon with nmax=2 and smax=2. Immersions for k_f beyond those reported were not possible.

k_f	Helium	Lithium	Beryllium	Boron	Carbon
0.0	-2.85809	-7.43243	-14.57391	-24.530787	-37.6877019370
0.05	-2.85814	-7.43244	-14.57391	-24.530787	-37.6877019377
0.1	-2.85846	-7.43247	-14.57392	-24.530788	-37.6877019497
0.15	-2.85920	-7.43266	-14.57398	-24.530793	-37.6877020348
0.2	-2.86026	-7.43321	-14.57420	-24.530814	-37.6877023614
0.25	-2.86130	-7.43431	-14.57467	-24.530866	-37.6877031909
0.3	-2.86129	-7.43619	-14.57552	-24.530968	-37.6877047993
0.35	.	-7.43914	-14.57686	-24.531141	-37.6877074061
0.4	.	.	-14.57885	-24.531406	-37.6877111419
0.45	.	.	-14.58164	-24.531785	-37.6877160439
0.5	.	.	-14.58549	-24.532304	-37.6877220675
0.55	.	.	.	.	-37.6877291078
0.6	.	.	.	.	-37.6877370280
0.65	.	.	.	.	-37.6877456942
0.7	.	.	.	.	-37.6877550134
0.75	.	.	.	.	-37.6877649775
0.8	.	.	.	.	-37.6877756242

Null values are due to a breakdown in the convergence. The asymptotic expansion in Equation 5.20 is no longer valid and the energy increase to positive infinity very rapidly. Carbon has the least change in total energy, on the micro-hartree scale. This is encouraging as pure carbon is non-metal and should not have an energy advantage to a metallic state.

The immersion energy data can be more useful if it is expressed as the difference from a free atom. This can show the extent of the energy advantage of an immersed atom.

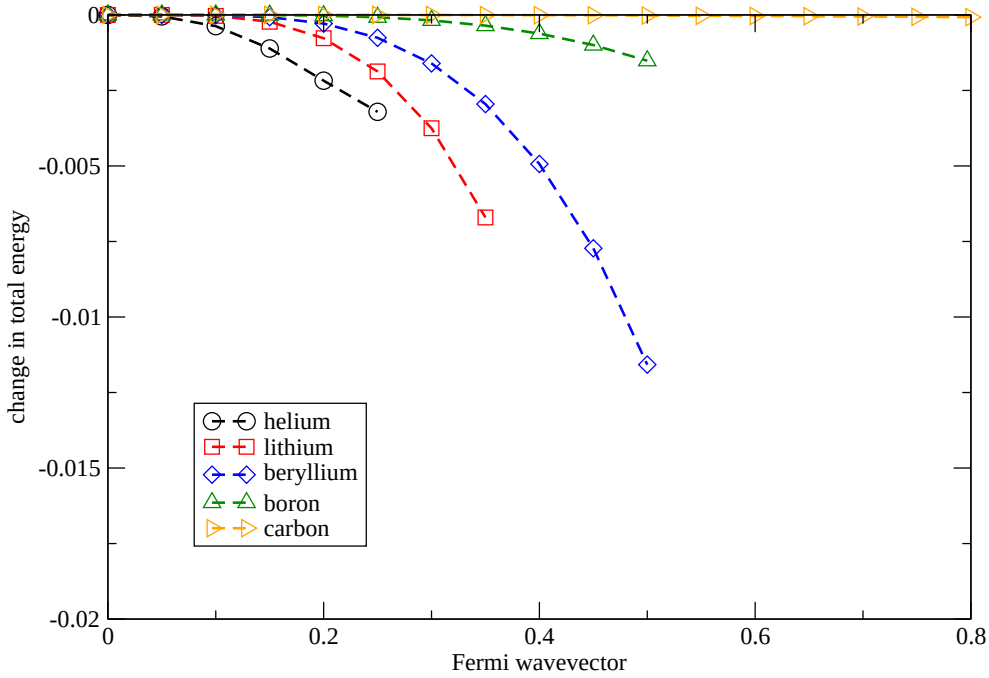

FIGURE 5.6: Change total energy vs k_f for helium through carbon immersed in an electron gas. Convergence was possible with nmax=2 and smax=2.

One general feature of the data in Figure 5.6 is the relative change in energy for atoms of different metallic properties. Lithium and beryllium have the greatest drop in immersion energy. Both of these are metals. Boron has a change that is in between the non-metal carbon and the previously stated metals. This fits as boron is a semi-metal. Of course all these conclusions are done without consideration to helium, which doesn't fit the previous logic. Helium needs to be studied closer to understand the features exhibited here.

Each change in immersion energy appears to follow a similar dependence on k_f. In an attempt to create a slightly quantitative analysis the data will manipulated to extract

information on this k_f dependence. Carbon, although on a much smaller energy scale, exhibits the same general behavior as the other atoms. The top plot in Figure **??** is this immersion energy difference for carbon.

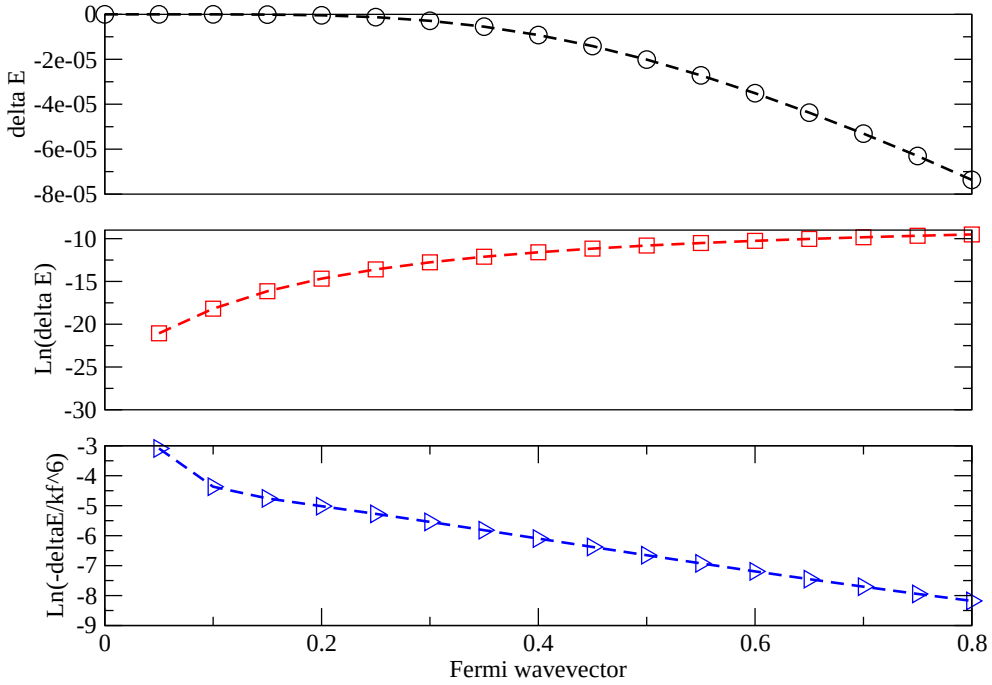

FIGURE 5.7: Data analysis of the k_f dependence of the total energy of carbon immersed in an electron gas. Convergence was possible with nmax=2 and smax=2.

The middle plot was to search for an exponential dependence. Much manipulation occurred next to find if any exponential, power, or combination of these dependencies simplified the connection. Finally it was discovered that a near-linear relationship existed for the natural log, of the absolute value, of the change in energy, divided by k_f to a power. For carbon the k_f power is six, which means $k_f^6 = n^2$. This would result in an immersion energy difference equal to the following:

$$\Delta E = -k_f^6 e^{-mk_f} = -n^2 e^{-m(3\pi^2 n)^{\frac{1}{3}}} \tag{5.51}$$

Here m is the absolute value of the slope of the linear portion of the bottom plot in figure

??, equal to roughly five.

With this assumed k_f dependence on the change of energy extrapolation to higher k_f could predict the expected behavior. Consider when the derivative to ΔE goes to zero.

$$\frac{d\Delta E}{dk_f} = \frac{6}{k_f}\Delta E - m\Delta E = 0 \tag{5.52}$$

When $k_f = 6/m$ this condition is satisfied. This would hint that the maximum change in energy for an immersion could be predicted. For the case of lithium this results in a maximum change in energy at $k_f = 6/5$. The Fermi wave vector for metallic lithium is actually closer to 0.5 [13]. This preliminary result is on the correct order of magnitude and gives hope that the theory may have value.

The next logical question is if all the other atoms exhibited this type k_f dependent behavior. All but helium reach a near-linear relationships when the power k_f is six. Figure 5.8 shows the slope of each is also approximately the same.

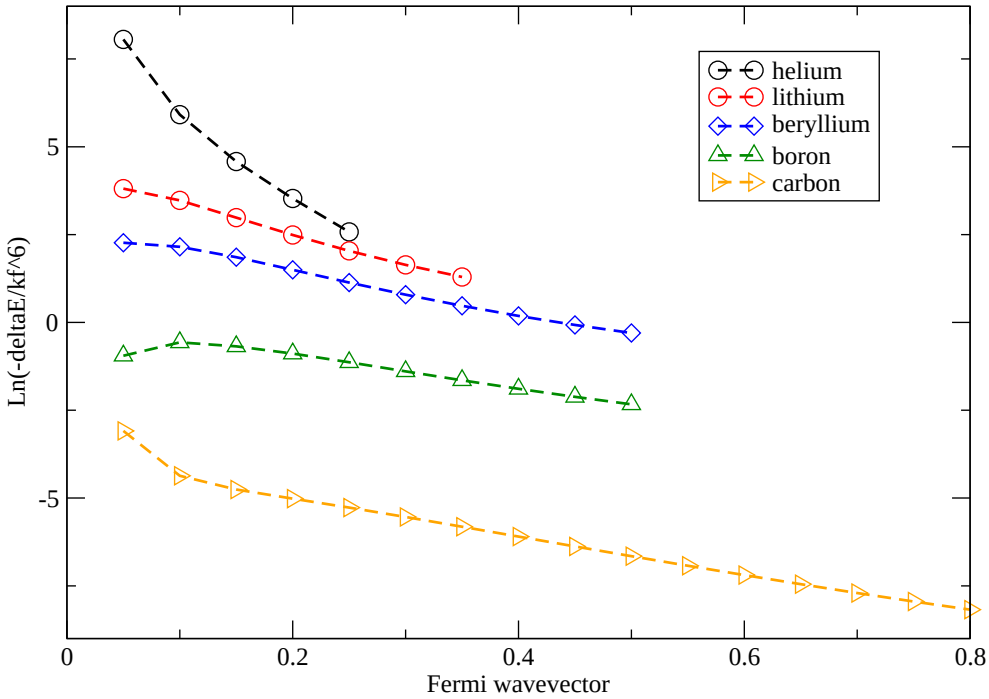

FIGURE 5.8: Immersion energy dependence on k_f for helium through carbon. Each follow similar k_f power dependence. Convergence was possible with nmax=2 and smax=2.

One question still unanswered is what happens to the charge density as the atom is immersed into the gas. The distribution of projections onto basis states helps to understand the shift in the charge density. Beryllium provides a simple example to explore the effect on the eigenvector coefficients because of its spin symmetry.

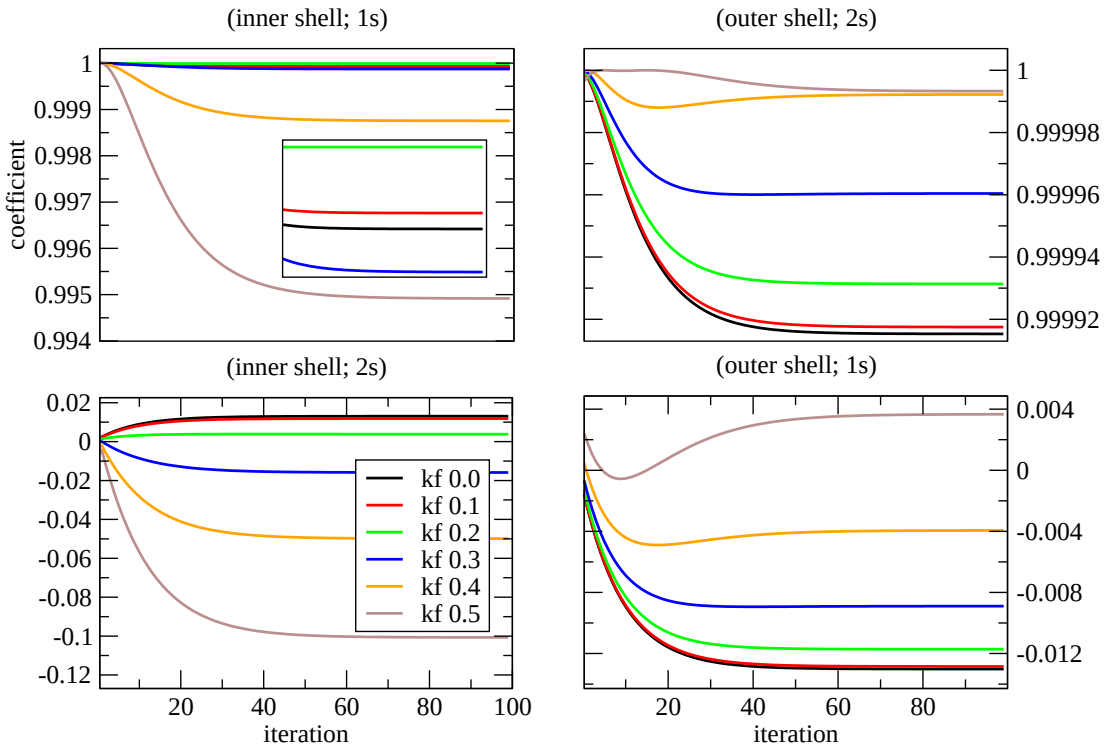

FIGURE 5.9: Immersed beryllium eigenvectors for nmax=2 and smax=2. The plot inset is to see the relative differences between the closely lying values in the top left plot.

In Figure 5.9 as k_f increases, the outer shell electrons 2s projection increase, which decreases the amount in the 1s state. The charge of the outer shell electron moves towards a greater $\langle r \rangle$. The inner shell electron is more complicated. As the electron density in the gas increases the 2s coefficient initially decreases to zero. Between $k_f = 0.2$ and $k_f = 0.3$ this 2s coefficient switches from a positive to negative number. Immersion greater than this and more charge moves into the 2s state. So initially the inner shell electron's charge density moves towards the nucleus but as k_f increases this effect switches and the charge moves out. The coefficients for the outer shell electron vary an order of magnitude less than the inner. This would conclude that the inner shell change in density would dominate the overall shift in charge. Since the energy decreased as the immersion increased no definitive conclusion can be made about the shift in the immersed charge densities effect on total

energy. What can be said is the charge initially moved towards the nucleus. When k_f went from 0.2 to 0.3 this effect reversed and beyond $k_f = 0.3$ the charge density continued to move away from the nucleus.

All of the data from the immersion calculations show that the perturbation method used is promising. Shortfalls of the chosen expansions used during the derivation of the immersion energy have been identified. Further work could overcome some of these difficulties and make the model more robust. Understanding the behavior of immersed helium could have light shed onto it by extending the program to the next noble gas, neon.

6. CONCLUSION

The many-body Schrödinger equation has been solved for free atoms and atoms immersed in an electron gas. The method uses converged DFT states as the basis for spin orbital states in unrestricted Hartree-Fock theory.

Parameters used when generating the basis sets, combined with an adjustable basis size, serve as tools to find the most complete basis for a given electronic configuration. The ideal basis set can yield values for the total energy of a free helium through carbon atom, within millihartrees of those calculated with a complete Roothaan basis.

Breaking of spherical symmetry lifts degeneracies in the eigenvalues of the Fock matrix and the total energy. The post-Hartree-Fock method of configuration interaction can be used to account for correlation and create total wave functions that are eigenstates of L and S. When compared to spectroscopic data, the energy of the transition of boron from the ground state to the first excited state only differed by 6.165×10^{-3} hartrees.

The immersion of the atoms into an electron gas was accomplished, without increasing state space, by a method of perturbation [8]. For the range of system convergence, the energy of the atom is lowered as the charge density of the background increases. Lithium and beryllium exhibited the greatest energy shifts, on the order of milliHartrees, followed by boron, which was less than a milliHartree. Still following the same immersion dependence but on a scale nearly six orders of magnitude less, carbon showed the least energy advantage.

This work has shown that modelling free atoms in the context of Hartree-Fock theory, with sets of basis states generated from converged DFT, can produce viable energies for free atoms. Immersing these atoms into an electron gas with the use of perturbation theory is possible.

Future work should include free atom total energy calculations for heavier atoms.

Each of these atoms should have configuration interaction calculations for L and S symmetry. These values can then be compared with spectroscopic experiment. A MCHF approach could go even further in accounting for electron correlation. The derivation for the immersed Fock matrix needs to be made more robust. The obvious solution to this is not performing the asymptotic expansion that separates the Bessel functions r and k dependence. Calculations for greater k_f could then produce results for maximum energy advantages of atoms immersed in an electron gas. Post-Hartree-Fock methods such as CI and MCHF could then be done on the immersed electronic configurations.

In short, we've created and tested a set of fundamental tools for modelling many-body interactions. The number of systems that could be explored, with this work as a jump-off point, are endless.

BIBLIOGRAPHY

1. A.P. Albus, *Immersion Energies of Atoms in Jellium*, M.S. Thesis, Oregon State University (1999)
2. M.J. Puska, R.M. Nieminen, M. Manninen, *Atoms embedded in an electron gas: Immersion energies* Phys. Rev. B **24**, 3037 (1981)
3. J.H. Song, *Impurities in a Homogeneous Electron Gas*, Ph.D. Thesis, Oregon State University (2005)
4. S. Dorsett, *Breaking of Spherical Symmetry in Electronic Structure, Free and Immersed Atoms in an Electron Gas*, Ph.D. Thesis, Oregon State University (2007)
5. F. Hund, Zeitschrift fr Physik, **33**, 345-371 (1925)
6. C. Kittel, *Quantum Theory of Solids*, Wiley (1987)
7. E. Wigner, Phys. Rev. **46**, 1002 (1934)
8. Per-Olov Löwdin, *A Note on the Quantum-Mechanical Perturbation Theory*, J. Chem. Phys., Vol. 19, Num. 11, (november 1951)
9. G. Arfken, H. Weber, *Mathematical Methods for Physicists*, pg **724** Academic Press (2001)
10. M. Abramowitz, I.A. Stegun, *Handbook of Mathematical Functions*, Dover (1965)
11. B.H. Bransden, C.J. Joachain, *Physics of Atoms and Molecules*, Addison Wesley Longman Ltd. (1983)
12. C.F. Fischer, T. Brage, P. Jönsson, *Computational Atomic Structure: An MCHF Approach*, IOP Publishing Ltd., (1997)
13. M. Marder, *Condensed Matter Physics*, John Wiley & Sons, Inc., New York.(2000)
14. J.C. Slater *Quantum Theory of Atomic Structure*, Vol. I. New York, McGraw-Hill Publishing Company, Inc. (1960)
15. R.G. Parr, W. Yang, *Density-Functional Theory of Atoms and Molecules*, Oxford University Press (1989)
16. P. Hohenberg, W. Kohn, Phys. Rev. **136**, B864 (1964)
17. W. Kohn, L.J. Sham, Phys. Rev. **140**, 4A, A1133 (1965)

18. J.D. Jackson, *Classical Electrodynamics, 3rd Edition*, John Wiley & Sons (1999)

19. R.H. Landau, M.J. Páez, C.C. Bordeianu, *A Survey of Compuational Physics*, Princeton University Press (2008)

20. G. Drake, *Atomic, Molecular, and Optical Physics Handbook*, AIP Press (1996)

21. J. Carlsson, P. Jönsson, L. Sturesson, C. Froese Fischer, *Lifetimes and transition probabilities of the boron atom calculated with the active-space multiconfiguration Hartree-Fock method*, Phys. Rev. A, Vol. 49, Num. 5, (may 1994)

22. J.C. Morrison, C.F. Fischer, *Multiconfiguration Hartree-Fock method and many-body perturbation theory: A unified approach*, Phys. Rev. A, Vol. 35, Num. 6, (March 1987)

23. C. F. Bunge, J. A. Barrientos, A. V. Bunge, J.A. Cogordan, *Hartree-Fock and Roothaan-Hartree-Fock energies for the ground states of He through Xe*, Phys. Rev. A, Vol. 46, Num. 7, (october 1992)

24. C.C.J. Roothaan, Rev. Mod. Phys. **23**, 69 (1951); **32**, 179 (1960)

25. National Institute of Standards and Technology (NIST) website (http://physics.nist.gov/PhysRefData/ASD/index.html) for spectroscopic data

26. J.J. Sakurai, *Modern Quantum Mechanics*, Benjamin/Cummings (1985)

27. A. N. Andriotis,*Impurity Atoms/Ions Embedded in Metals*, Europhys. Lett., **17** (4), (january 1992)

28. J.E. Inglesfield, *A method of embedding*, Phys. C: Solid State Phys., **14** (1981)

29. S. Lundqvist, N.H. March *Theoy of the Inhomogeneous Electron Gas*, Plenum (1983)

30. E. Clemnti and C. Roetti, At. Data Nucl. Data Tables **14**, 177 (1974)

31. A.N. Andriotis, *A non-local Hartree-Fock approach to embedding*, J. Phys.:Condens. Matter **2**, (1990)